Transverse mode coupling instability with space charge at the CERN SPS

X. Buffat and H. Bartosik

Many thanks to the F. Asvesta, S. Albright, M. Coly, A. Huschauer, B. Salvant, A. Lasheen, H. Damerau, G. Papotti and the PSB, PS and SPS operation crews for their help !

Content

- Transverse mode coupling instability with space-charge
- Self-consistent simulations setup
- Experimental studies
- Conclusion

The Transverse Mode Coupling Instability (TMCI)

- The intensity per bunch in a synchrotron is often limited by the TMCI driven by the machine impedance

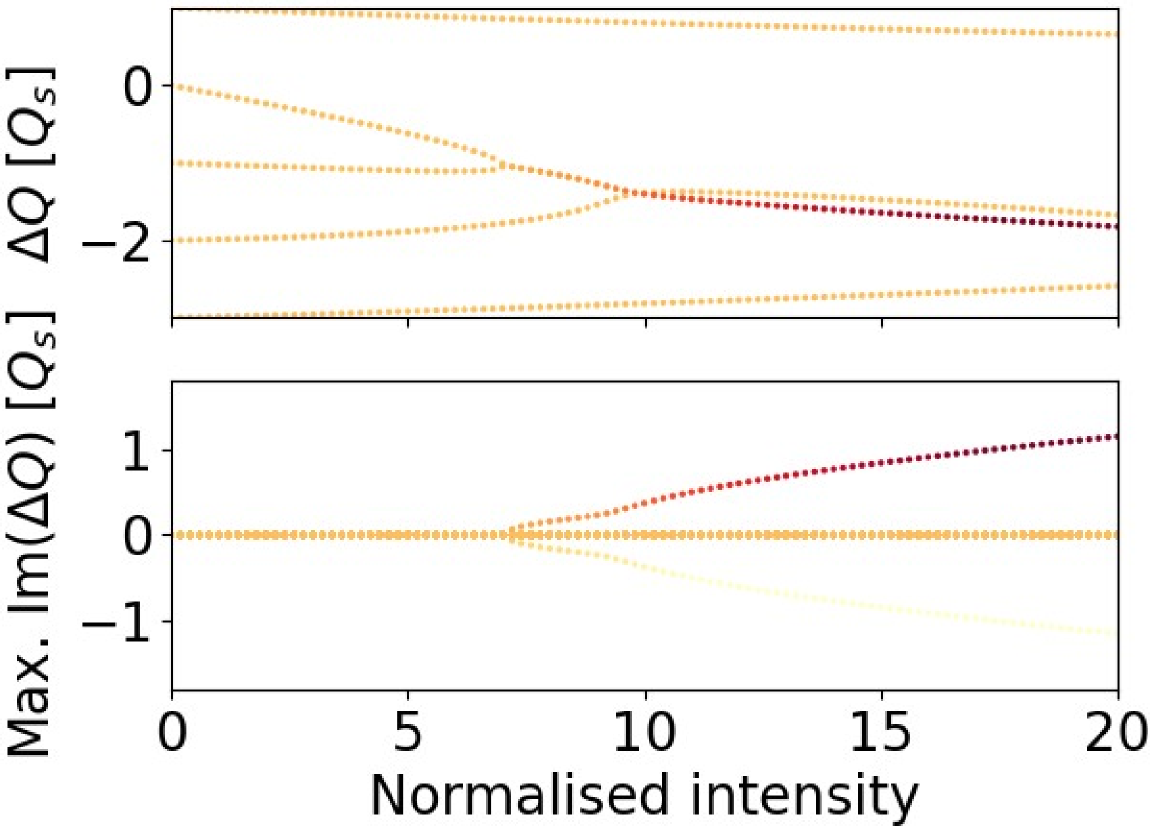

The Transverse Mode Coupling Instability (TMCI)

- The intensity per bunch in a synchrotron is often limited by the TMCI driven by the machine impedance

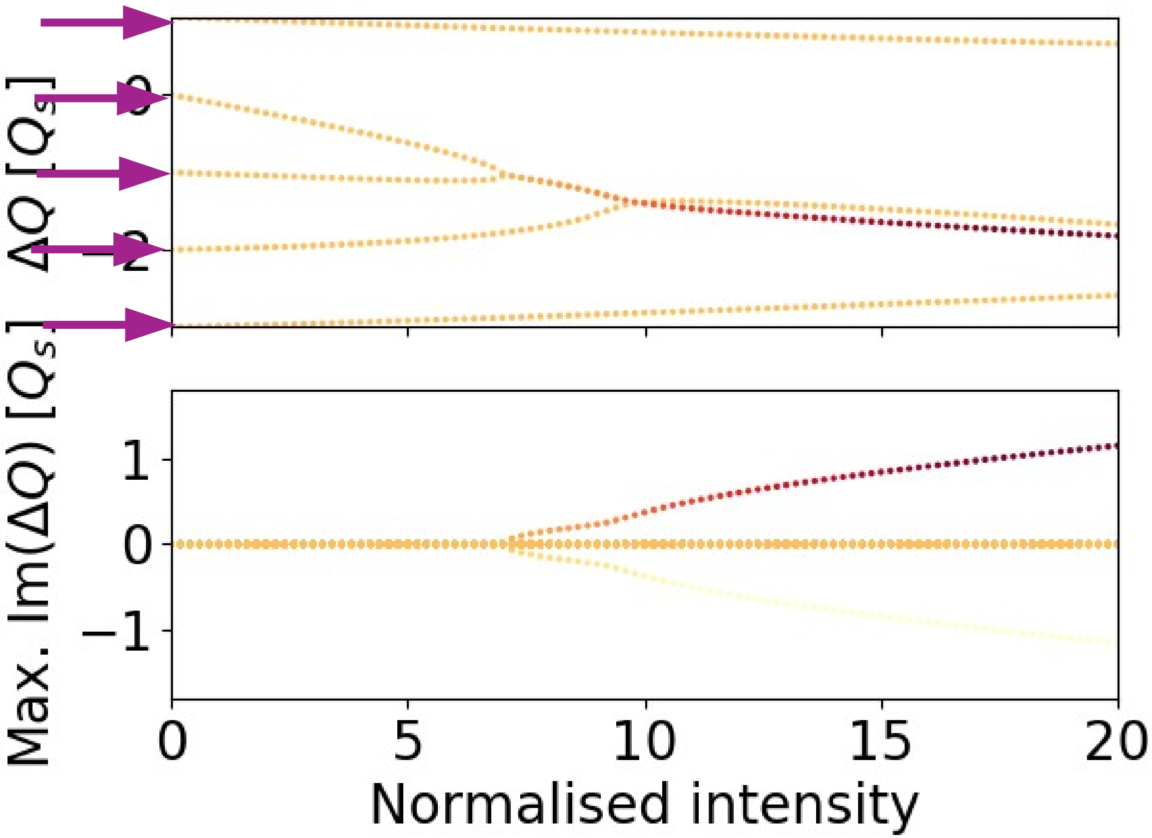

The Transverse Mode Coupling Instability (TMCI)

- The intensity per bunch in a synchrotron is often limited by the TMCI driven by the machine impedance

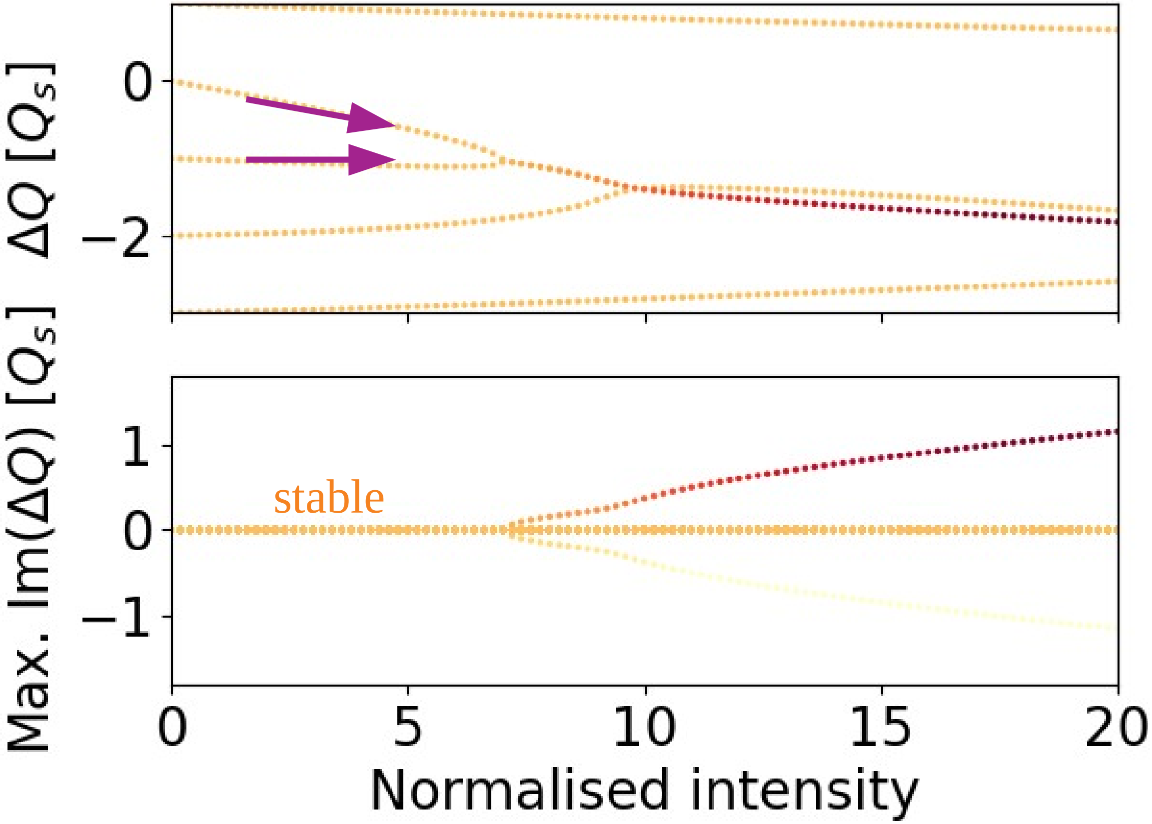

The Transverse Mode Coupling Instability (TMCI)

- The intensity per bunch in a synchrotron is often limited by the TMCI driven by the machine impedance

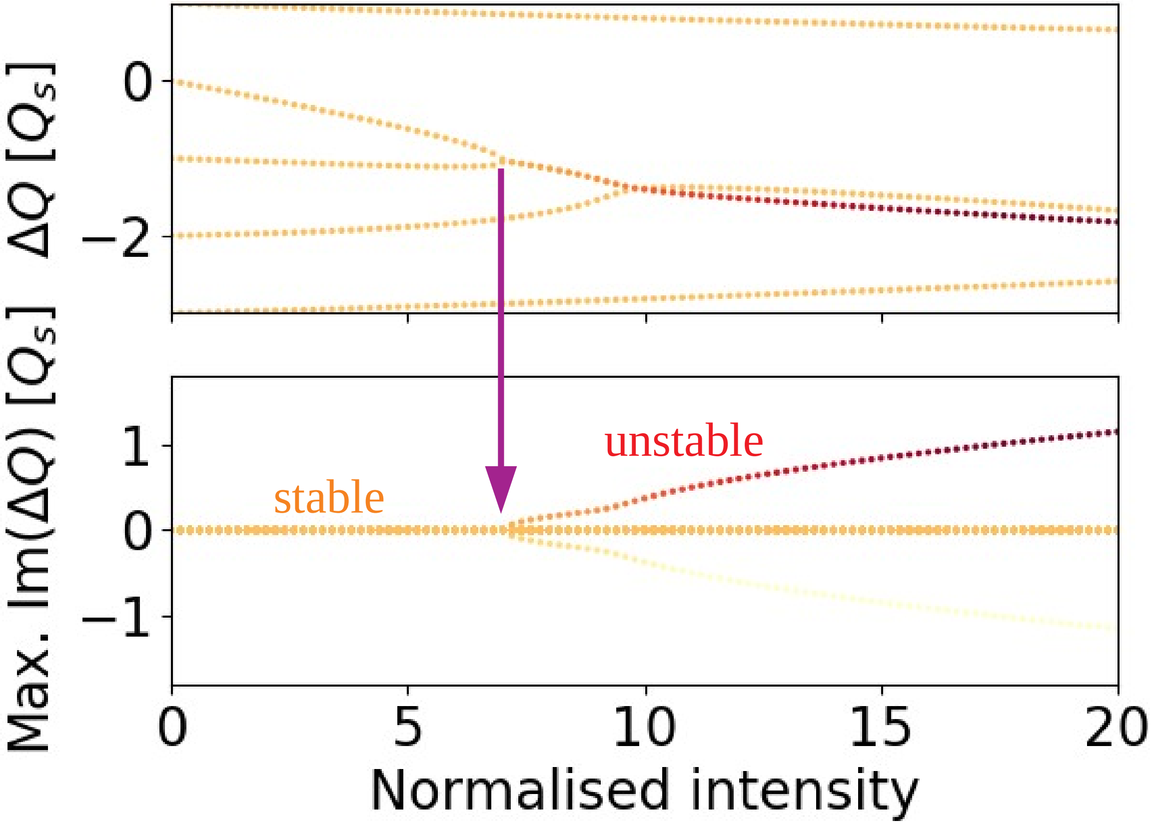

The Transverse Mode Coupling Instability (TMCI)

- The intensity per bunch in a synchrotron is often limited by the TMCI driven by the machine impedance

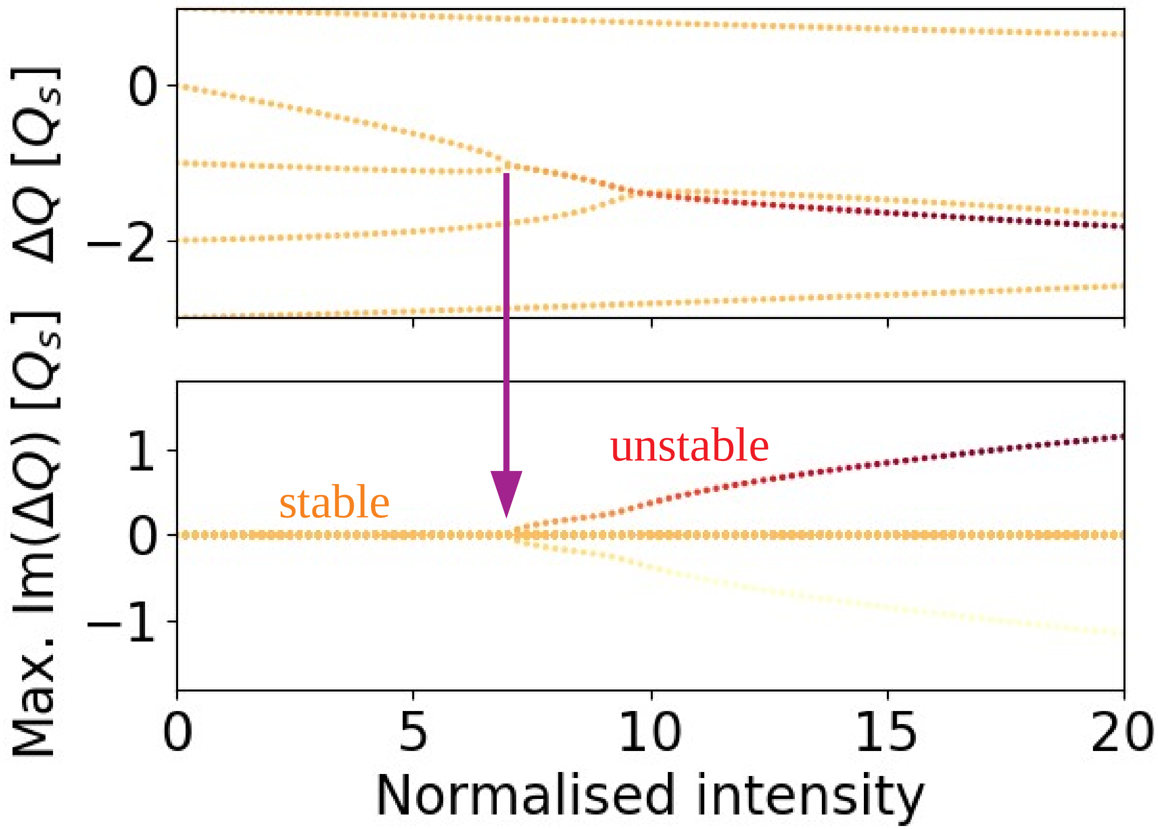

→ Models including both the impedance and space-charge forces are relevant to understand performance limitations in existing and future machines (e.g. high intensity proton drivers)

Impact of space-charge within the airbag model

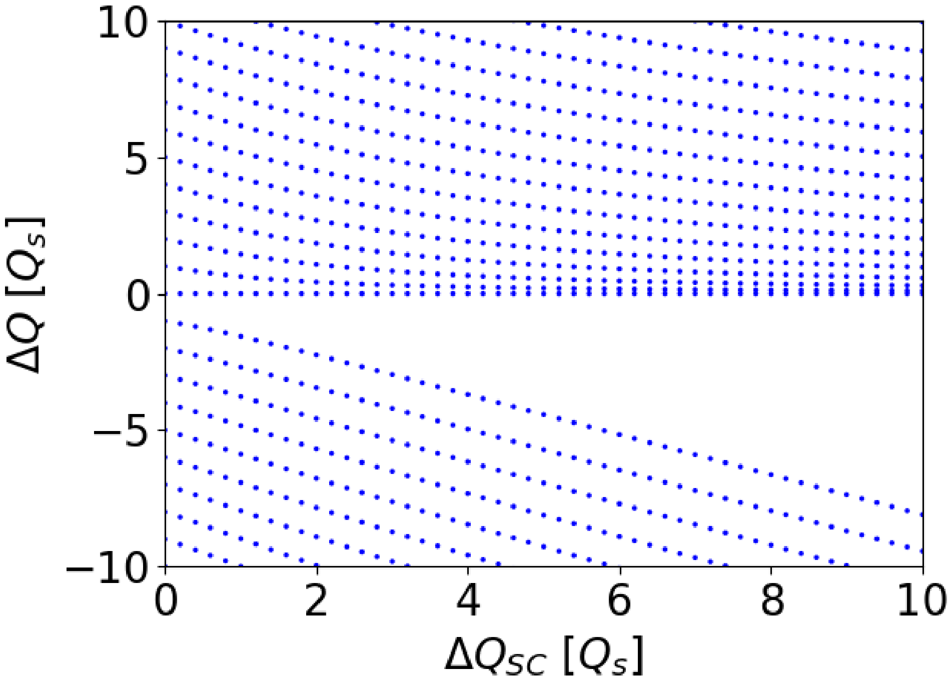

- Due to space-charge, the frequency of head-tail modes is reduced
  - The positive head-tail modes' frequency saturates above the bare tune

Impact of space-charge within the airbag model

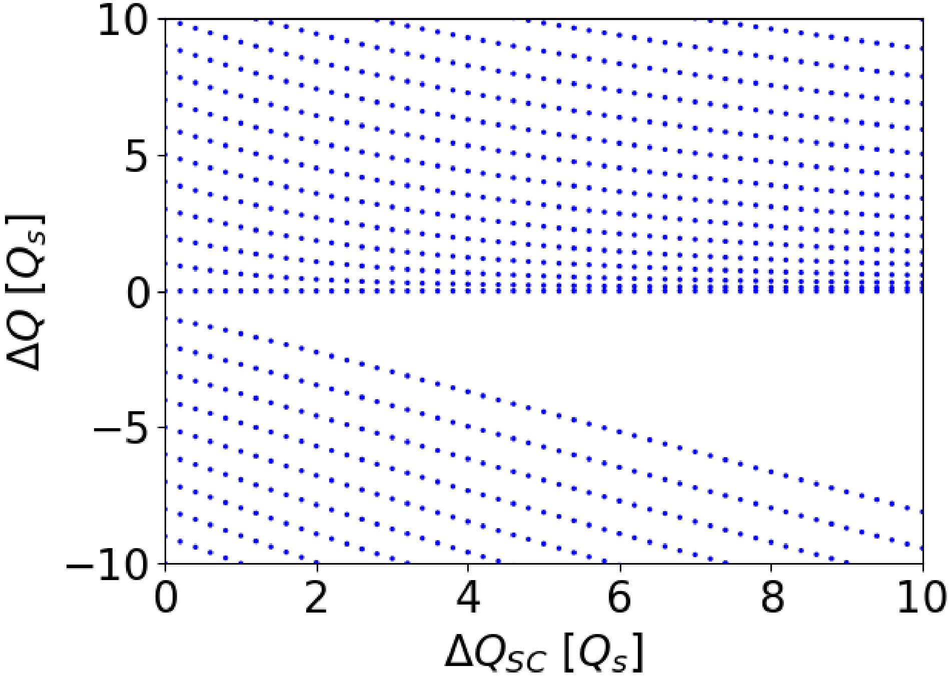

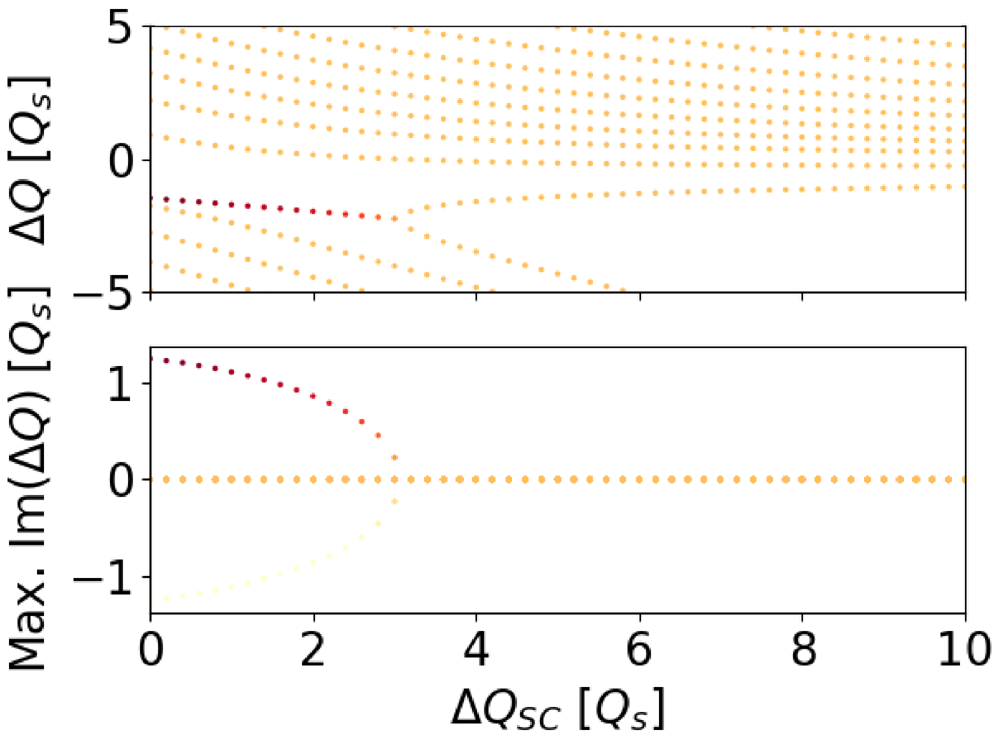

- Due to space-charge, the frequency of head-tail modes is reduced
  - The positive head-tail modes’ frequency saturates above the bare tune

Impact of space-charge within the airbag model

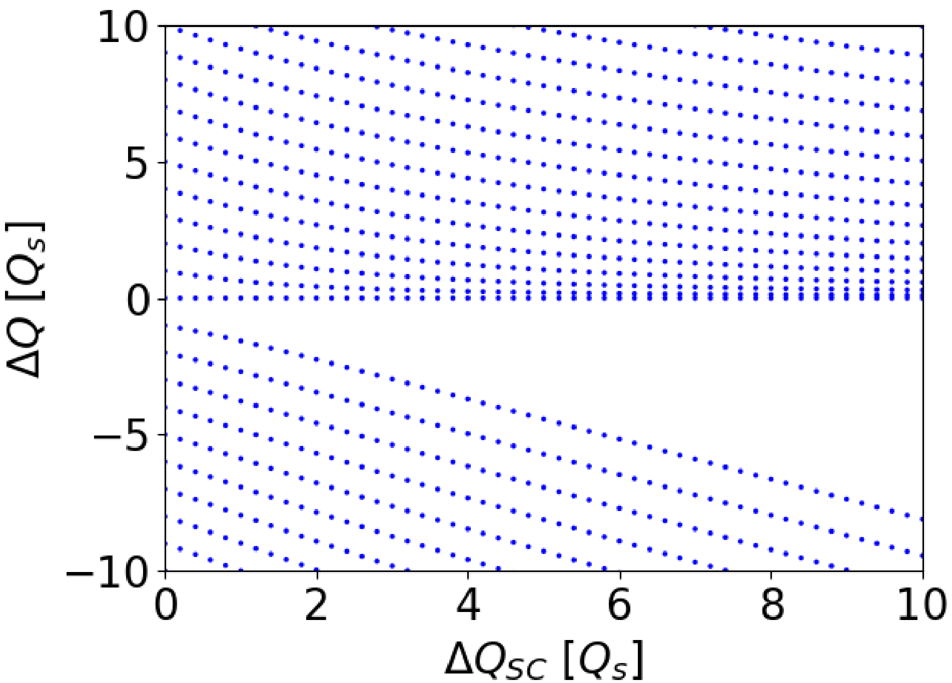

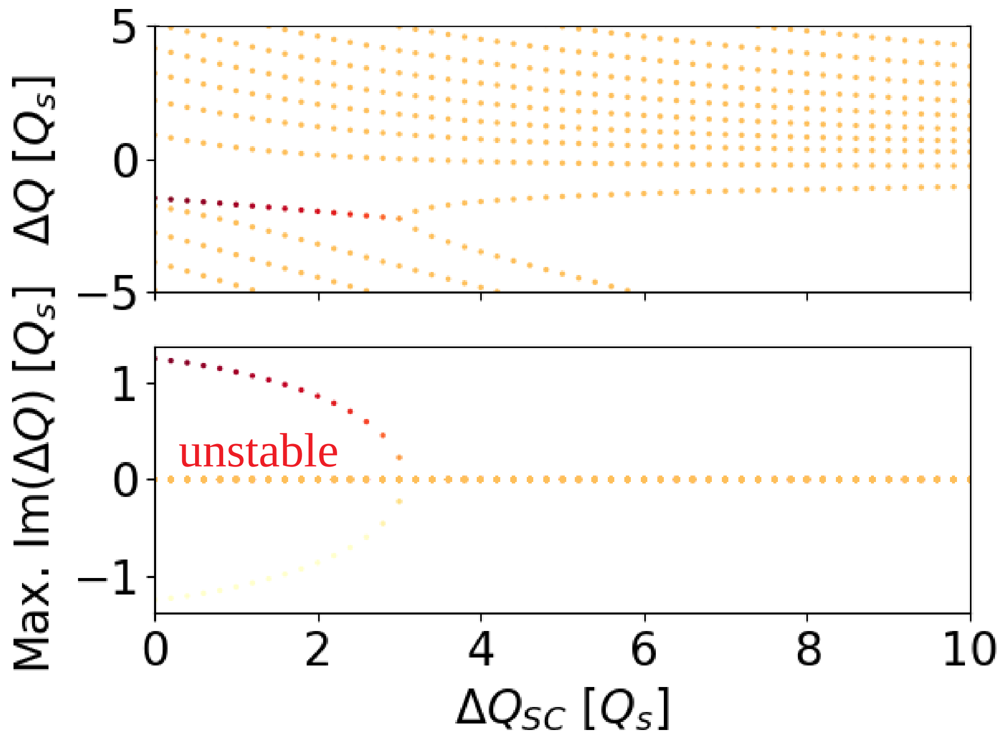

- Due to space-charge, the frequency of head-tail modes is reduced
  - The positive head-tail modes' frequency saturates above the bare tune

Impact of space-charge within the airbag model

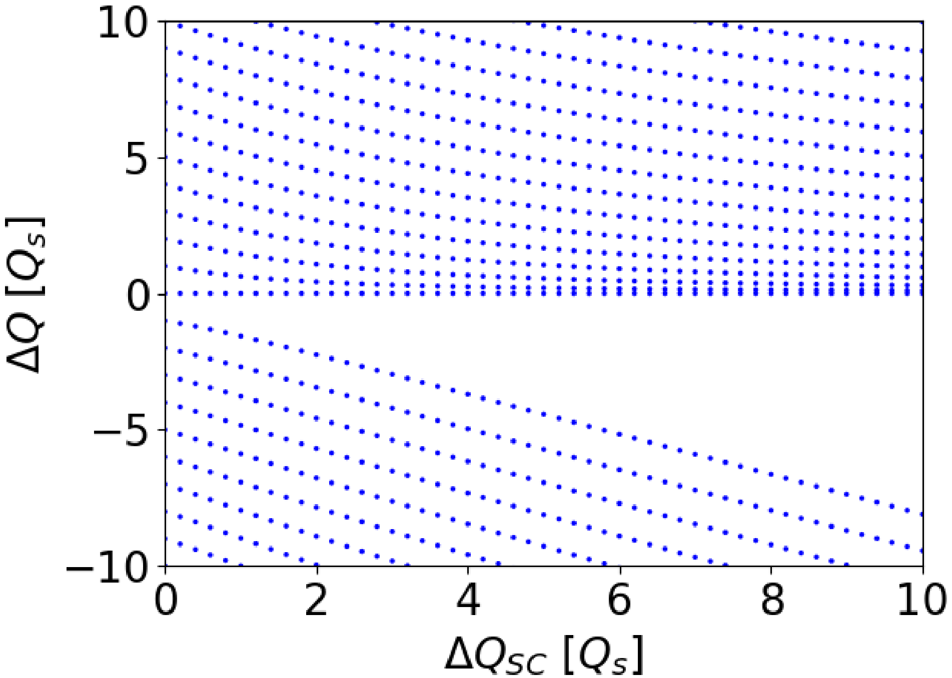

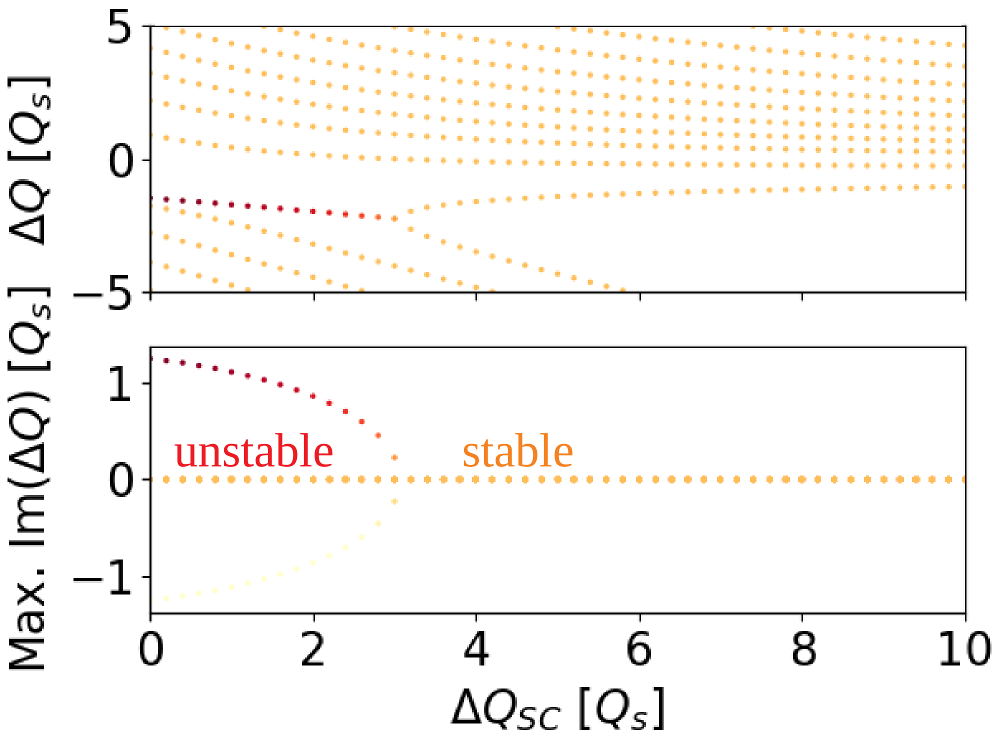

- Due to space-charge, the frequency of head-tail modes is reduced
  - The positive head-tail modes' frequency saturates above the bare tune

Impact of space-charge within the airbag model

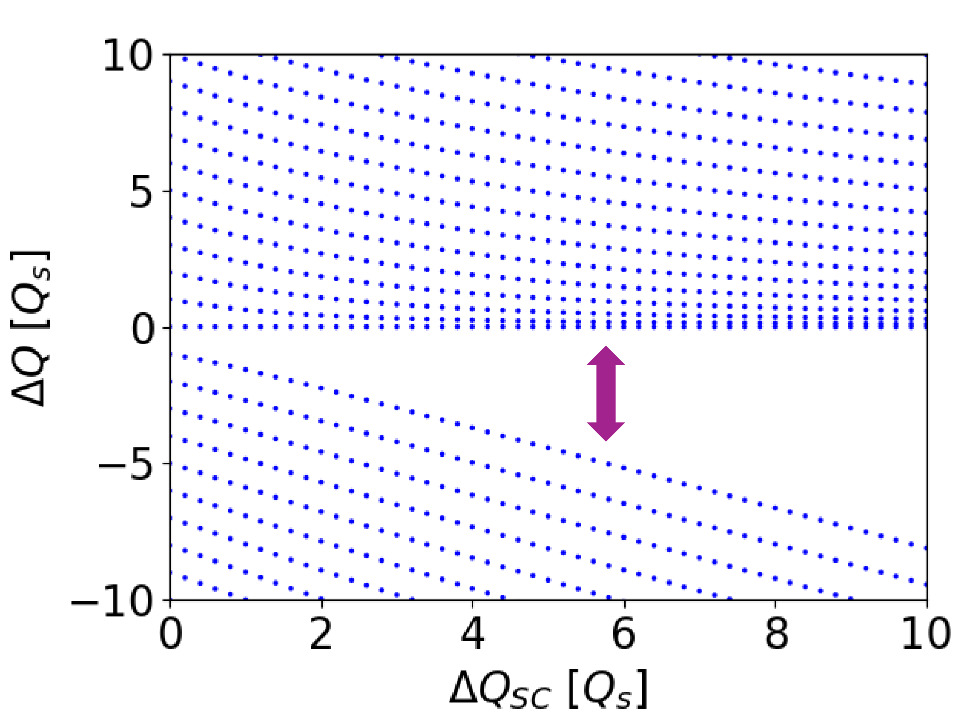

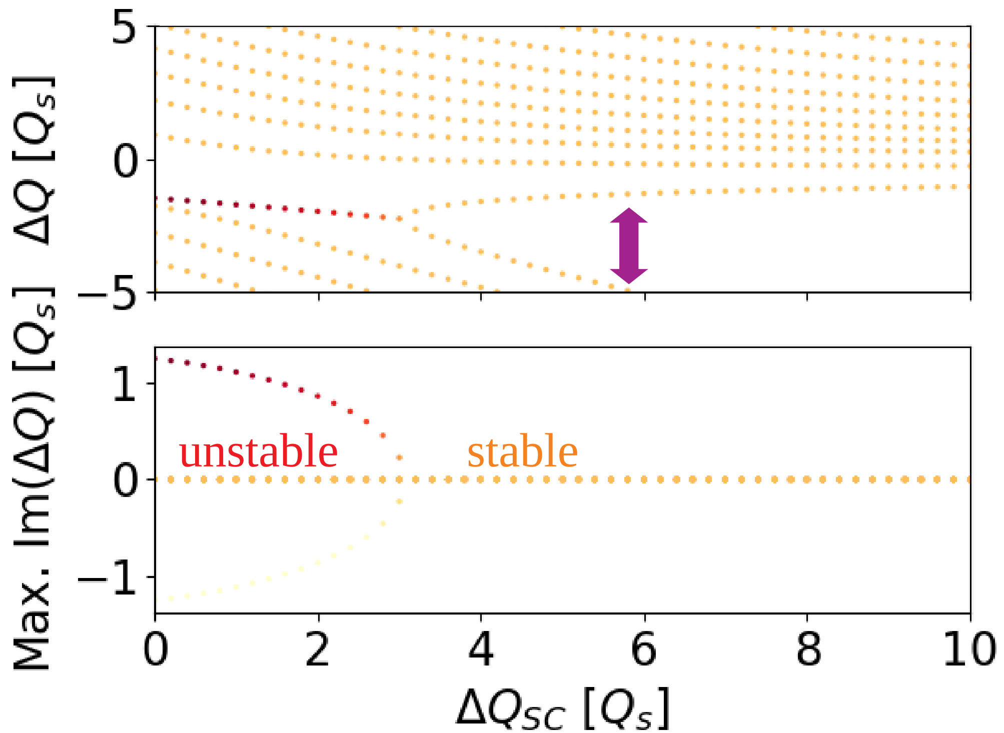

- Due to space-charge, the frequency of head-tail modes is reduced
  - The positive head-tail modes' frequency saturates above the bare tune
- Within the airbag model it was found that sufficiently strong space-charge forces suppress the TMCI *[Blaskiewicz]*

[Blaskiewicz] M. Blaskiewicz, Phys. Rev. ST Accel. Beams 1, 044201 (1998)

Impact of space-charge within the airbag model

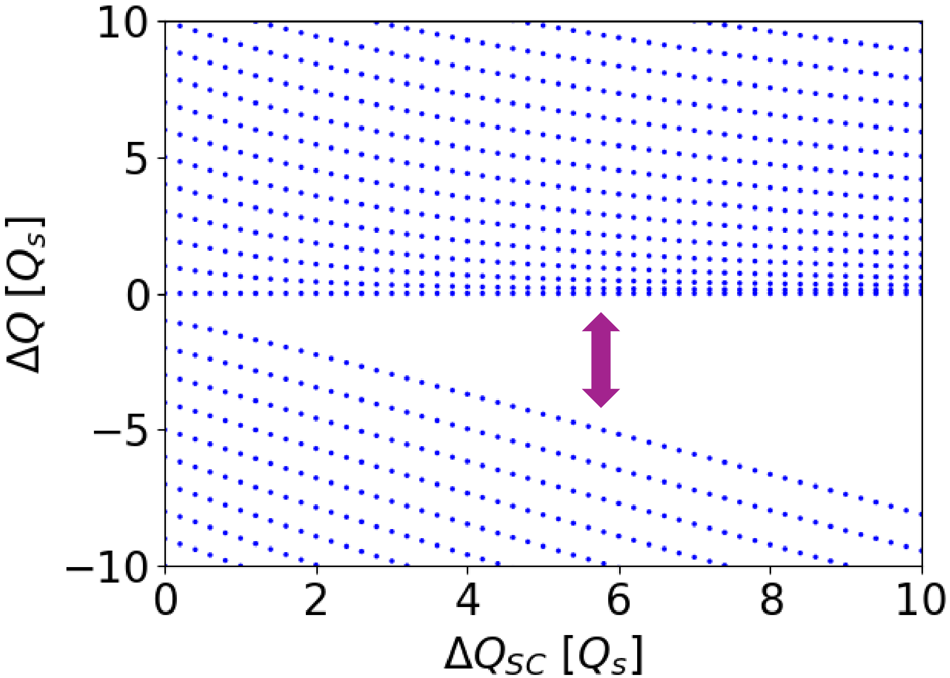

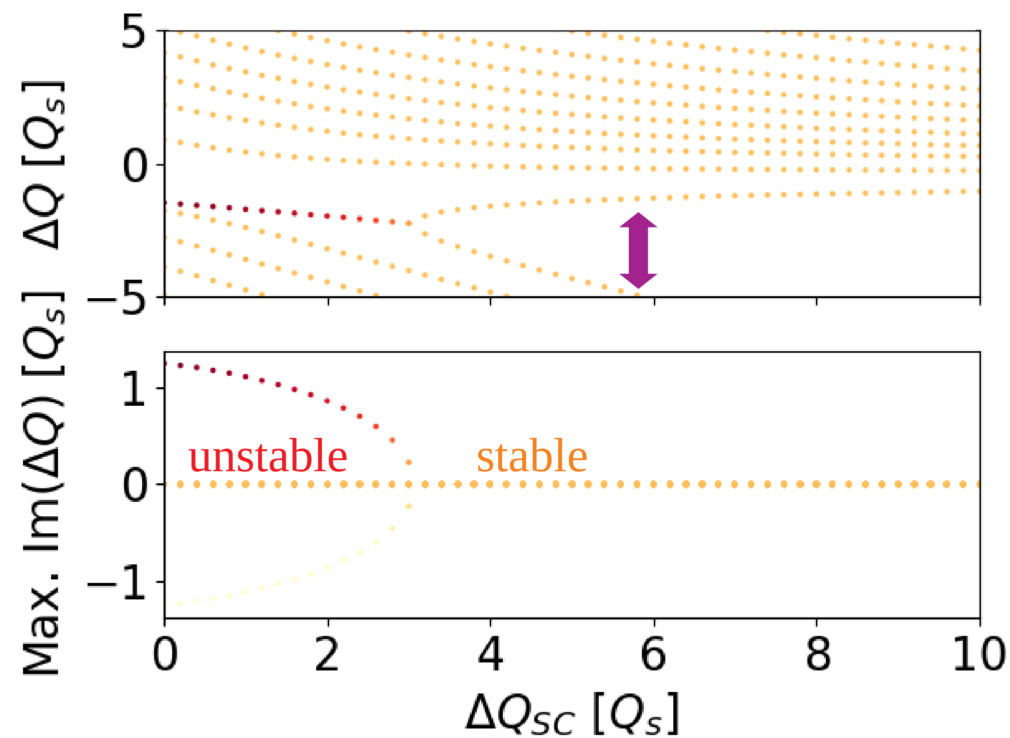

- Due to space-charge, the frequency of head-tail modes is reduced
  - The positive head-tail modes' frequency saturates above the bare tune
- Within the airbag model it was found that sufficiently strong space-charge forces suppress the TMCI *[Blaskiewicz]*

→ **Experimentally, transverse instabilities are observed in spite of space-charge**

[Blaskiewicz] M. Blaskiewicz, Phys. Rev. ST Accel. Beams 1, 044201 (1998)

Impact of space-charge: Radial modes

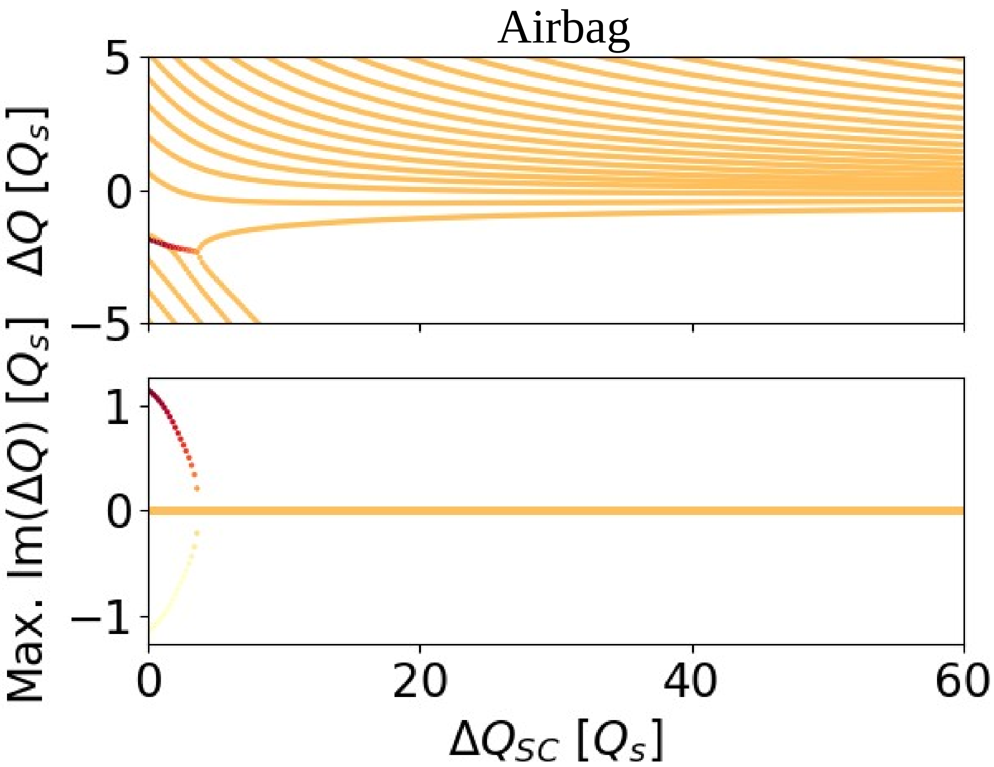

Impact of space-charge: Radial modes

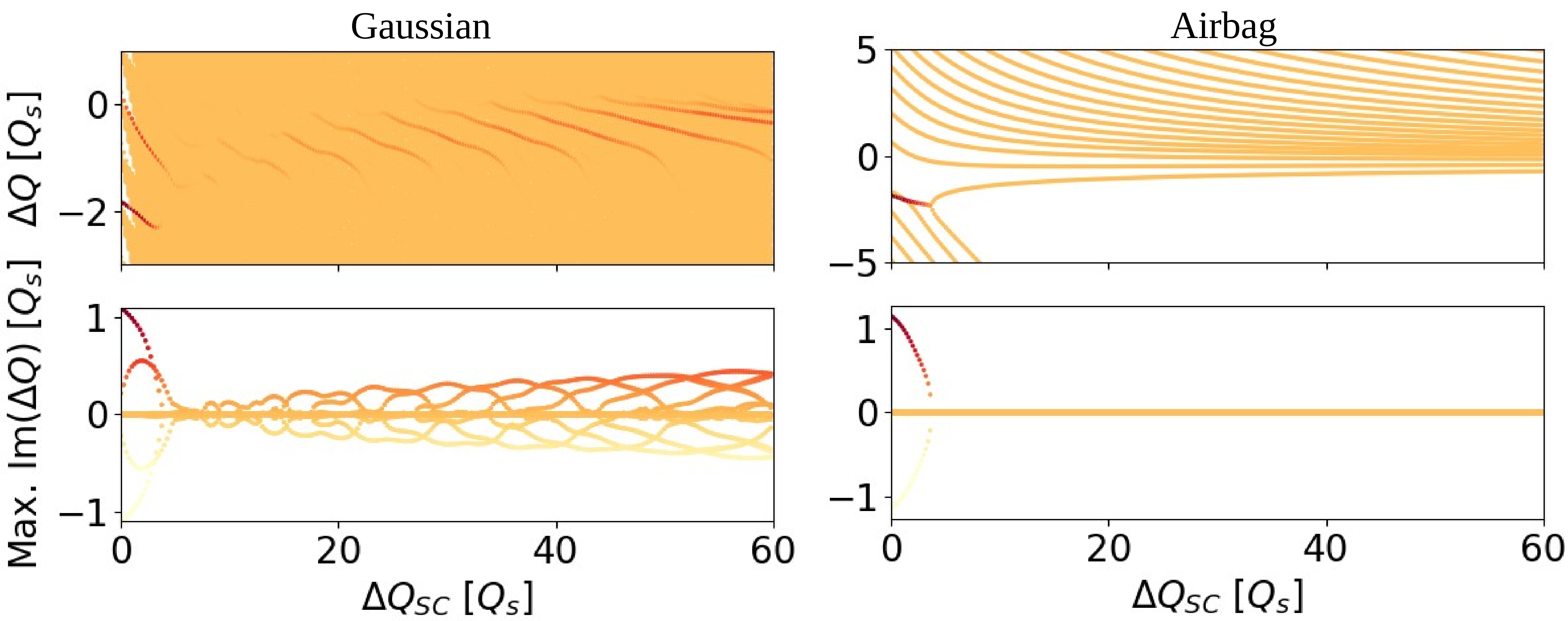

Impact of space-charge: Radial modes

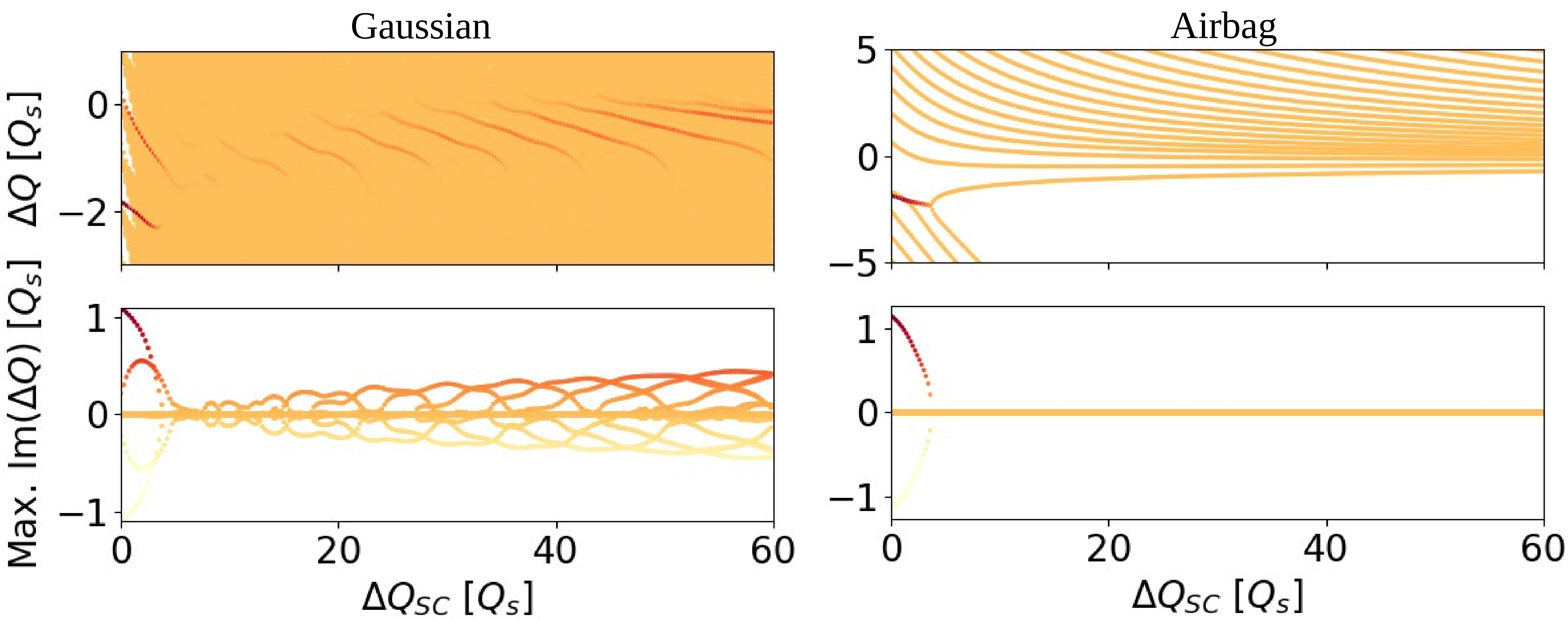

- Space-charge lifts the degeneracy of the head-tail modes, leading to a forest of head-tail mode

Impact of space-charge: Radial modes

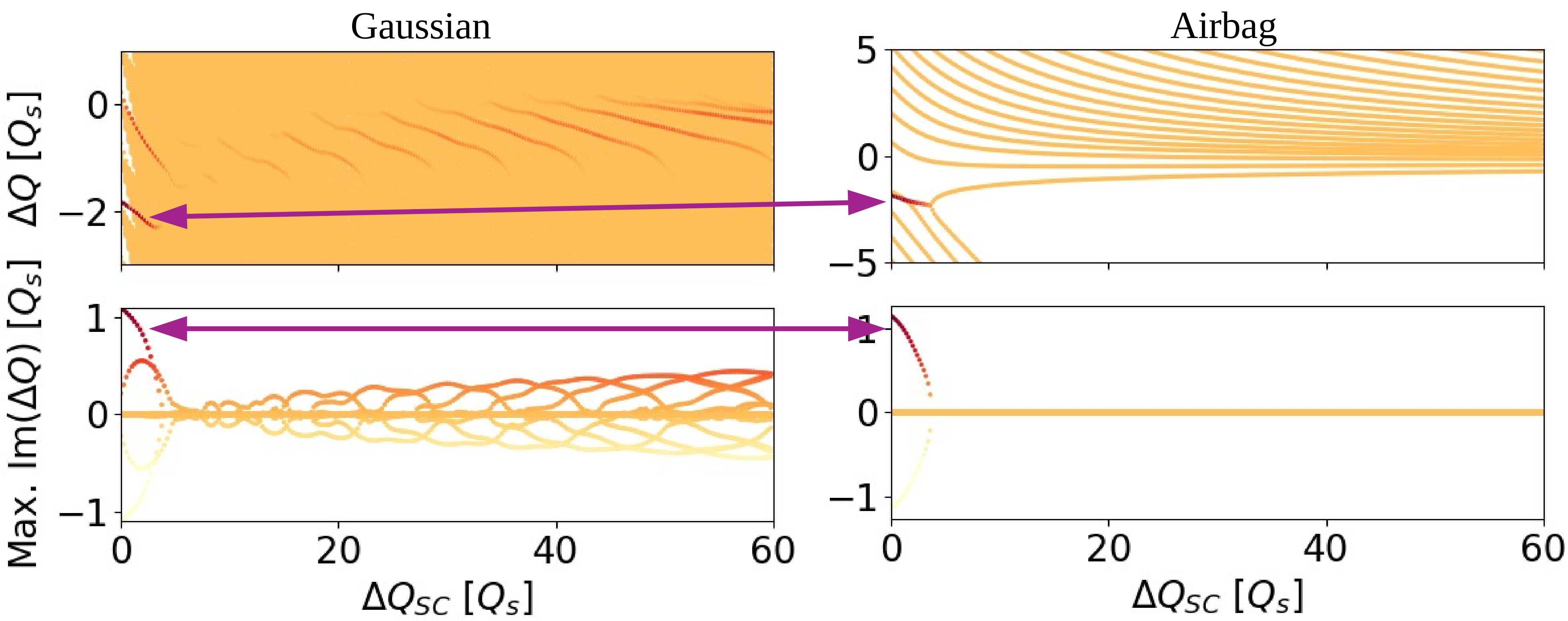

- Space-charge lifts the degeneracy of the head-tail modes, leading to a forest of head-tail mode
- The original TMCI is still lifted, as predicted by the airbag model

Impact of space-charge: Radial modes

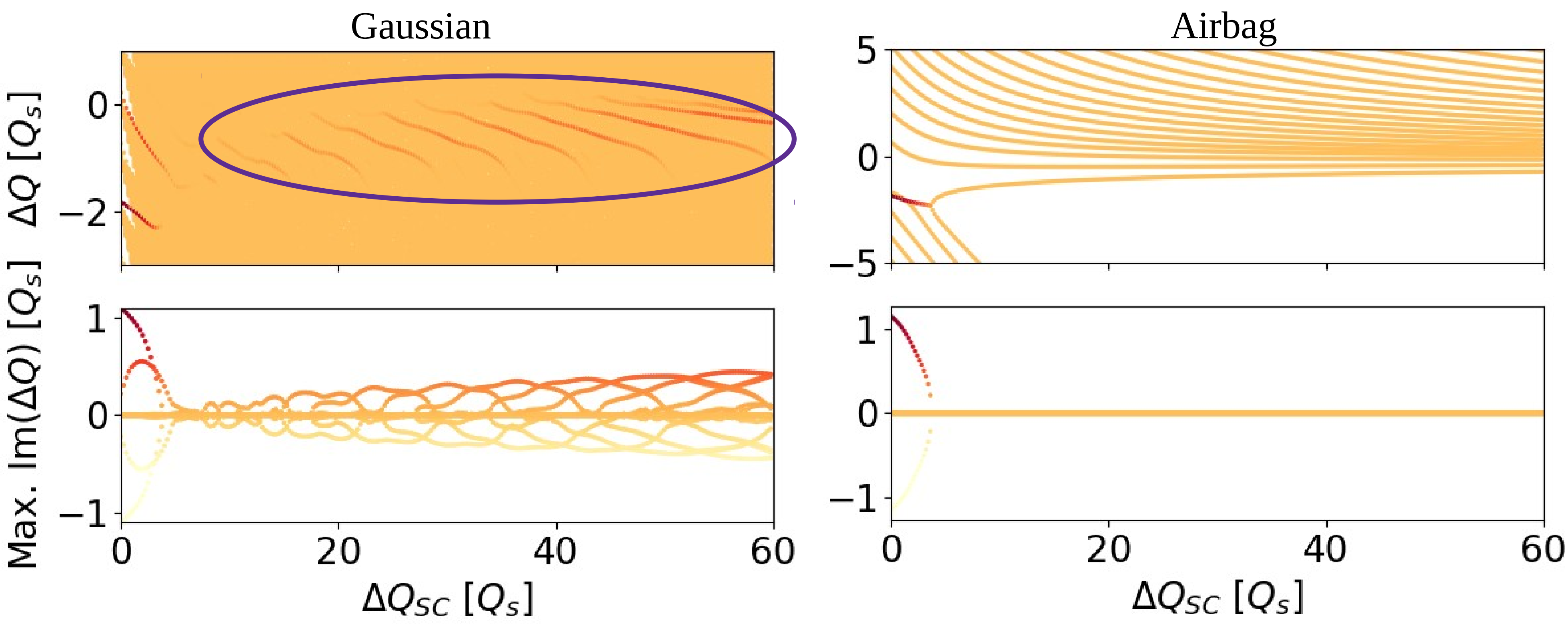

- Space-charge lifts the degeneracy of the head-tail modes, leading to a forest of head-tail mode
- The original TMCI is still lifted, as predicted by the airbag model
- Positive head-tail modes lead a succession of mode coupling instabilities that are not predicted by Airbag model

TMCI with space-charge

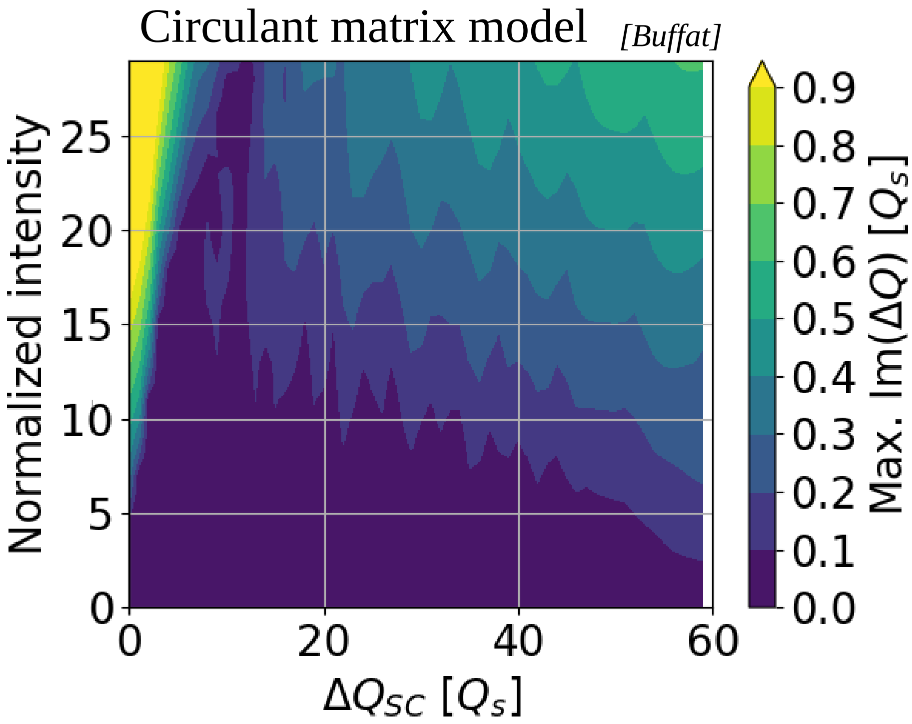

TMCI with space-charge

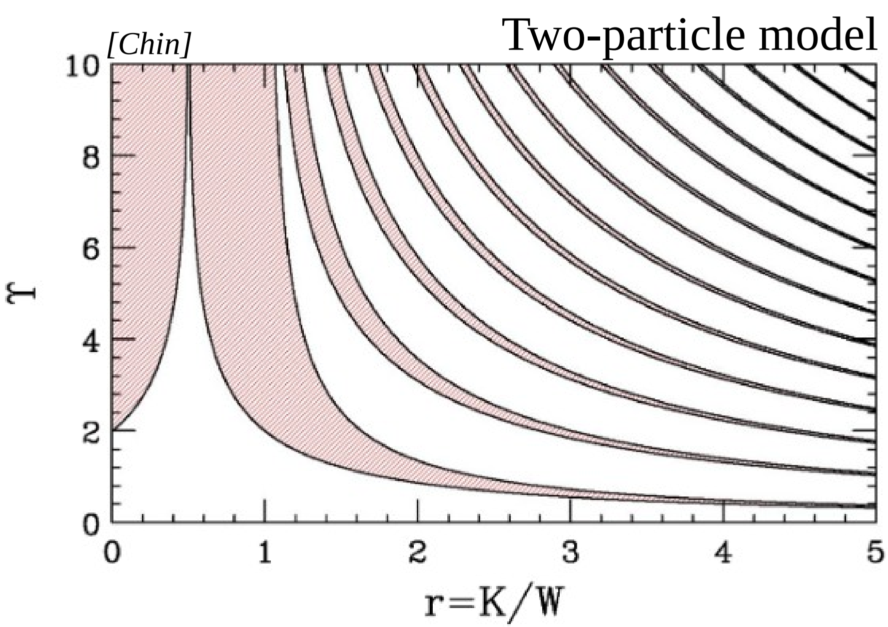

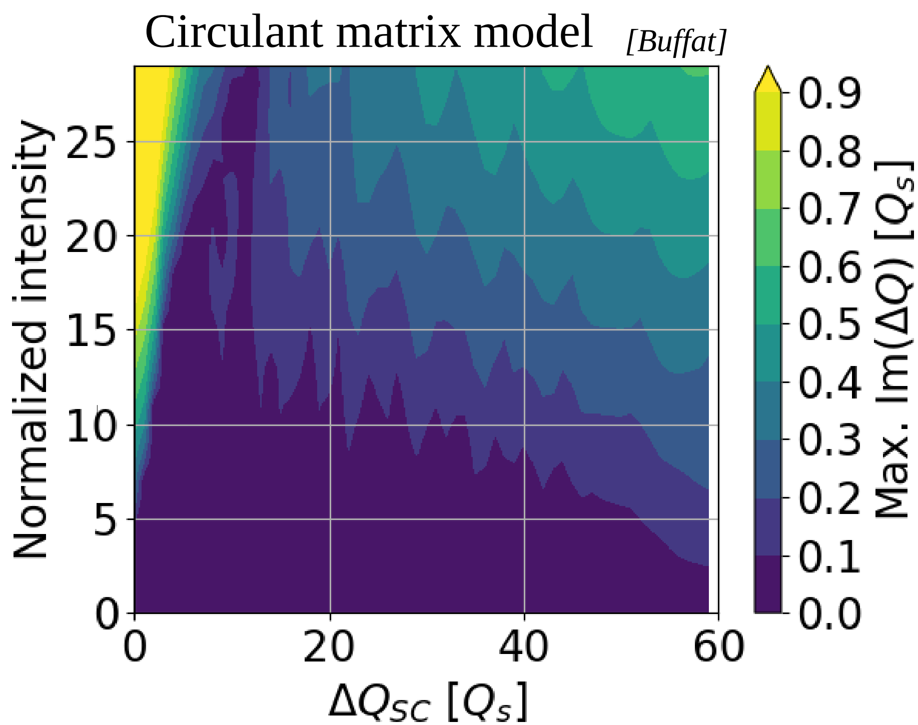

[Chin] Y. H. Chin, A. W. Chao, and M. Blaskiewicz, Phys. Rev. Accel. Beams 19, 014201 (2016)
[Buffat] X. Buffat, et al. Phys. Rev. Accel. Beams 24, 060101 (2021)

TMCI with space-charge

Weak space-charge
→ ‘original’ TMCI

[Chin] Two-particle model

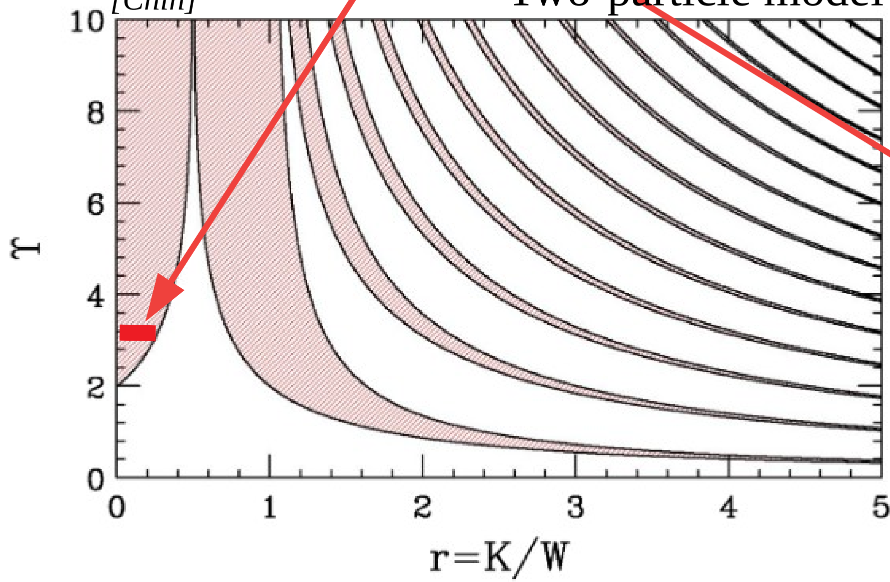

Circulant matrix model *[Buffat]*

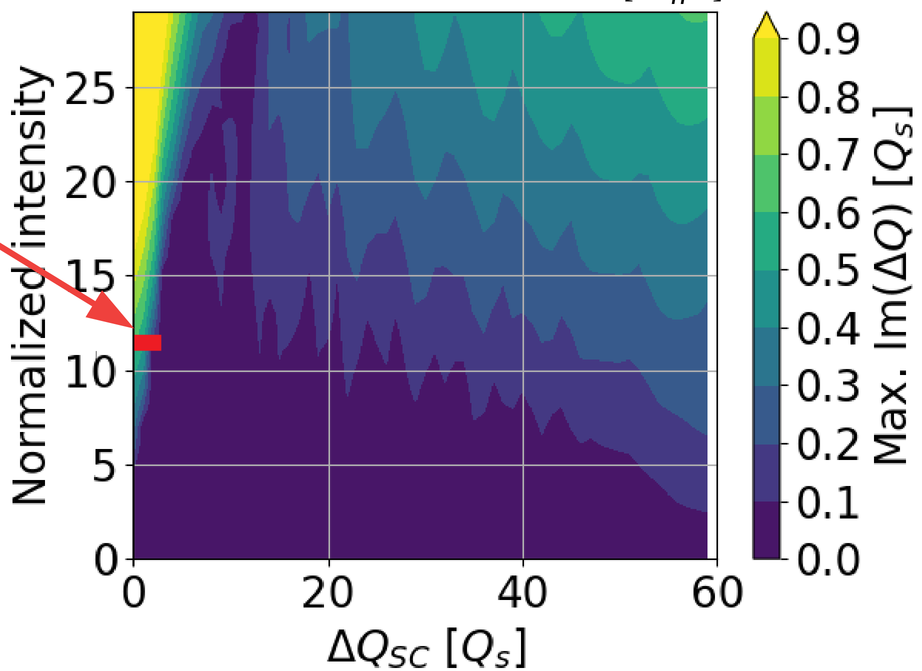

[Chin] Y. H. Chin, A. W. Chao, and M. Blaskiewicz, Phys. Rev. Accel. Beams 19, 014201 (2016)
[Buffat] X. Buffat, et al. Phys. Rev. Accel. Beams 24, 060101 (2021)

TMCI with space-charge

Weak space-charge
→ ‘original’ TMCI

Intermediate space-charge
→ stable

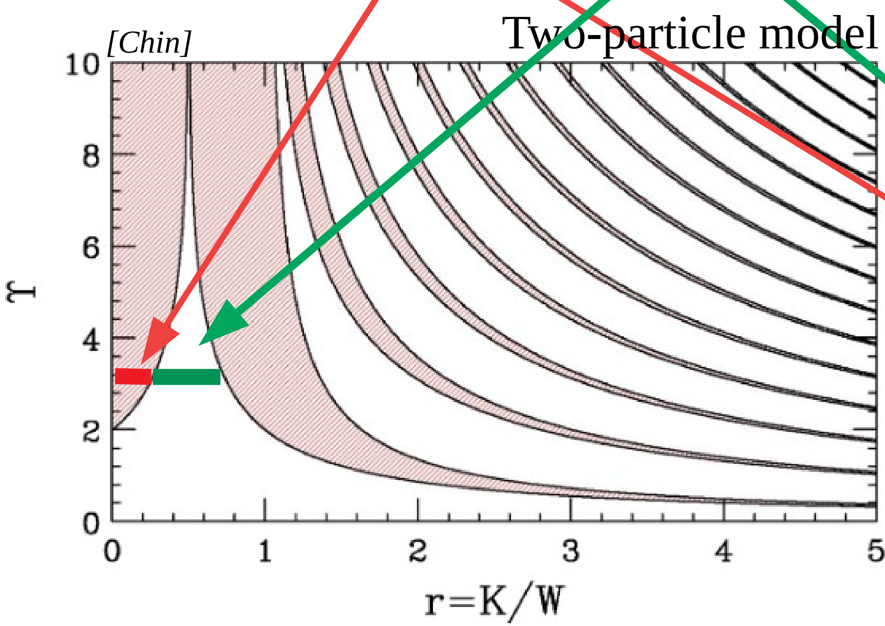

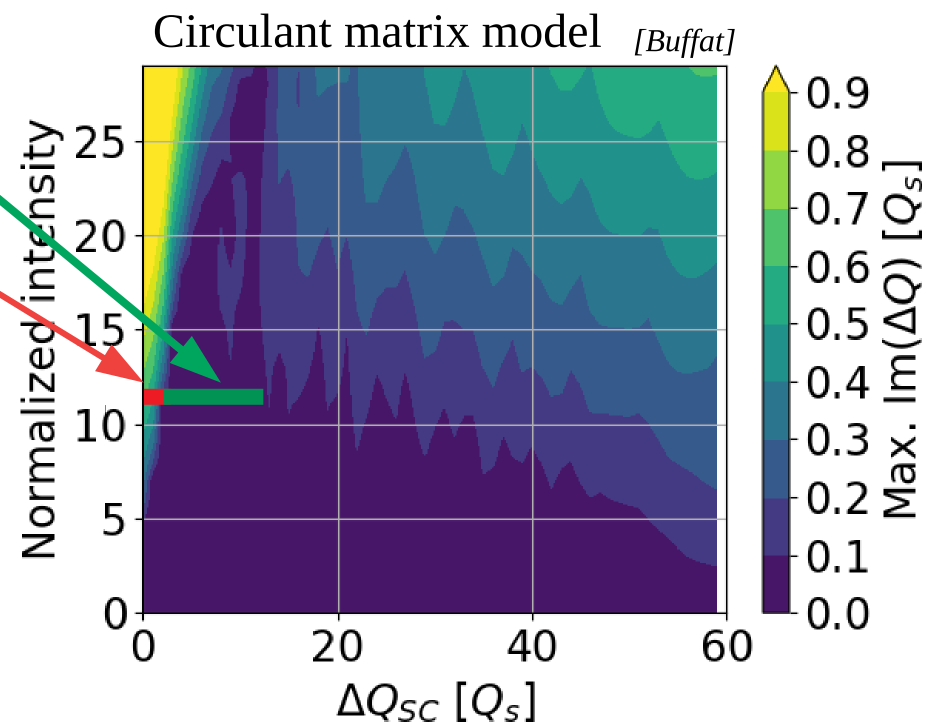

[Chin] Y. H. Chin, A. W. Chao, and M. Blaskiewicz, Phys. Rev. Accel. Beams 19, 014201 (2016)
[Buffat] X. Buffat, et al. Phys. Rev. Accel. Beams 24, 060101 (2021)

TMCI with space-charge

Weak space-charge
→ 'original' TMCI

Intermediate space-charge
→ stable

Strong space-charge
→ Coupling / decoupling of Positive head-tail modes

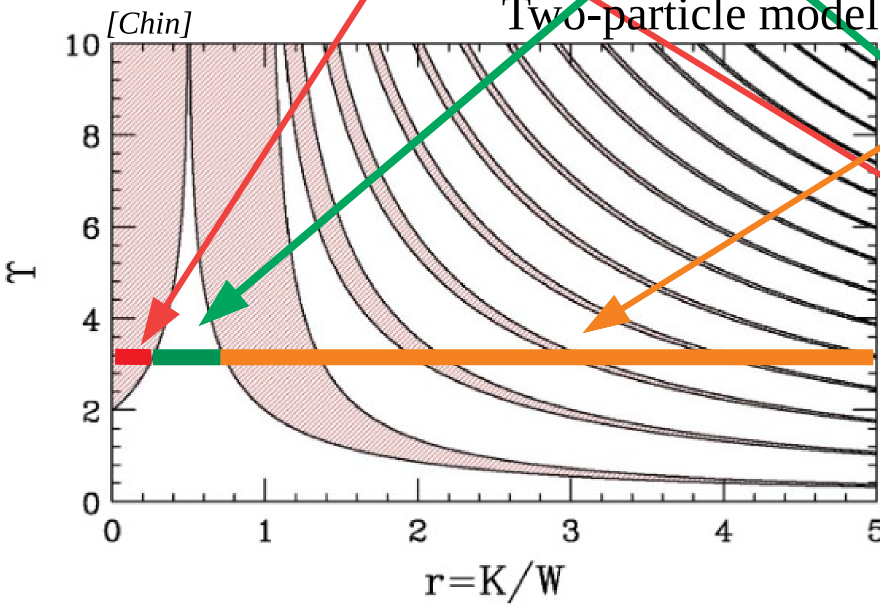

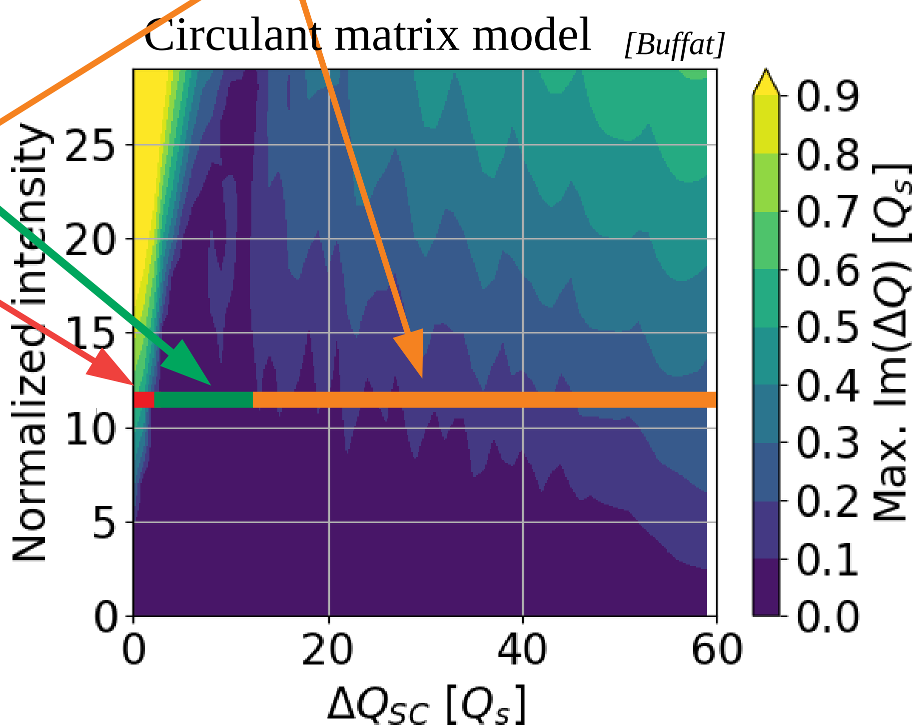

[Chin] Y. H. Chin, A. W. Chao, and M. Blaskiewicz, Phys. Rev. Accel. Beams 19, 014201 (2016)
[Buffat] X. Buffat, et al. Phys. Rev. Accel. Beams 24, 060101 (2021)

TMCI with space-charge

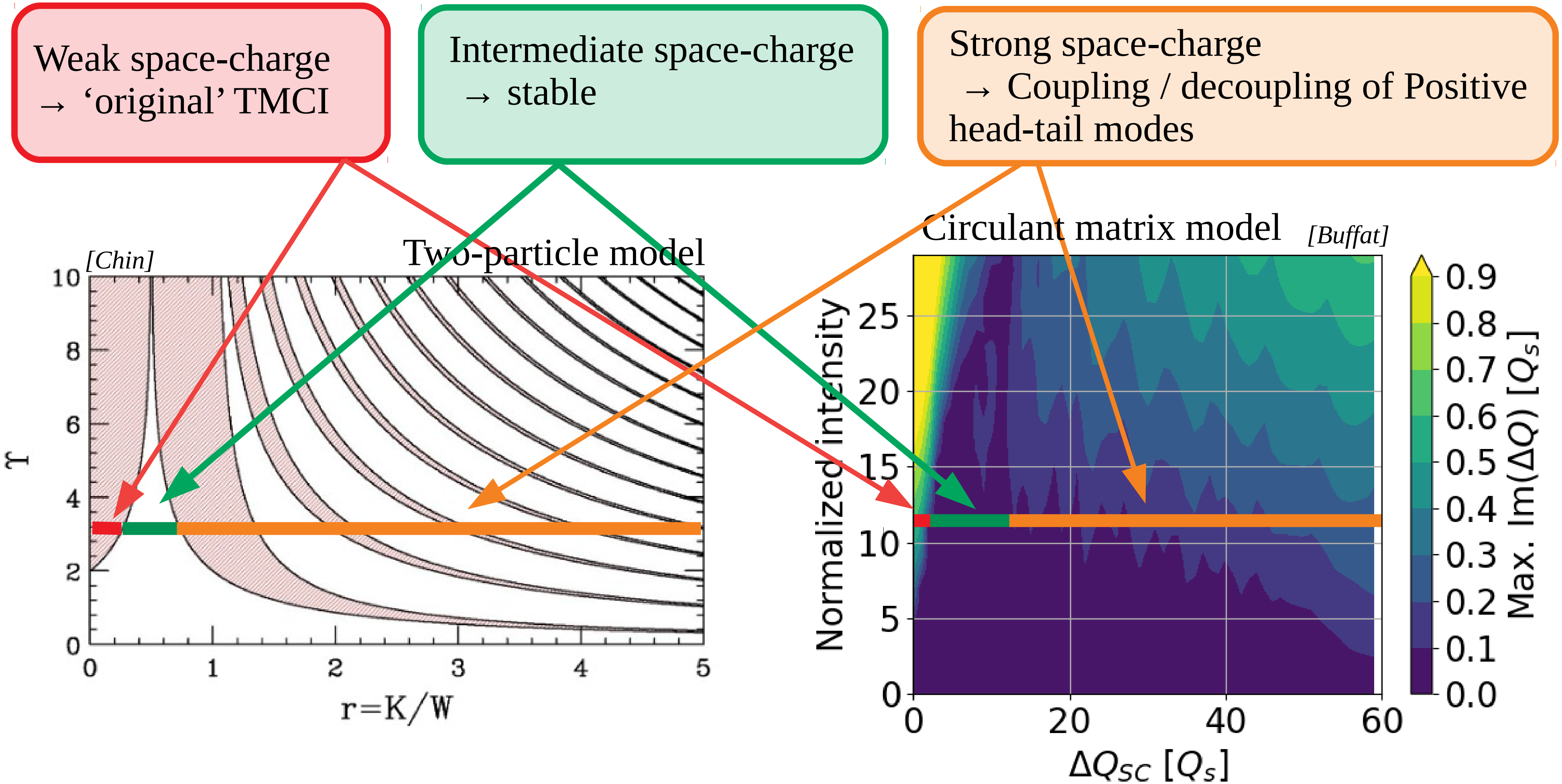

- The weak-space charge regime cannot easily be tested experimentally at the SPS (Intensities / longitudinal emittances beyond the TMCI necessarily imply strong space-charge)

[Chin] Y. H. Chin, A. W. Chao, and M. Blaskiewicz, Phys. Rev. Accel. Beams 19, 014201 (2016)
[Buffat] X. Buffat, et al. Phys. Rev. Accel. Beams 24, 060101 (2021)

TMCI with space-charge

Weak space-charge
→ ‘original’ TMCI

Intermediate space-charge
→ stable

Strong space-charge
→ Coupling / decoupling of Positive head-tail modes

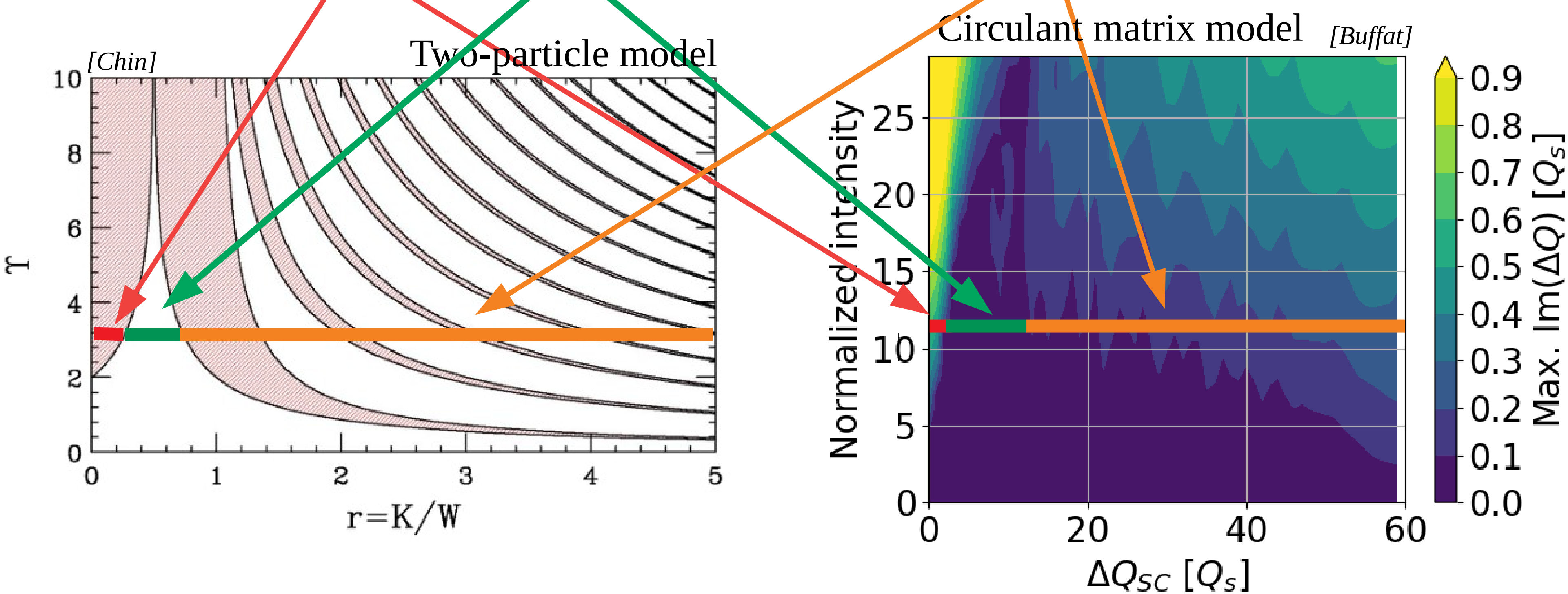

- The weak-space charge regime cannot easily be tested experimentally at the SPS (Intensities / longitudinal emittances beyond the TMCI necessarily imply strong space-charge)

→ We aim at probing the stability threshold in the strong space-charge regime

[Chin] Y. H. Chin, A. W. Chao, and M. Blaskiewicz, Phys. Rev. Accel. Beams 19, 014201 (2016)
[Buffat] X. Buffat, et al. Phys. Rev. Accel. Beams 24, 060101 (2021)

Tracking simulation setup

- Element-by-element tracking through the lattice (sixtracklib) including self-consistent space-charge kicks (PyPIC) and wake-fields (PyHEADTAIL)

Machine / beam parameter	
Energy [GeV]	26
Bunch intensity [10^{11} p/b]	1.5 to 2.4
Norm. trans. Emit [mum]	0.5 to 6
Long. emit. [eVs]	0.25 to 0.4
H/V tune	26.15 /26.22
H/V Chromaticity	3.0/2.0
H/V 2nd order chroma. [10^2]	2.8/1.2
H/V 3nd order chroma. [10^5]	-5.0/3.2
Synchrotron tune [10^{-3}]	4.2
RF 200 MHz	1 MV
RF 800 MHz	0.1 MV
Flat bottom length [turn]	130000
Optics	Q26

Simulation parameter	
Number of macroparticles	10^6
Number of space-charge kicks	540
Field solver	GPUFFTPoissonSolver_2_5D from PyPIC
Field solver grid size	128x128
Number of slices for space-charge	50
Longitudinal cut	$\pm 3\sigma_z$
Dipole errors	b3, b5, b7
Wake model	Complete, 2018
Number of slices for wakes	500

Tracking simulation setup

- Element-by-element tracking through the lattice (sixtracklib) including self-consistent space-charge kicks (PyPIC) and wake-fields (PyHEADTAIL)

Machine / beam parameter	
Energy [GeV]	26
Bunch intensity [10^{11} p/b]	1.5 to 2.4
Norm. trans. Emit [mum]	0.5 to 6
Long. emit. [eVs]	0.25 to 0.4
H/V tune	26.15 /26.22
H/V Chromaticity	3.0/2.0
H/V 2nd order chroma. [10^2]	2.8/1.2
H/V 3nd order chroma. [10^5]	-5.0/3.2
Synchrotron tune [10^{-3}]	4.2
RF 200 MHz	1 MV
RF 800 MHz	0.1 MV
Flat bottom length [turn]	130000
Optics	Q26

Simulation parameter	
Number of macroparticles	10^6
Number of space-charge kicks	540
Field solver	GPUFFTPoissonSolver_2_5D from PyPIC
Field solver grid size	128x128
Number of slices for space-charge	50
Longitudinal cut	$\pm 3\sigma_z$
Dipole errors	b3, b5, b7
Wake model	Complete, 2018
Number of slices for wakes	500

Tracking simulation setup

- Element-by-element tracking through the lattice (sixtracklib) including self-consistent space-charge kicks (PyPIC) and wake-fields (PyHEADTAIL)

Machine / beam parameter	
Energy [GeV]	26
Bunch intensity [10^{11} p/b]	1.5 to 2.4
Norm. trans. Emit [mum]	0.5 to 6
Long. emit. [eVs]	0.25 to 0.4
H/V tune	26.13 /26.22
H/V Chromaticity	3.0/2.0
H/V 2nd order chroma. [10^2]	2.8/1.2
H/V 3rd order chroma. [10^5]	-5.0/3.2
Synchrotron tune [10^{-3}]	4.2
RF 200 MHz	1 MV
RF 800 MHz	0.1 MV
Flat bottom length [turn]	130000
Optics	Q26

Simulation parameter	
Number of macroparticles	10^6
Number of space-charge kicks	540
Field solver	GPUFFTPoissonSolver_2_5D from PyPIC
Field solver grid size	128x128
Number of slices for space-charge	50
Longitudinal cut	$\pm 3\sigma_z$
Dipole errors	b3, b5, b7
Wake model	Complete, 2018
Number of slices for wakes	500

Tracking simulation setup

- Element-by-element tracking through the lattice (sixtracklib) including self-consistent space-charge kicks (PyPIC) and wake-fields (PyHEADTAIL)

Machine / beam parameter	
Energy [GeV]	26
Bunch intensity [10^{11} p/b]	1.5 to 2.4
Norm. trans. Emit [mum]	0.5 to 6
Long. emit. [eVs]	0.25 to 0.4
H/V tune	26.15 /26.22
H/V Chromaticity	3.0/2.0
H/V 2nd order chroma. [10^2]	2.8/1.2
H/V 3rd order chroma. [10^5]	-5.0/3.2
Synchrotron tune [10^{-3}]	4.2
RF 200 MHz	1 MV
RF 800 MHz	0.1 MV
Flat bottom length [turn]	130000
Optics	Q26

Simulation parameter	
Number of macroparticles	10^6
Number of space-charge kicks	540
Field solver	GPUFFTPoissonSolver_2_5D from PyPIC
Field solver grid size	128x128
Number of slices for space-charge	50
Longitudinal cut	$\pm 3\sigma_z$
Dipole errors	b3, b5, b7
Wake model	Complete, 2018
Number of slices for wakes	500

Tracking simulation setup

- Element-by-element tracking through the lattice (sixtracklib) including self-consistent space-charge kicks (PyPIC) and wake-fields (PyHEADTAIL)

Machine / beam parameter	
Energy [GeV]	26
Bunch intensity [10^{11} p/b]	1.5 to 2.4
Norm. trans. Emit [mum]	0.5 to 6
Long. emit. [eVs]	0.25 to 0.4
H/V tune	26.15 /26.22
H/V Chromaticity	3.0/2.0
H/V 2nd order chroma. [10^2]	2.8/1.2
H/V 3rd order chroma. [10^5]	-5.0/3.2
Synchrotron tune [10^{-3}]	4.2
RF 200 MHz	1 MV
RF 800 MHz	0.1 MV
Flat bottom length [turn]	130000
Optics	Q26

Simulation parameter	
Number of macroparticles	10^6
Number of space-charge kicks	540
Field solver	GPUFFTPoissonSolver_2_5D from PyPIC
Field solver grid size	128x128
Number of slices for space-charge	50
Longitudinal cut	$\pm 3\sigma_z$
Dipole errors	b3, b5, b7
Wake model	Complete, 2018
Number of slices for wakes	500

Tracking simulation setup

- Element-by-element tracking through the lattice (sixtracklib) including self-consistent space-charge kicks (PyPIC) and wake-fields (PyHEADTAIL)

Machine / beam parameter	
Energy [GeV]	26
Bunch intensity [10^{11} p/b]	1.5 to 2.4
Norm. trans. Emit [mum]	0.5 to 6
Long. emit. [eVs]	0.25 to 0.4
H/V tune	26.15 /26.22
H/V Chromaticity	3.0/2.0
H/V 2nd order chroma. [10^2]	2.8/1.2
H/V 3rd order chroma. [10^5]	-5.0/3.2
Synchrotron tune [10^{-3}]	4.2
RF 200 MHz	1 MV
RF 800 MHz	0.1 MV
Flat bottom length [turn]	130000
Optics	Q26

Simulation parameter	
Number of macroparticles	10^6
Number of space-charge kicks	540
Field solver	GPUFFTPoissonSolver_2_5D from PyPIC
Field solver grid size	128x128
Number of slices for space-charge	50
Longitudinal cut	$\pm 3\sigma$
Dipole errors	b3, b5, b7
Wake model	Complete, 2018
Number of slices for wakes	500

Tracking simulation setup

- Element-by-element tracking through the lattice (sixtracklib) including self-consistent space-charge kicks (PyPIC) and wake-fields (PyHEADTAIL)

→ Simulation of the full flat bottom (3.1s) takes about two weeks using a NVIDIA V100

Machine / beam parameter	
Energy [GeV]	26
Bunch intensity [10^{11} p/b]	1.5 to 2.4
Norm. trans. Emit [mum]	0.5 to 6
Long. emit. [eVs]	0.25 to 0.4
H/V tune	26.15 /26.22
H/V Chromaticity	3.0/2.0
H/V 2nd order chroma. [10^2]	2.8/1.2
H/V 3rd order chroma. [10^5]	-5.0/3.2
Synchrotron tune [10^{-3}]	4.2
RF 200 MHz	1 MV
RF 800 MHz	0.1 MV
Flat bottom length [turn]	130000
Optics	Q26

Simulation parameter	
Number of macroparticles	10^6
Number of space-charge kicks	540
Field solver	GPUFFTPoissonSolver_2_5D from PyPIC
Field solver grid size	128x128
Number of slices for space-charge	50
Longitudinal cut	$\pm 3\sigma_z$
Dipole errors	b3, b5, b7
Wake model	Complete, 2018
Number of slices for wakes	500

Tracking simulation output

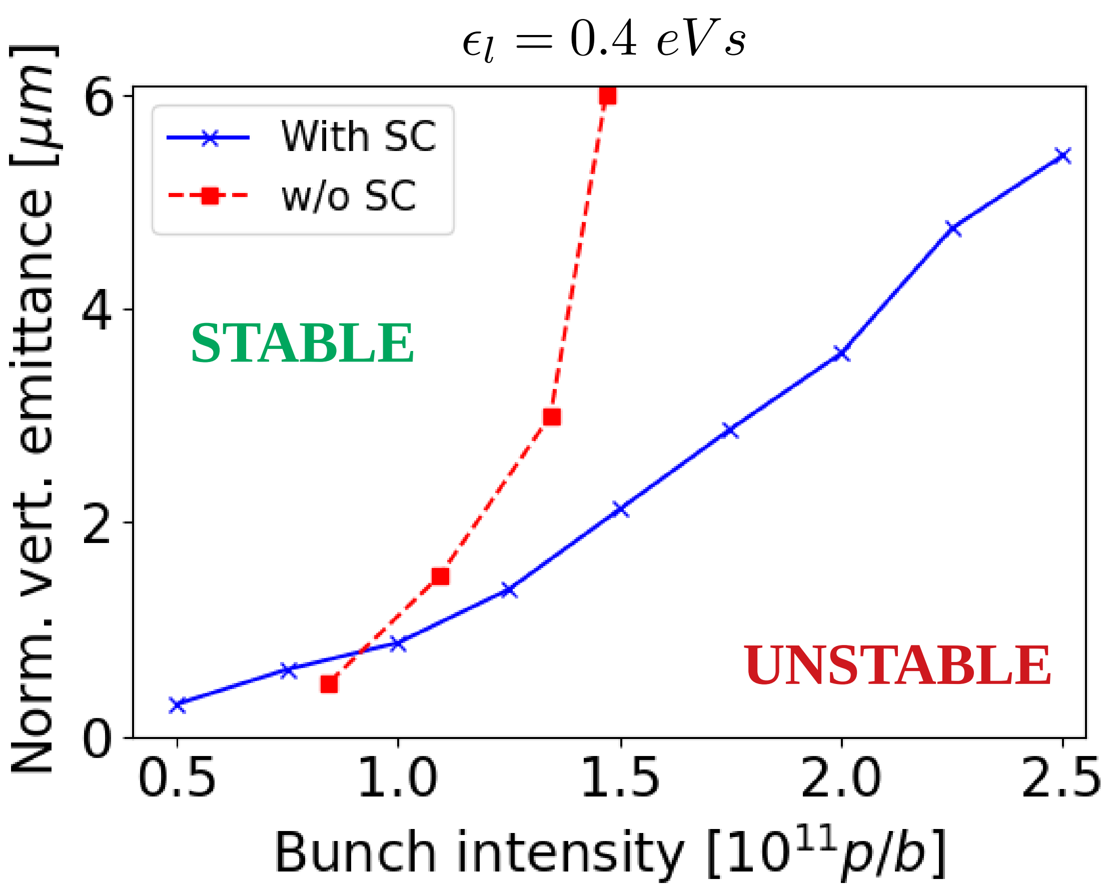

- With fixed intensity and longitudinal emittance, the strength of the wake fields is constant. The transverse emittance is used to vary the strength of space-charge
  - The transverse emittance also impacts the tune spread driven by the lattice non-linearity

Instability threshold

- The bunch intensity was varied at fixed longitudinal and transverse emittance using the H- injection into the PS Booster.
- The transverse emittances were varied using a tune bump towards the integer tune at the PS

- Each cycle is characterised by the corresponding intensity transmission, given that instabilities lead to significant beam losses
- The stability threshold is in good agreement with simulations

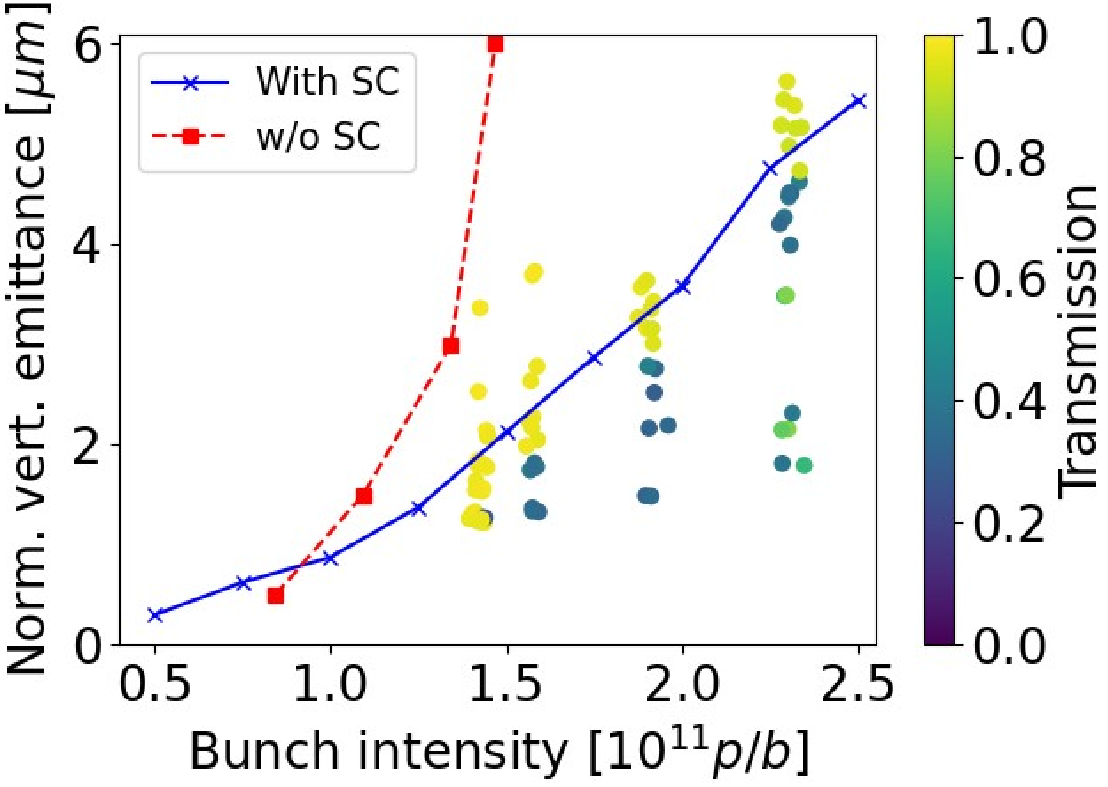

Instability threshold

- The bunch intensity was varied at fixed longitudinal and transverse emittance using the H- injection into the PS Booster.
- The transverse emittances were varied using a tune bump towards the integer tune at the PS

$$\Delta Q_{SC,y} \approx -0.12 \approx 30[Q_s]$$

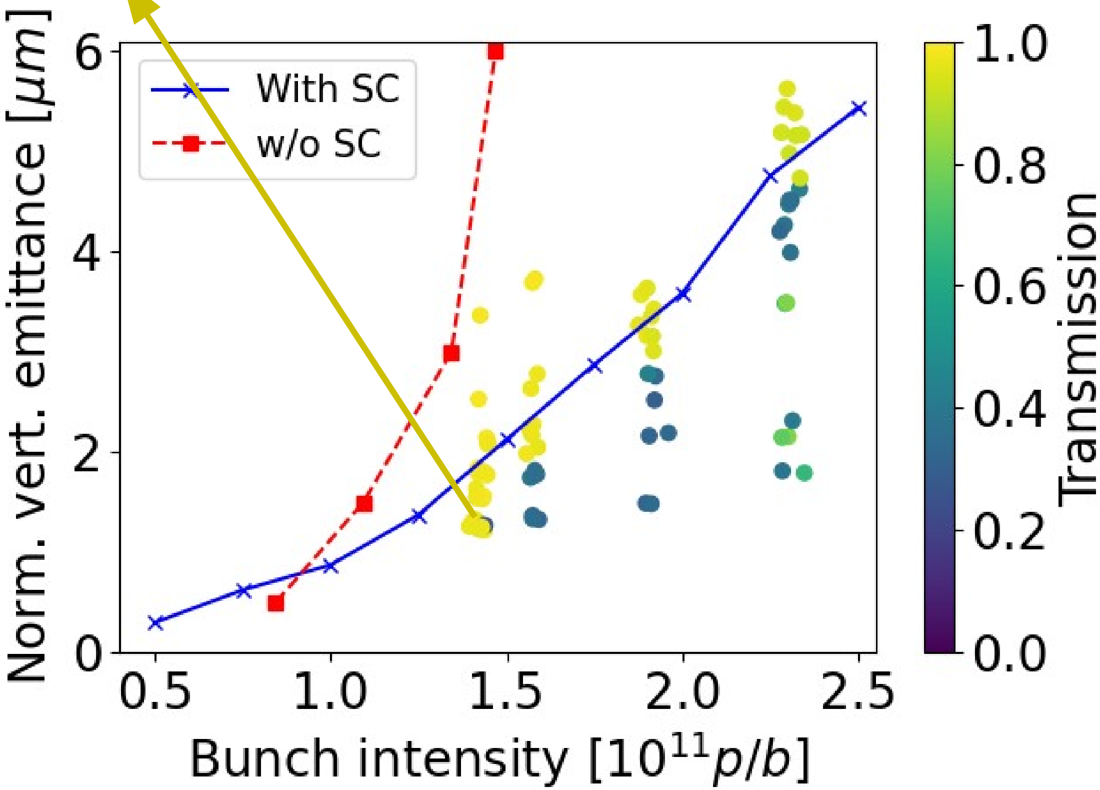

- Each cycle is characterised by the corresponding intensity transmission, given that instabilities lead to significant beam losses
- The stability threshold is in good agreement with simulations

Instability threshold

- The bunch intensity was varied at fixed longitudinal and transverse emittance using the H- injection into the PS Booster.
- The transverse emittances were varied using a tune bump towards the integer tune at the PS

$$\Delta Q_{SC,y} \approx -0.12 \approx 30[Q_s]$$

$$\Delta Q_{SC,y} \approx -0.07 \approx 17[Q_s]$$

- Each cycle is characterised by the corresponding intensity transmission, given that instabilities lead to significant beam losses
- The stability threshold is in good agreement with simulations

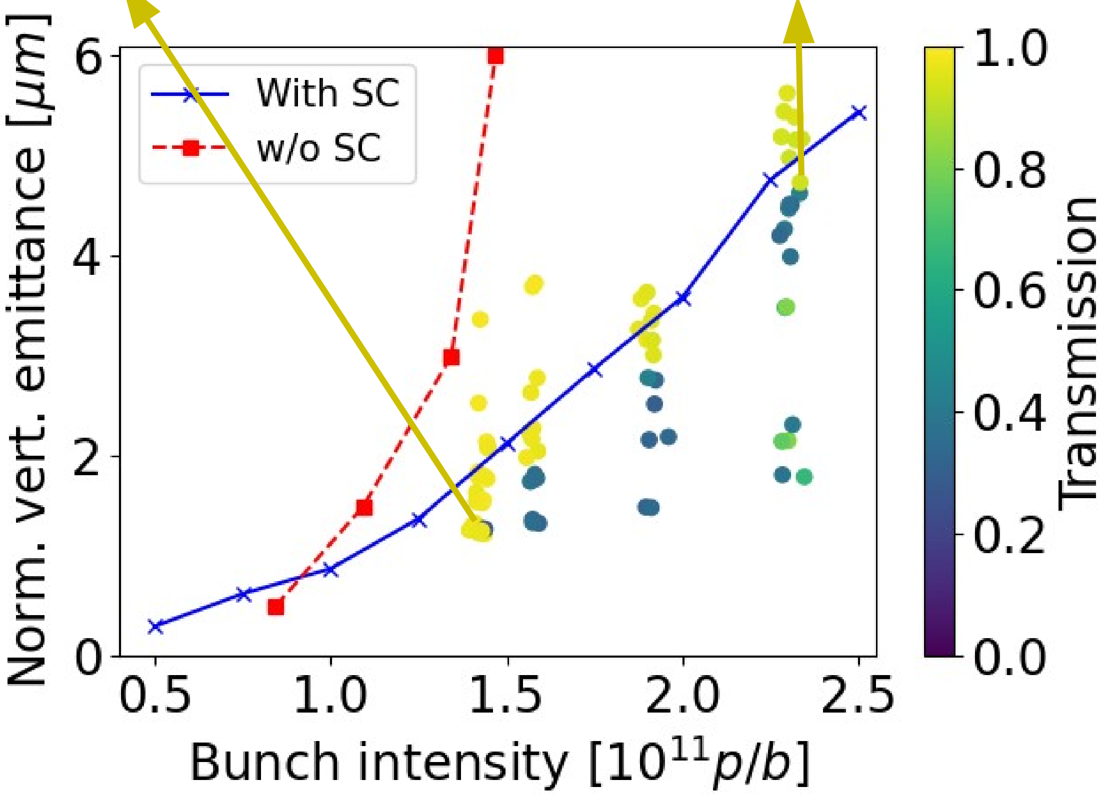

Instability threshold

- The bunch intensity was varied at fixed longitudinal and transverse emittance using the H- injection into the PS Booster.
- The transverse emittances were varied using a tune bump towards the integer tune at the PS

$$\Delta Q_{SC,y} \approx -0.12 \approx 30[Q_s]$$

$$\Delta Q_{SC,y} \approx -0.07 \approx 17[Q_s]$$

- Each cycle is characterised by the corresponding intensity transmission, given that instabilities lead to significant beam losses
- The stability threshold is in good agreement with simulations

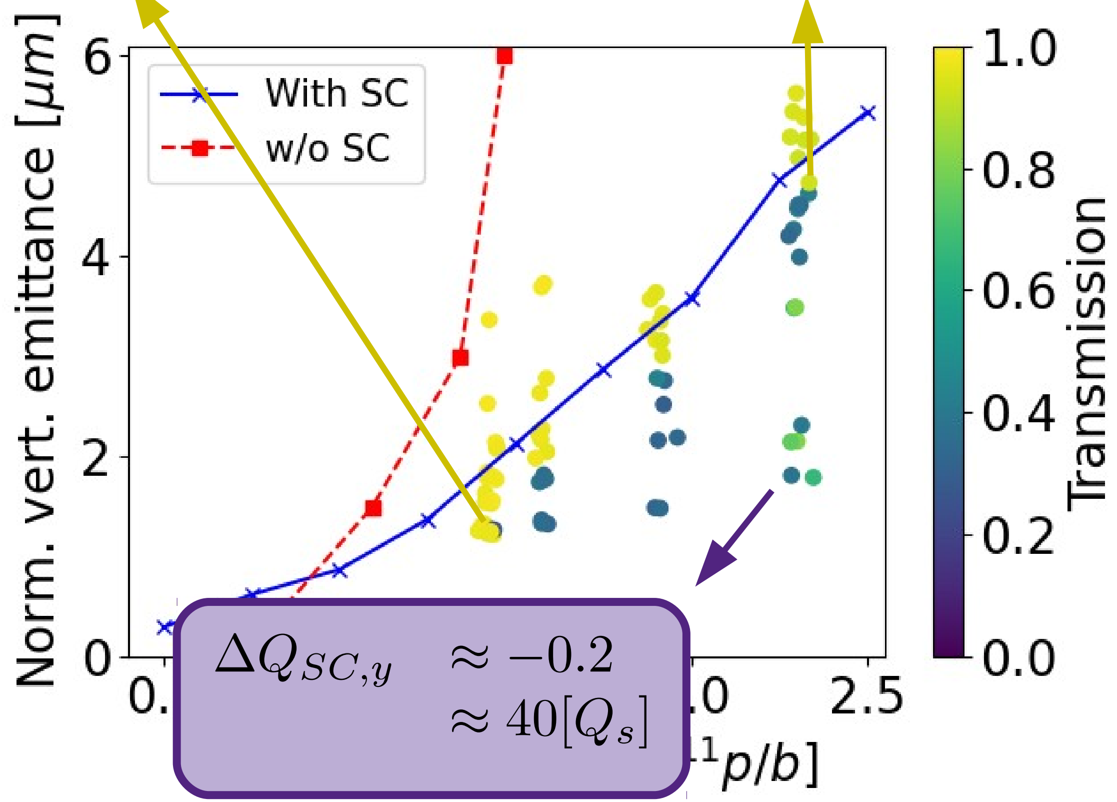

$$\Delta Q_{SC,y} \approx -0.2 \approx 40[Q_s]$$

Complex tune shift

- The tune shift of the instability mostly depends on the intensity

  → Consistently with the predicted coupling/decoupling of positive headtail modes just above mode 0 tune (unperturbed by space-charge, but shifted down by the impedance)

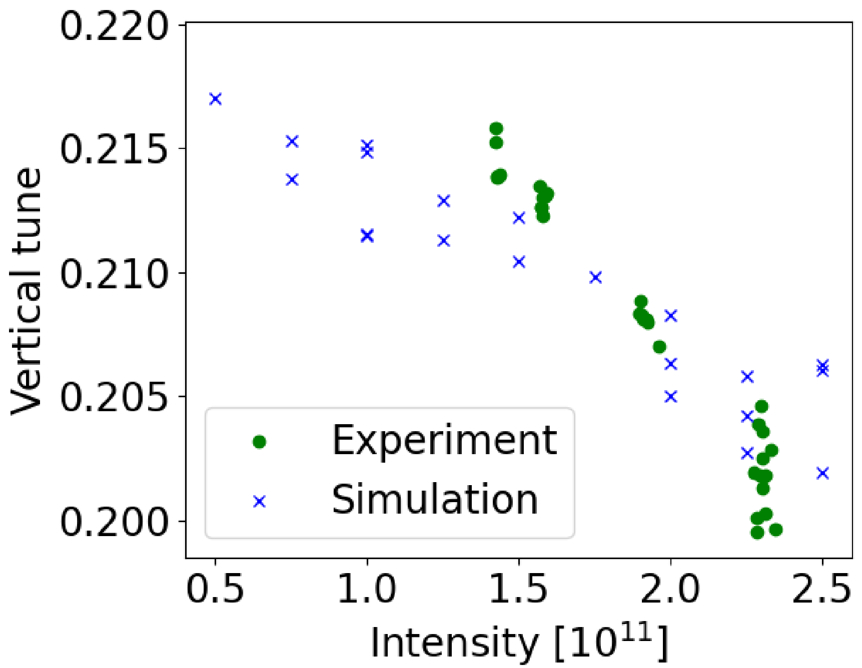

- The tune shift of the instability mostly depends on the intensity

  → Consistently with the predicted coupling/decoupling of positive headtail modes just above mode 0 tune (unperturbed by space-charge, but shifted down by the impedance)

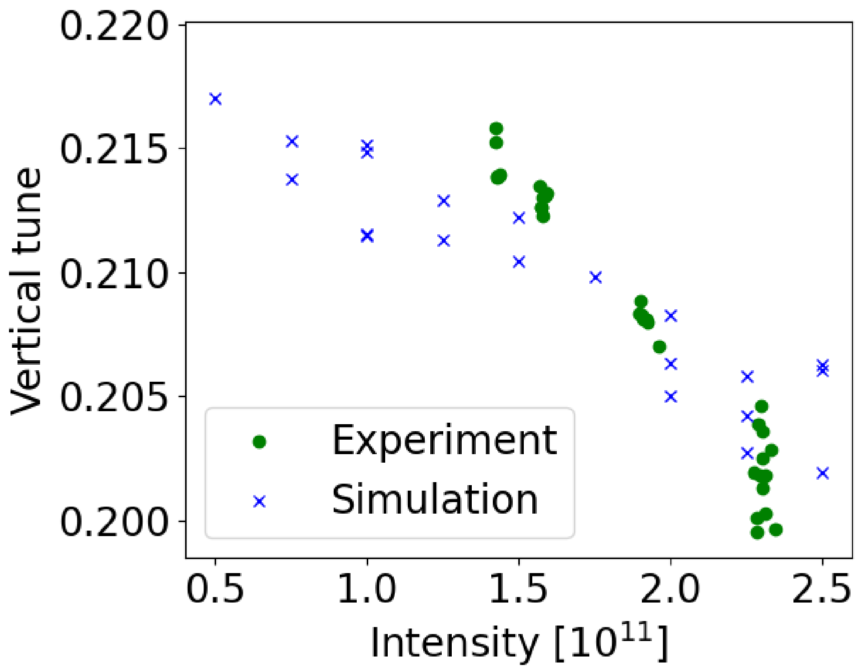

- The instability growth rate match the simulated ones

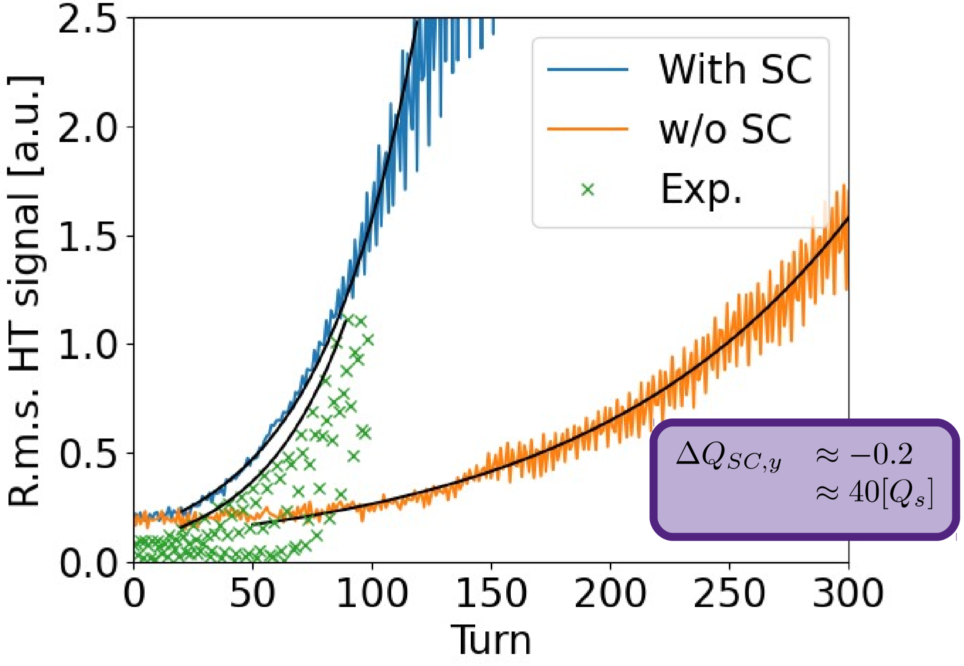

Head-tail motion

- Simulations with and without space-charge show a shift of the head-tail motion towards the tail of the bunch caused by space-charge

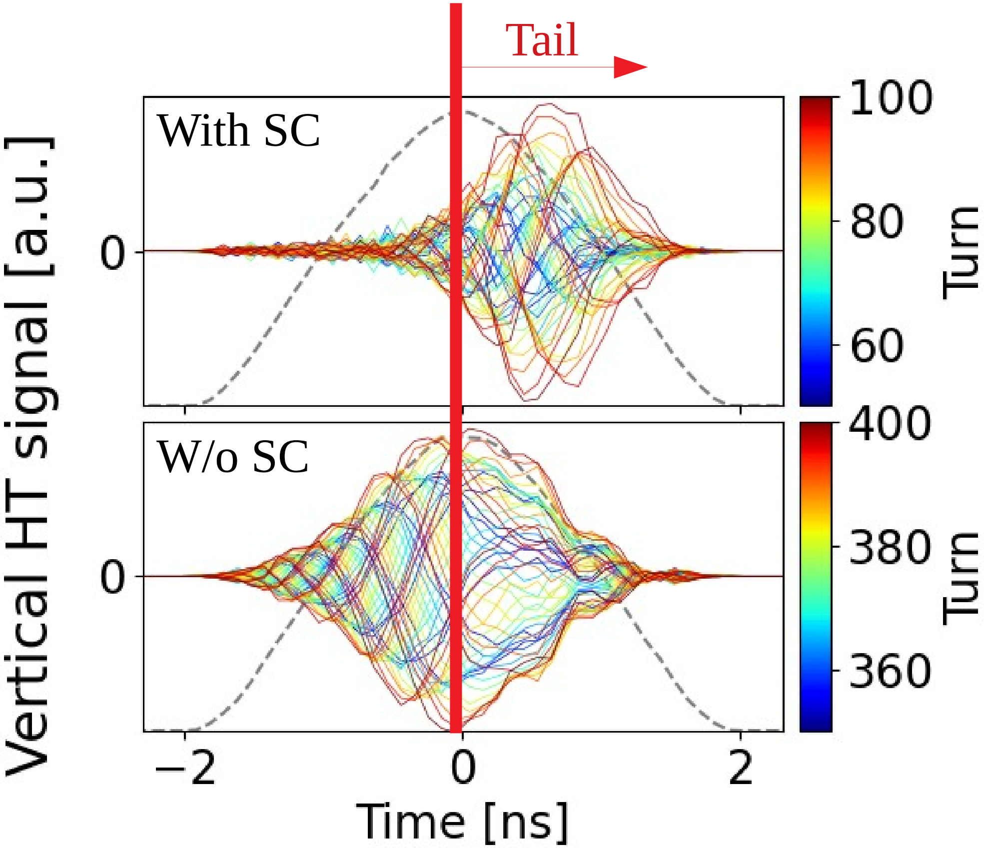

Head-tail motion

- Simulations with and without space-charge show a shift of the head-tail motion towards the tail of the bunch caused by space-charge

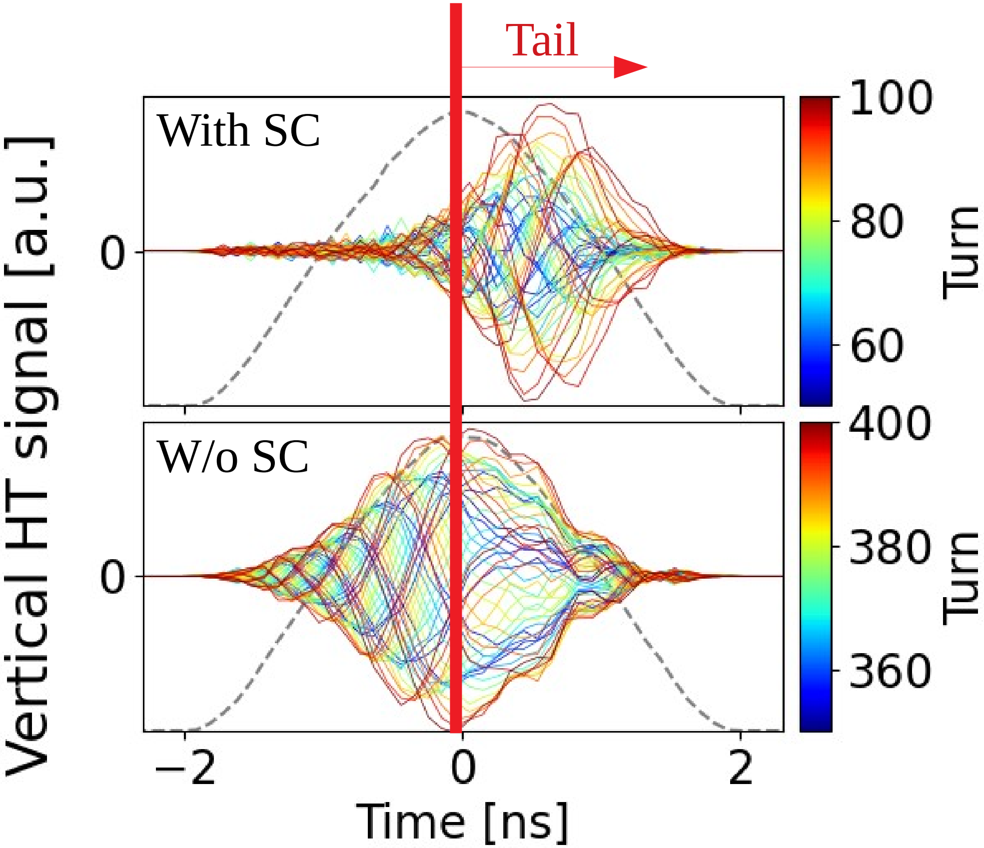

- Experimental data obtain with a wideband pickup exhibit the same behaviour

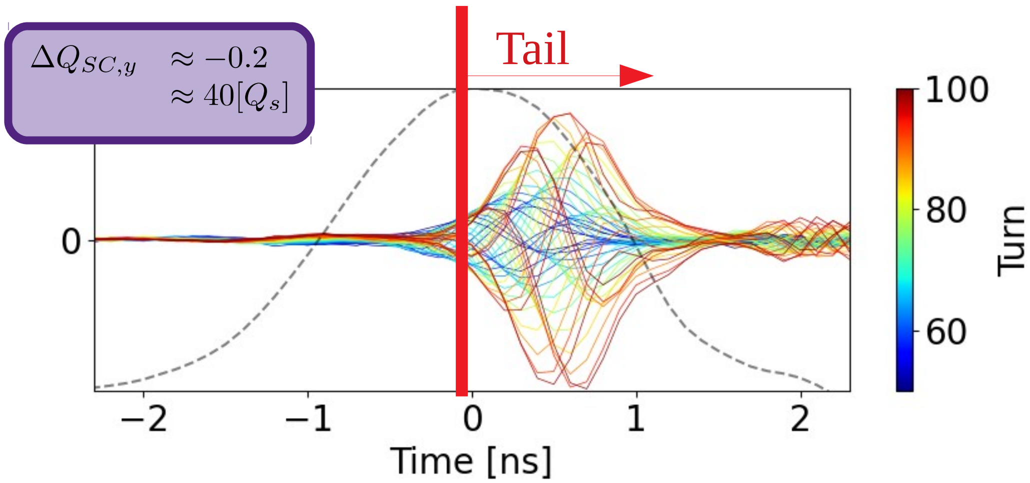

Head-tail motion

- Simulations with and without space-charge show a shift of the head-tail motion towards the tail of the bunch caused by space-charge

- Experimental data obtain with a wideband pickup exhibit the same behaviour

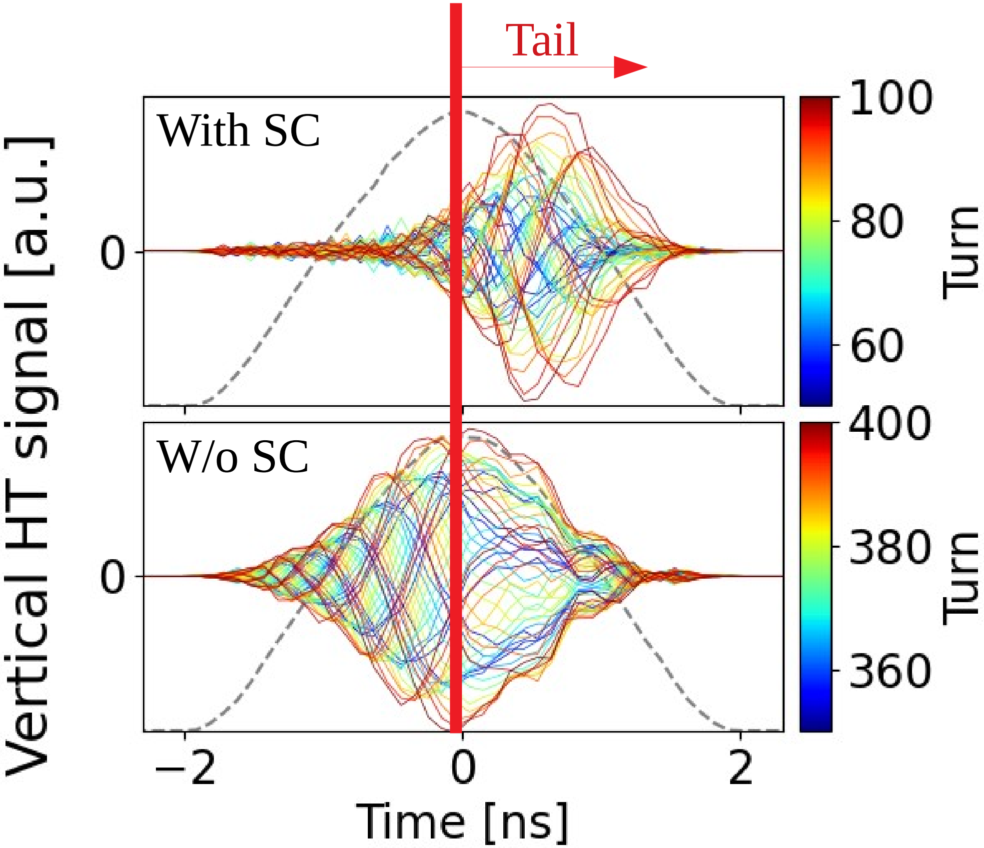

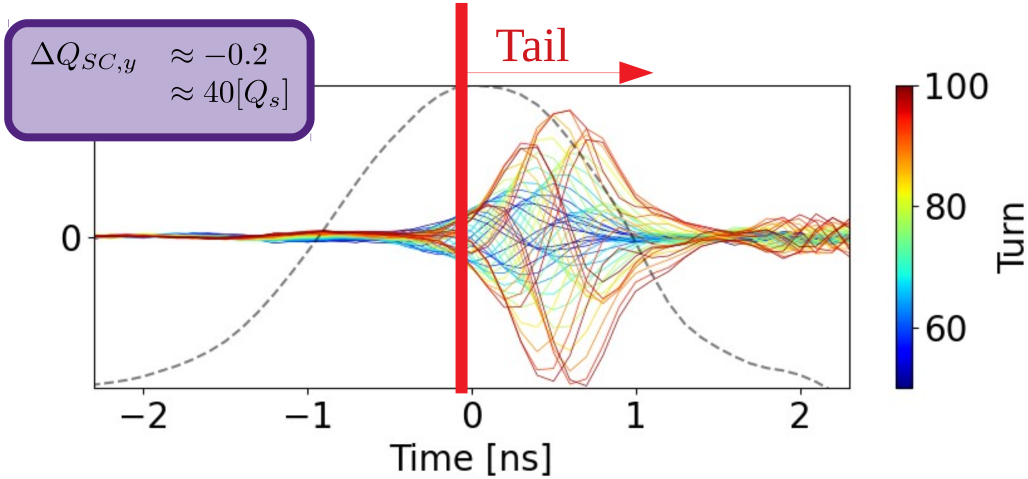

- The eigenmode corresponding to the most unstable eigenvalue obtained with the circulant matrix model features the same asymmetry

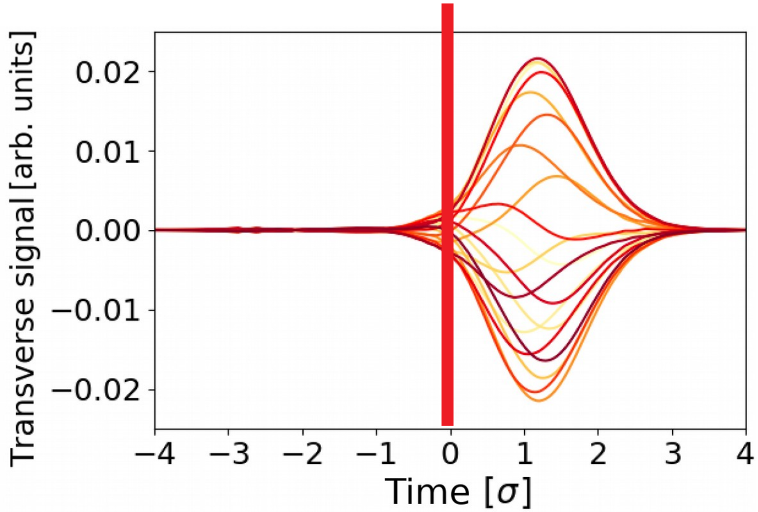

Summary slide, 5th ICFA mini-workshop on Space Charge
Theme: Bridging the gap in space charge dynamics

In 1-2 sentences, summarize the content of this presentation
(If relevant, specify type of facility, species, tune shift):

- *Single bunch instabilities with intermediate to strong space-charge (ΔQ_{SC} ~ 10 to 40 [Q_s]) at the CERN SPS are characterised experimentally.*
- *A good agreement was found with self-consistent space-charge simulations in terms of instability threshold with intensity and emittance, complex tune shift and head-tail signal.*
- *The existence of an instability threshold at lower bunch intensity for stronger space-charge is compatible with a regime of coupling/decoupling of positive head-tail modes predicted by the circulant matrix model for a Gaussian distribution including radial modes.*

[Alexahin] Y. Alexahin, in Proceedings of the ICFA Mini-workshop on Mitigation of Coherent instabilities in particle accelerators MCBI2019 (Zermatt, Switzerland, 2019).

Summary slide, 5th ICFA mini-workshop on Space Charge
Theme: Bridging the gap in space charge dynamics

In 1-2 sentences, summarize the content of this presentation
(If relevant, specify type of facility, species, tune shift):

- *Single bunch instabilities with intermediate to strong space-charge (ΔQ_{SC} ~ 10 to 40 [Q_s]) at the CERN SPS are characterised experimentally.*
- *A good agreement was found with self-consistent space-charge simulations in terms of instability threshold with intensity and emittance, complex tune shift and head-tail signal.*
- *The existence of an instability threshold at lower bunch intensity for stronger space-charge is compatible with a regime of coupling/decoupling of positive head-tail modes predicted by the circulant matrix model for a Gaussian distribution including radial modes.*

From your perspective, where is the gap regarding space charge effects? (understanding/control/mitigation/prediction/?)

- Accurate predictions require lengthy simulations. Analytical tools addressing Landau damping would be helpful, especially in the design of mitigation techniques.
- Experimental characterisation remains rather scarce. (Longer bunches, faster synchrotron motion, feedbacks, low space-charge regime, impact of an e-lens)

[Alexahin] Y. Alexahin, in Proceedings of the ICFA Mini-workshop on Mitigation of Coherent instabilities in particle accelerators MCBI2019 (Zermatt, Switzerland, 2019).

Summary slide, 5th ICFA mini-workshop on Space Charge
Theme: Bridging the gap in space charge dynamics

In 1-2 sentences, summarize the content of this presentation (If relevant, specify type of facility, species, tune shift):

- *Single bunch instabilities with intermediate to strong space-charge (ΔQ_{SC} ~ 10 to 40 [Q_s]) at the CERN SPS are characterised experimentally.*
- *A good agreement was found with self-consistent space-charge simulations in terms of instability threshold with intensity and emittance, complex tune shift and head-tail signal.*
- *The existence of an instability threshold at lower bunch intensity for stronger space-charge is compatible with a regime of coupling/decoupling of positive head-tail modes predicted by the circulant matrix model for a Gaussian distribution including radial modes.*

From your perspective, where is the gap regarding space charge effects? (understanding/control/mitigation/prediction/?)

- Accurate predictions require lengthy simulations. Analytical tools addressing Landau damping would be helpful, especially in the design of mitigation techniques.
- Experimental characterisation remains rather scarce. (Longer bunches, faster synchrotron motion, feedbacks, low space-charge regime, impact of an e-lens)

What is needed to bridge this gap?

- More powerful models (e.g. [Alexahin])
- Dedicated experiments

[Alexahin] Y. Alexahin, in Proceedings of the ICFA Mini-workshop on Mitigation of Coherent instabilities in particle accelerators MCBI2019 (Zermatt, Switzerland, 2019).

Self-consistent simulations vs CMM

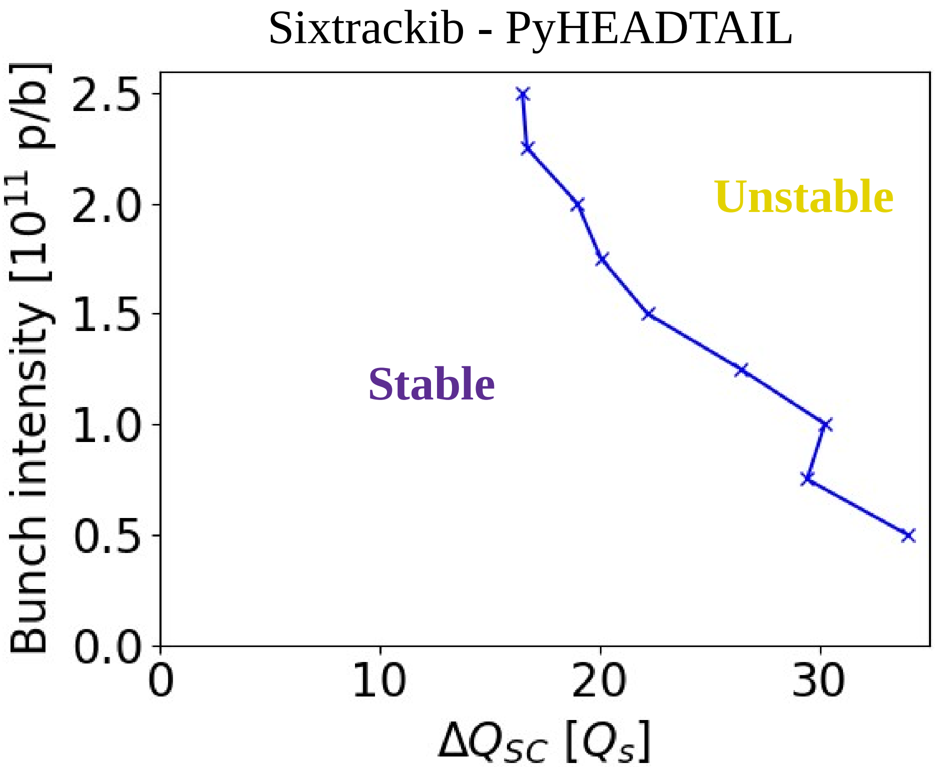

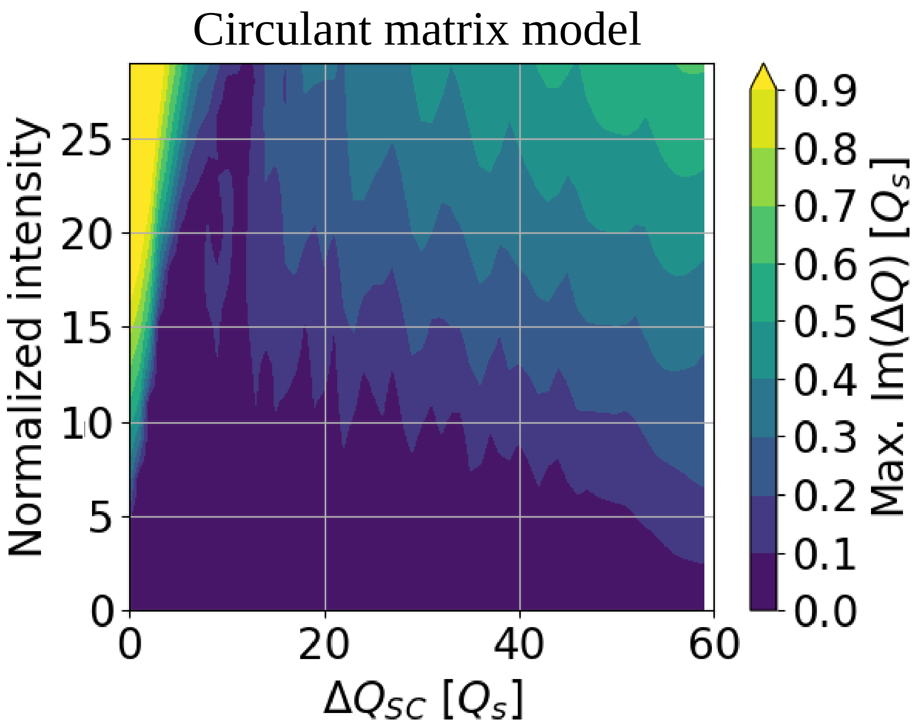

Instability threshold as a function of longitudinal emittance

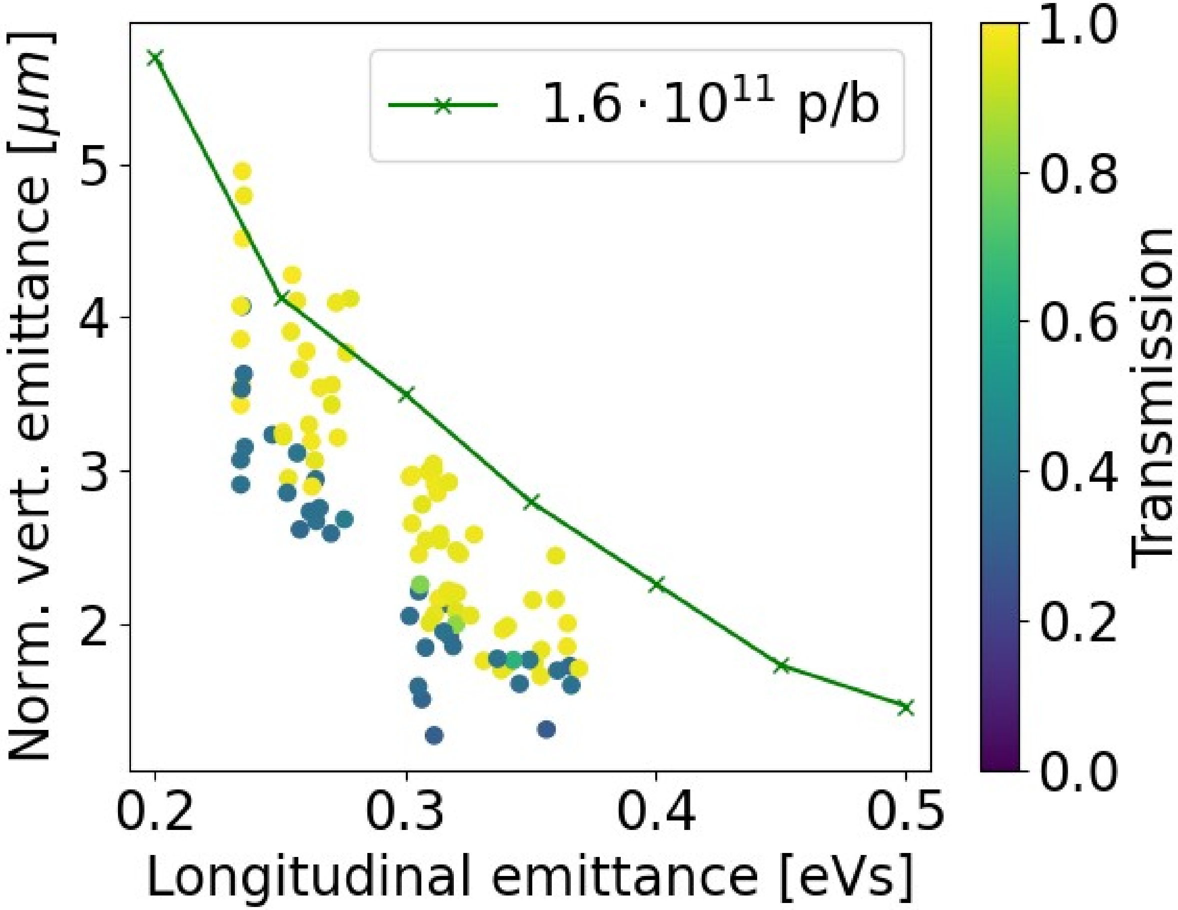

- While the behaviour of the instability threshold is consistent with simulation, the experimental data are systematically lower than the simulations
  - The measurement of the longitudinal emittance is done before the bunch rotation at extraction in the PS. Emittance growth before injection into the SPS cannot be excluded

Longitudinal emittance

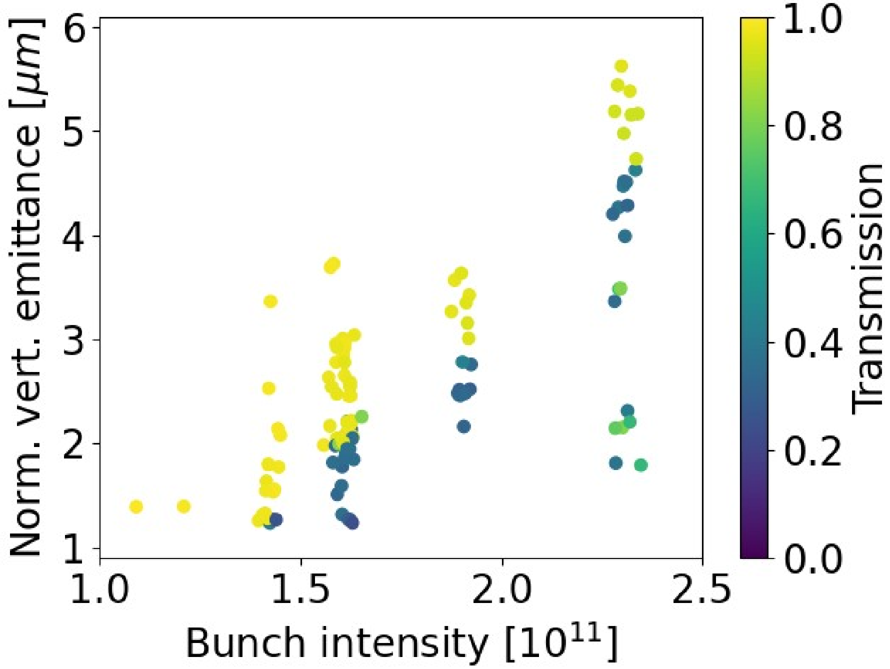

- The longitudinal emittance was kept constant at 0.3 eVs at the PS extraction

Longitudinal emittance

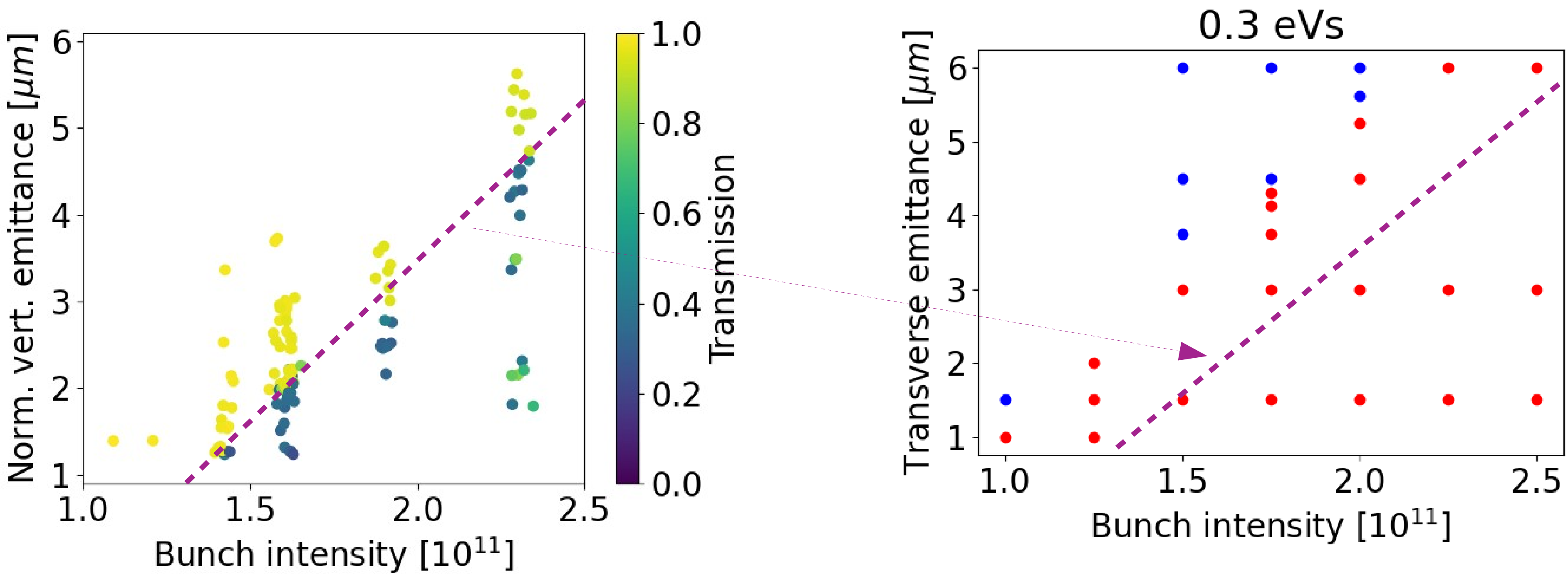

- The longitudinal emittance was kept constant at 0.3 eVs at the PS extraction
  - The corresponding matched bunch length at SPS flat bottom is 2.65 ns, yet it is measured at 3.5 ns (ABWLM) → longitudinal blowup at injection

Longitudinal emittance

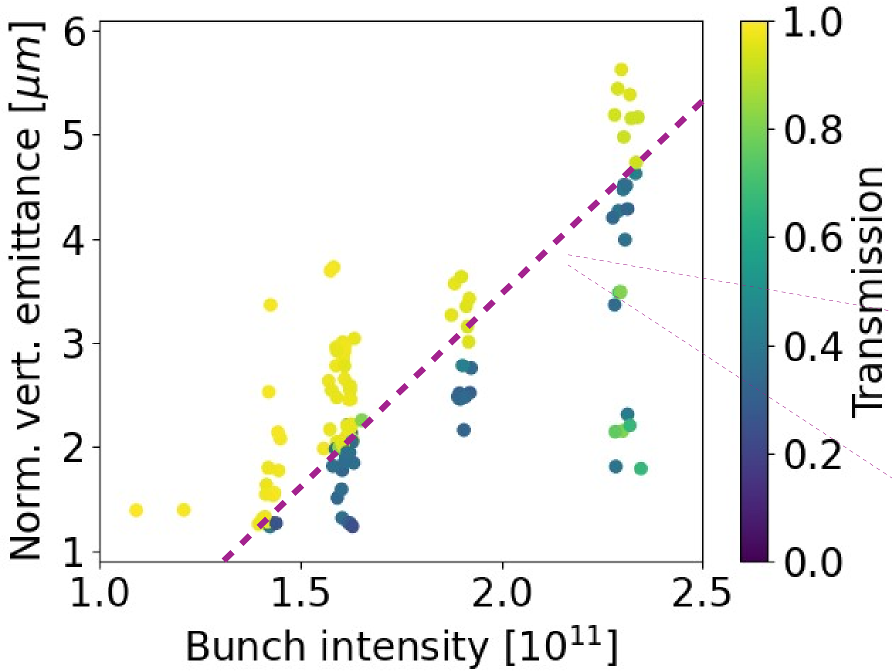

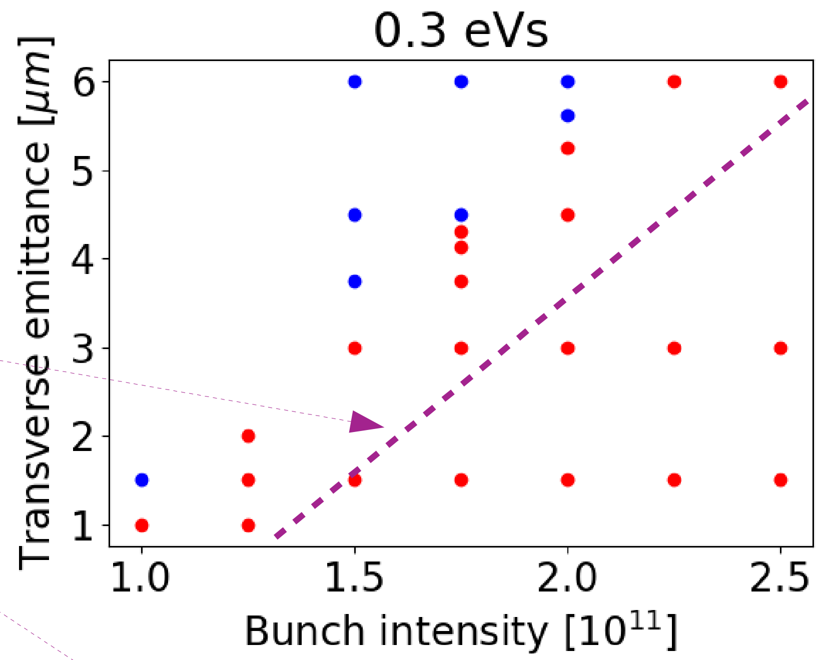

- The longitudinal emittance was kept constant at 0.3 eVs at the PS extraction
  - The corresponding matched bunch length at SPS flat bottom is 2.65 ns, yet it is measured at 3.5 ns (ABWLM) → longitudinal blowup at injection
- Simulation and data match well for 0.4 eVs (matched bunch length: 2.95 ns)

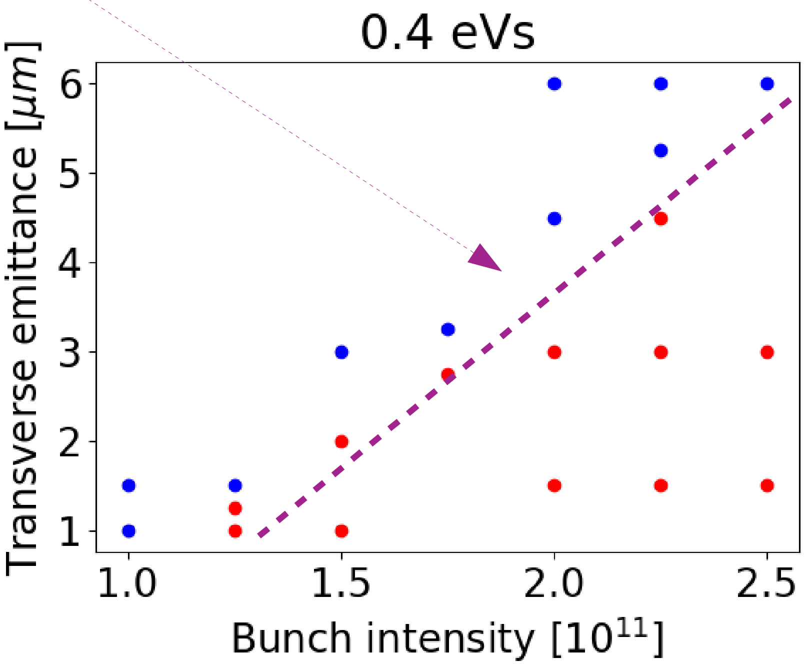

Control of intensity and longitudinal emittance at the booster

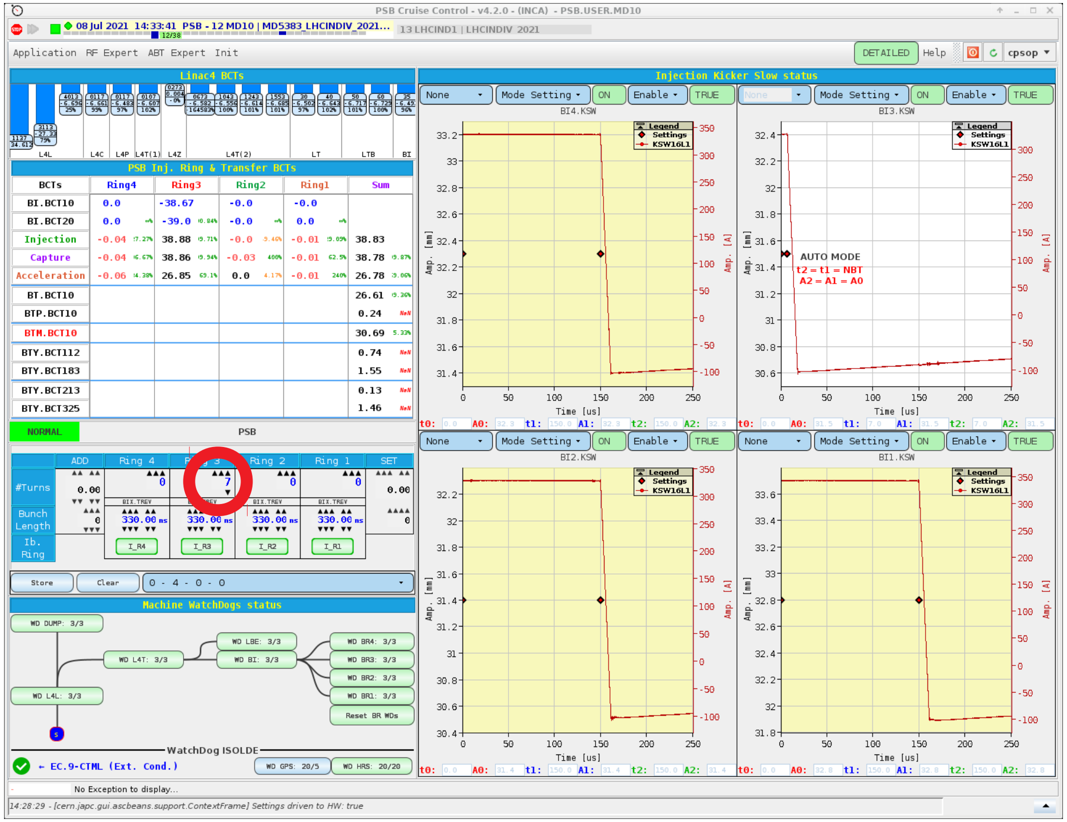

- Adjusting the number of injections into the PSB allows for a coarse control of the bunch intensity at constant longitudinal and transverse emittances

Control of intensity and longitudinal emittance at the booster

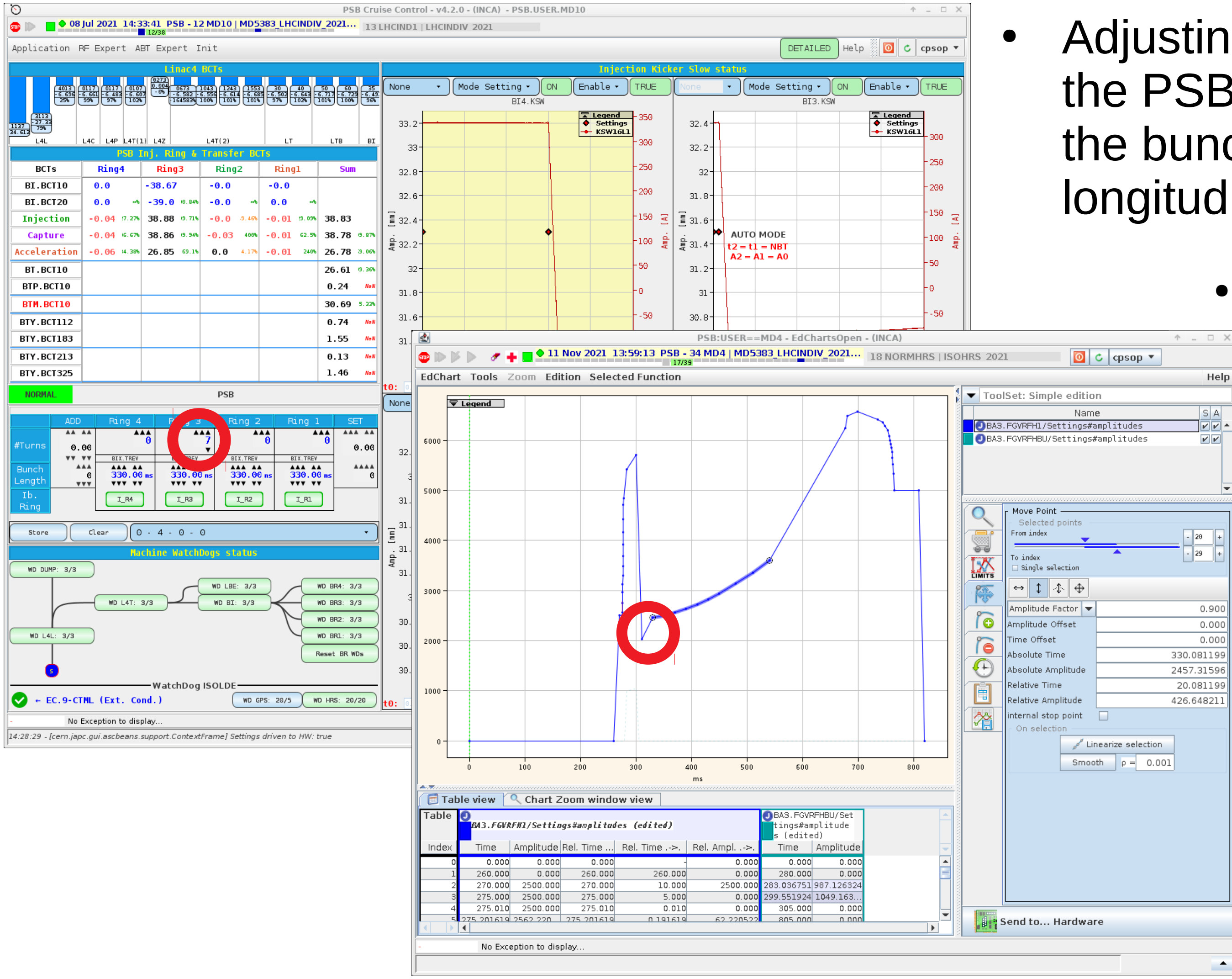

- Adjusting the number of injections into the PSB allows for a coarse control of the bunch intensity at constant longitudinal and transverse emittances
  - The RF voltage features a drop at the start of the ramp which lowers the bucket height (long. Shaving / choke). The depth of the drop define the longitudinal emittance.

Control of intensity and longitudinal emittance at the booster

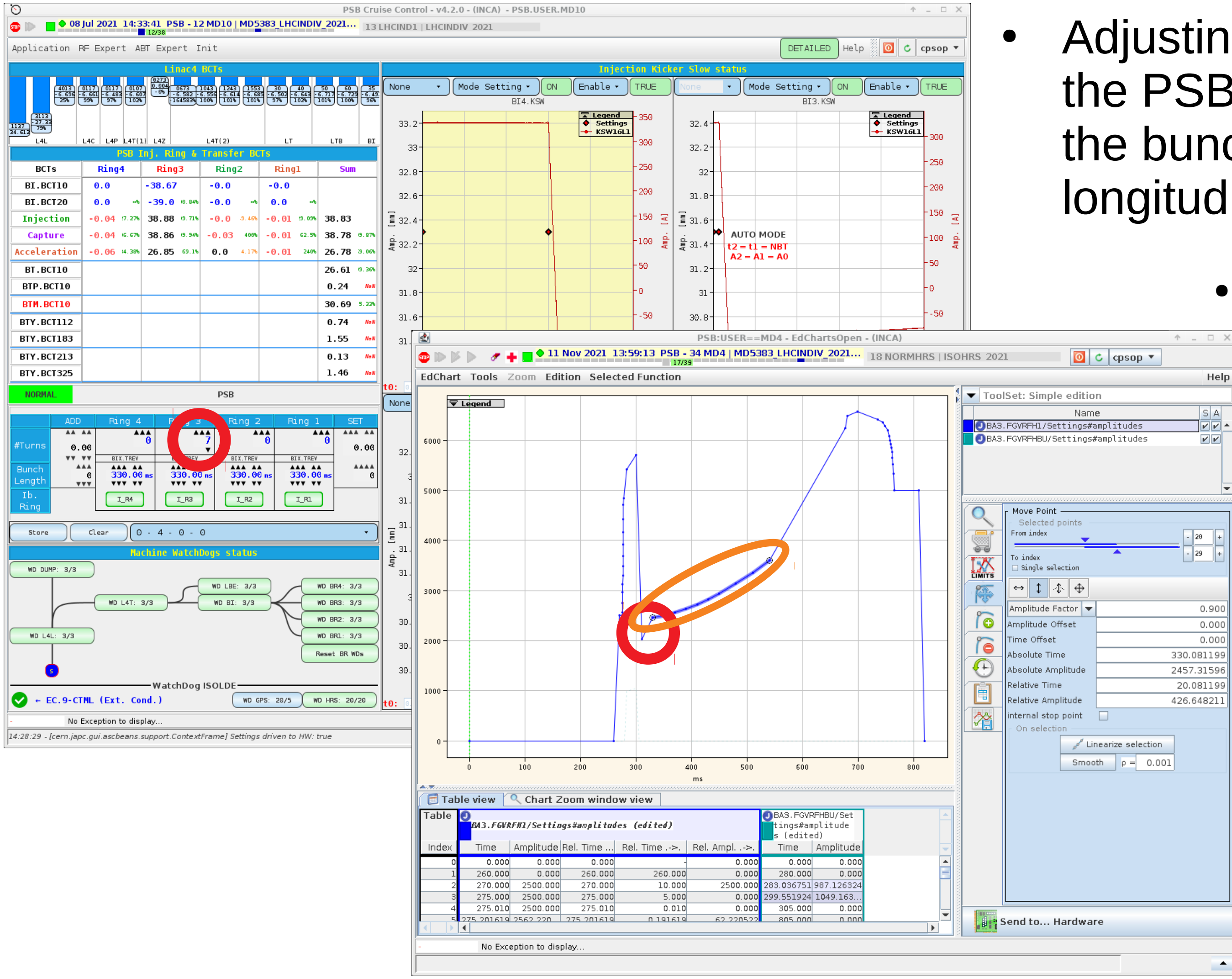

- Adjusting the number of injections into the PSB allows for a coarse control of the bunch intensity at constant longitudinal and transverse emittances
  - The RF voltage features a drop at the start of the ramp which lowers the bucket height (long. Shaving / choke). The depth of the drop define the longitudinal emittance.
- For high intensity and low longitudinal emittances, the RF voltage during the ramp should be reduced to maintain longitudinal Landau damping

Control of intensity and longitudinal emittance at the booster

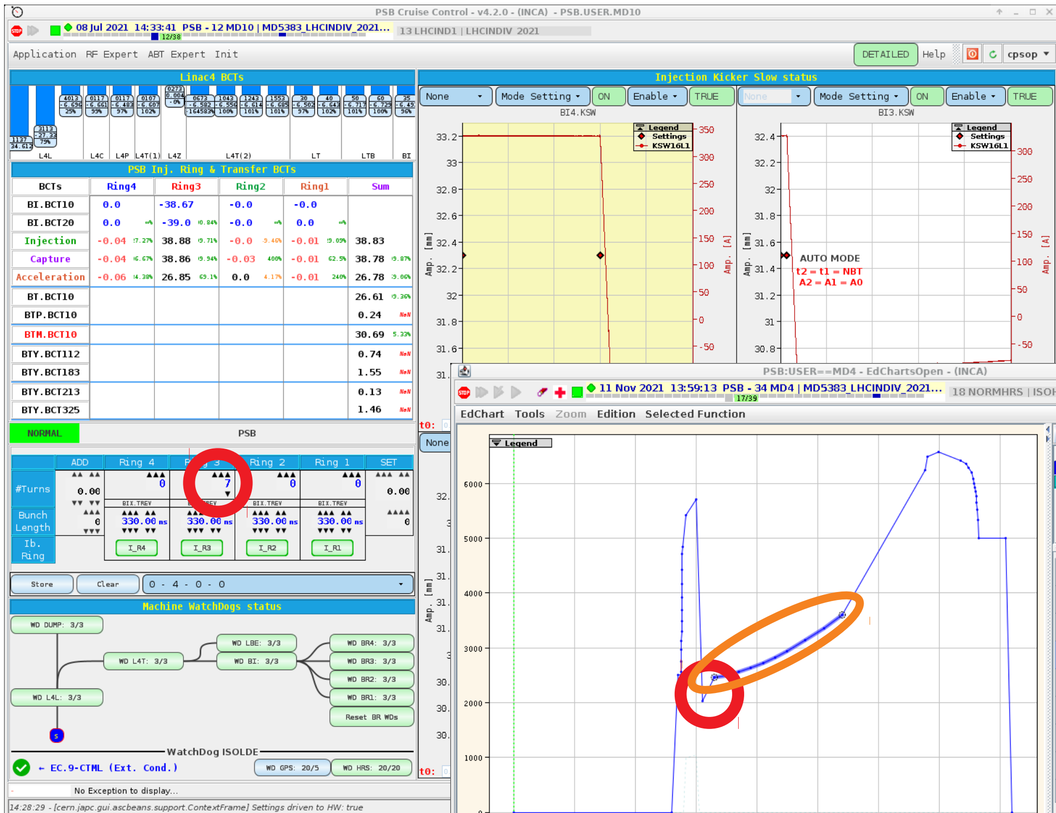

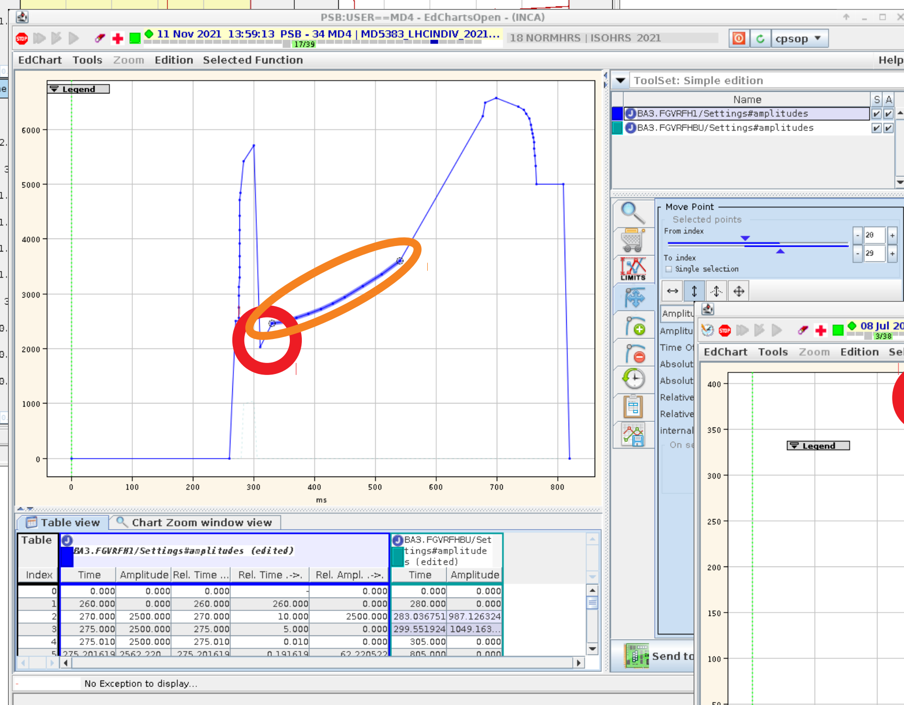

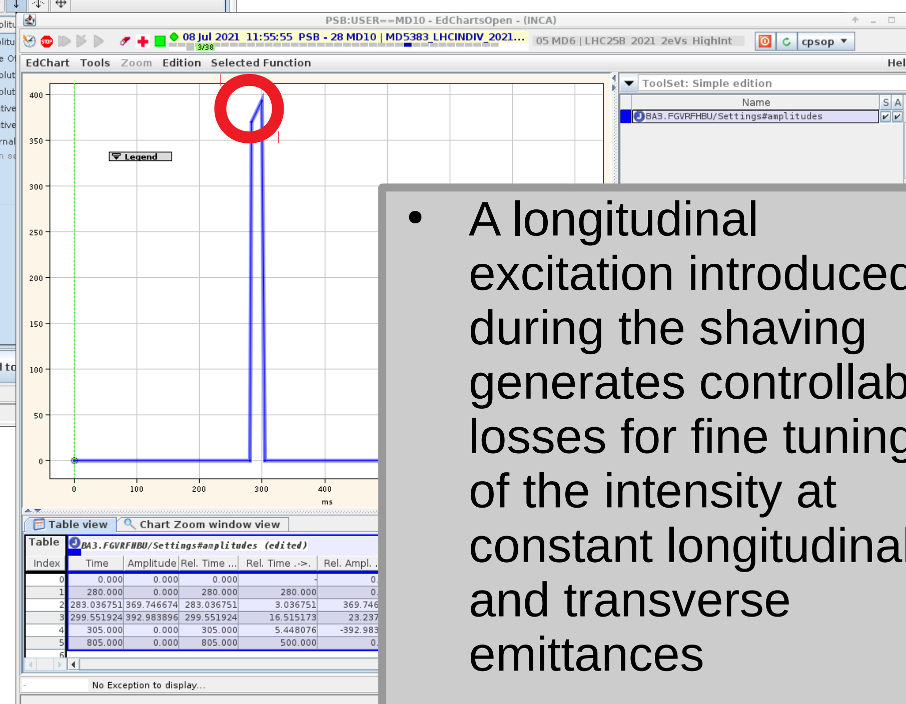

- Adjusting the number of injections into the PSB allows for a coarse control of the bunch intensity at constant longitudinal and transverse emittances
    - The RF voltage features a drop at the start of the ramp which lowers the bucket height (long. Shaving / choke). The depth of the drop define the longitudinal emittance.

- For high intensity and low longitudinal emittances, the RF voltage during the ramp should be reduced to maintain longitudinal Landau damping

- A longitudinal excitation introduced during the shaving generates controllable losses for fine tuning of the intensity at constant longitudinal and transverse emittances

Transverse emittance blowup at the PS

Transverse emittance blowup at the PS

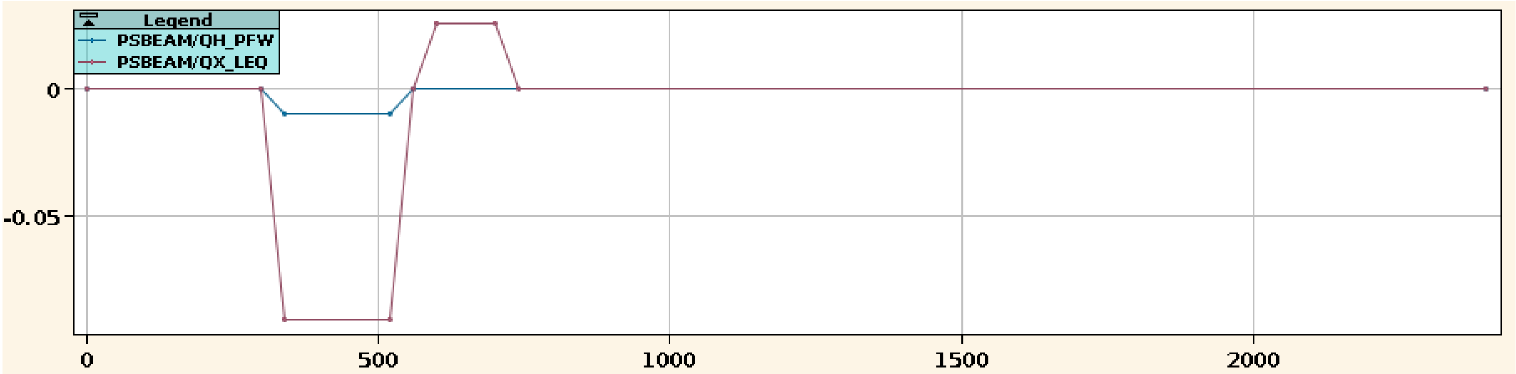

- Variations of the transverse emittance in the range 1.5 to 6 μm were obtained with a tune bump at the PS injection plateau

Transverse emittance blowup at the PS

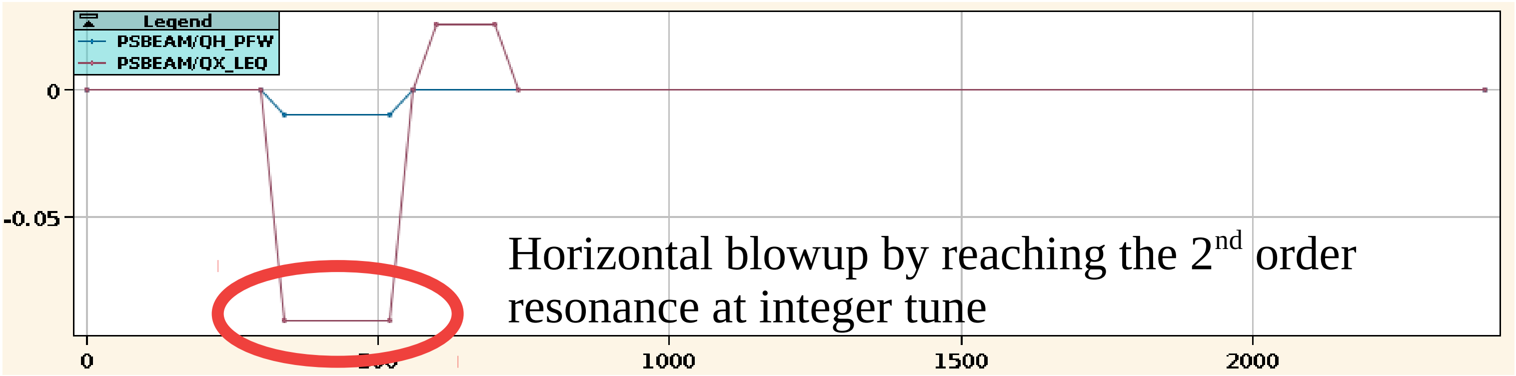

- Variations of the transverse emittance in the range 1.5 to 6 μm were obtained with a tune bump at the PS injection plateau

Transverse emittance blowup at the PS

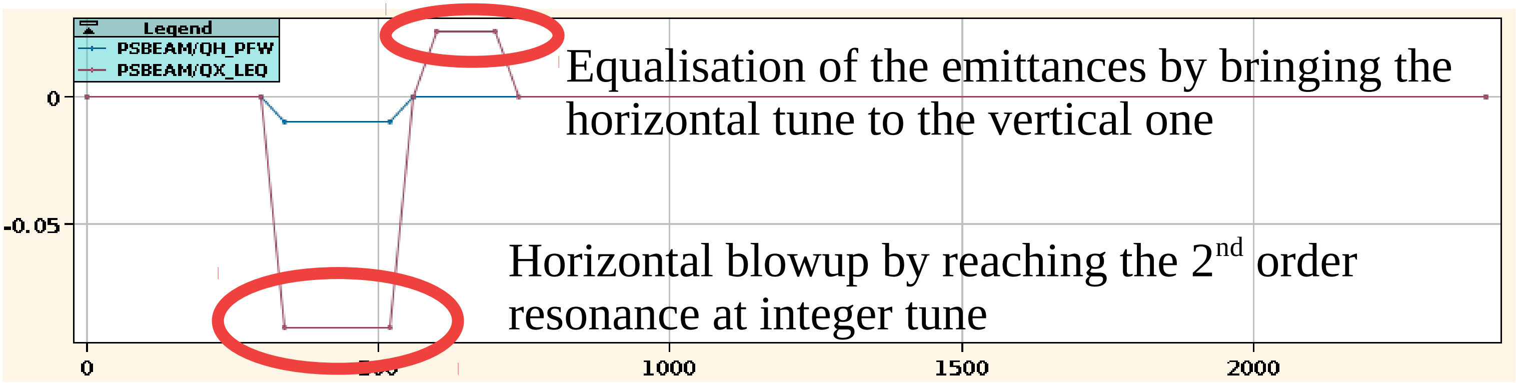

- Variations of the transverse emittance in the range 1.5 to 6 μm were obtained with a tune bump at the PS injection plateau

Transverse emittance blowup at the PS

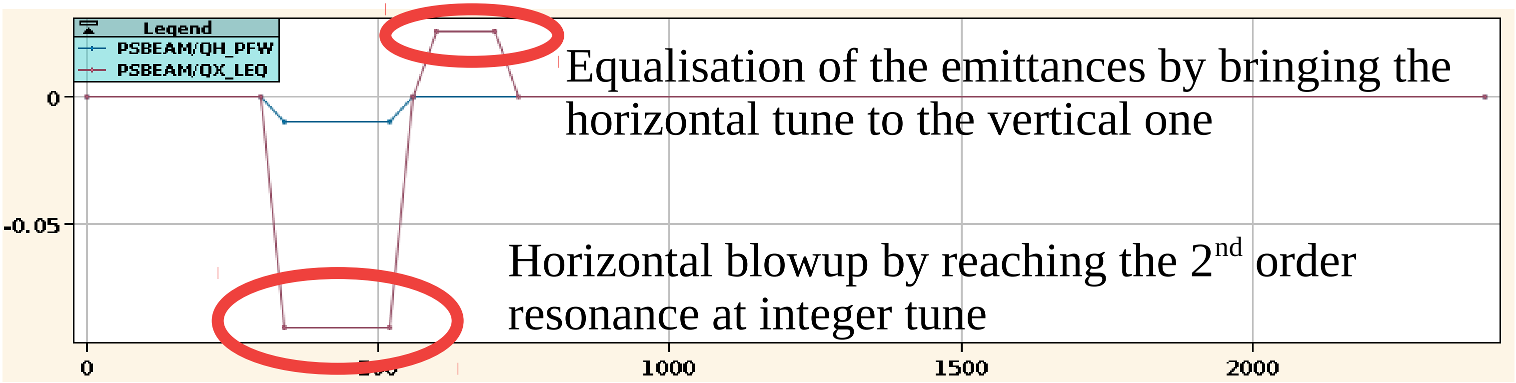

- Variations of the transverse emittance in the range 1.5 to 6 µm were obtained with a tune bump at the PS injection plateau

- The equalisation of the transverse emittances requires careful setup dependent of the beam parameters

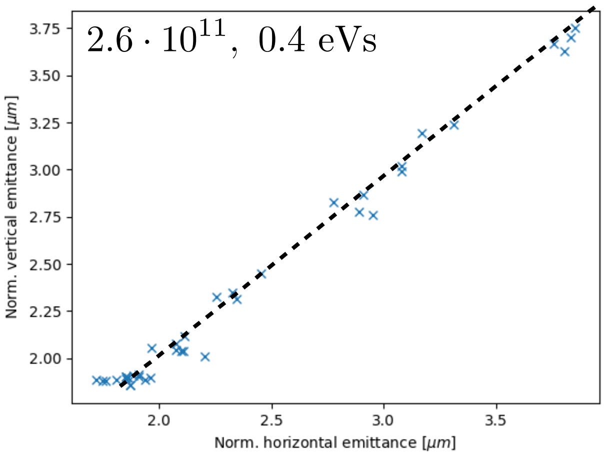

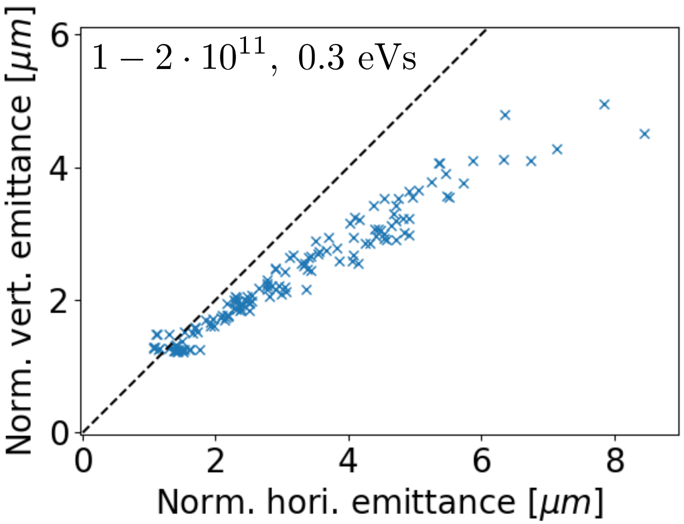

Issue with low longitudinal emittances at the PS transition

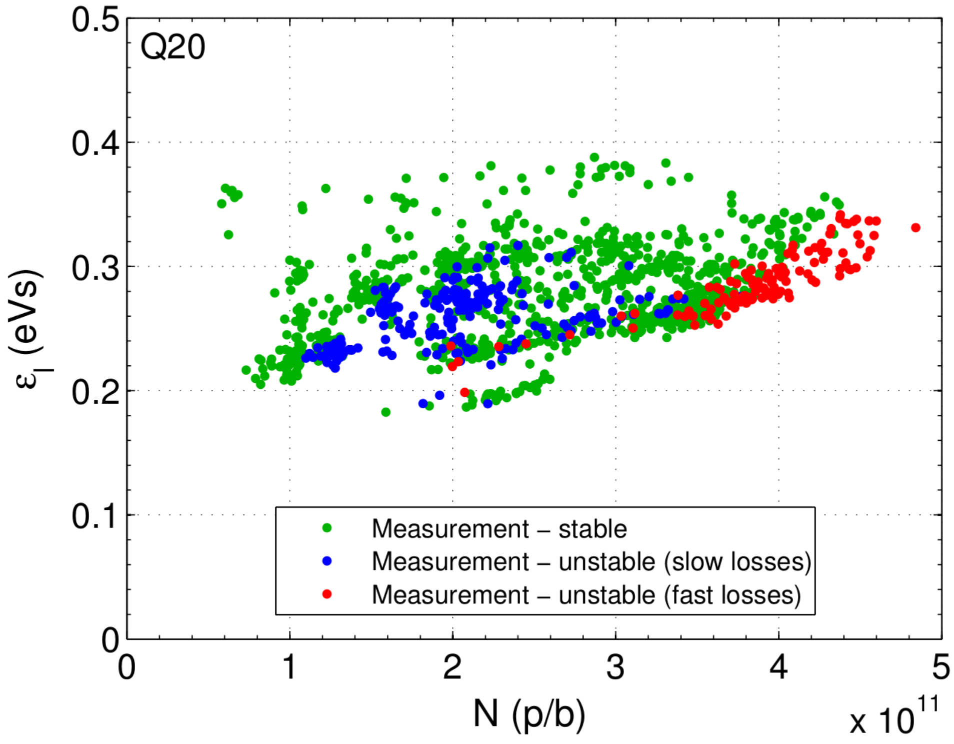

Issue with low longitudinal emittances at the PS transition

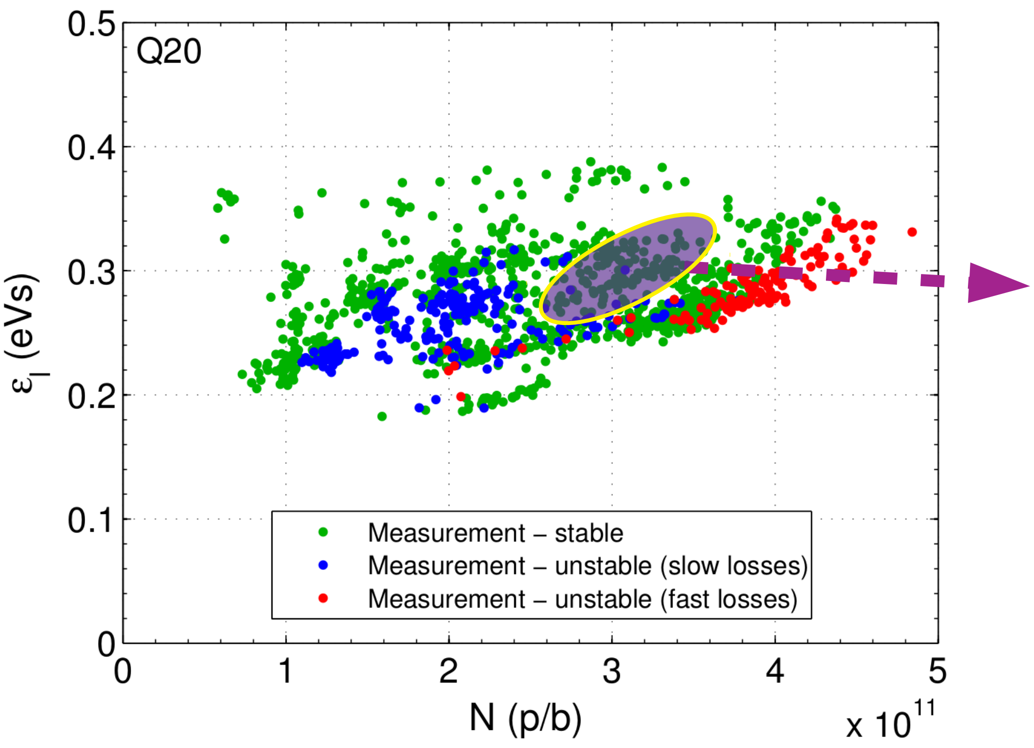

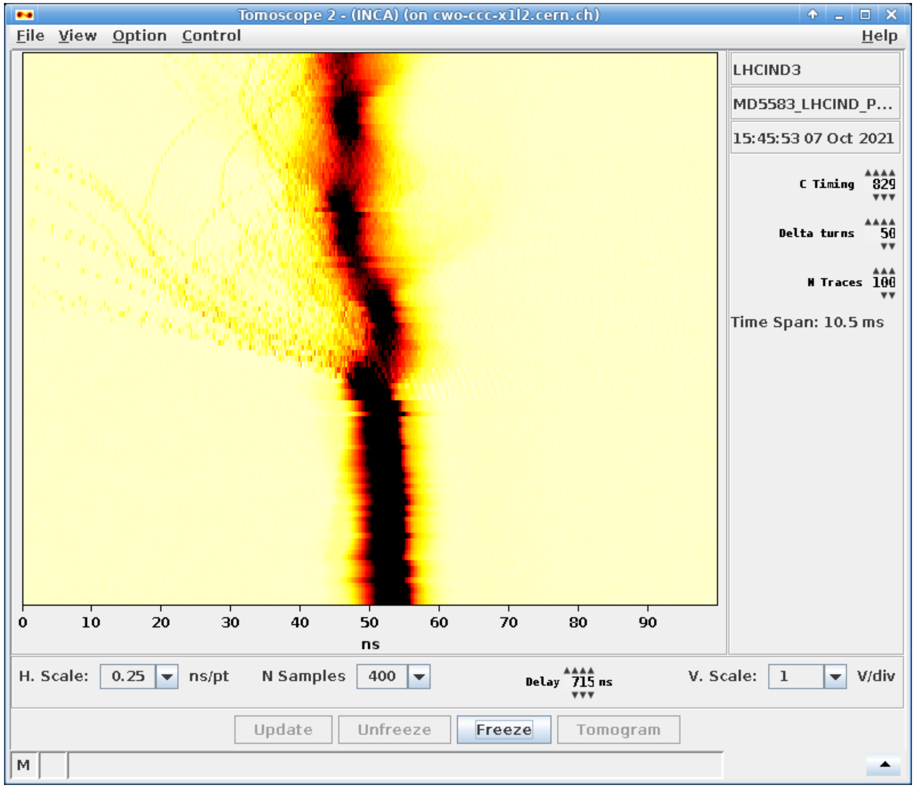

Issue with low longitudinal emittances at the PS transition

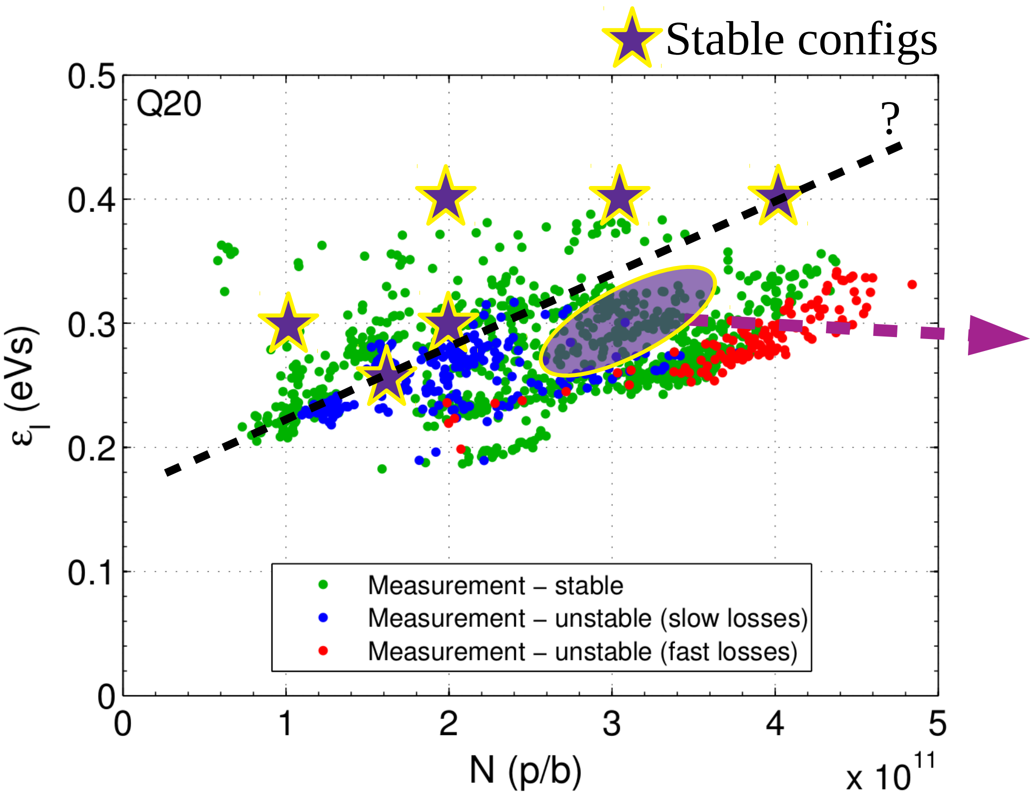

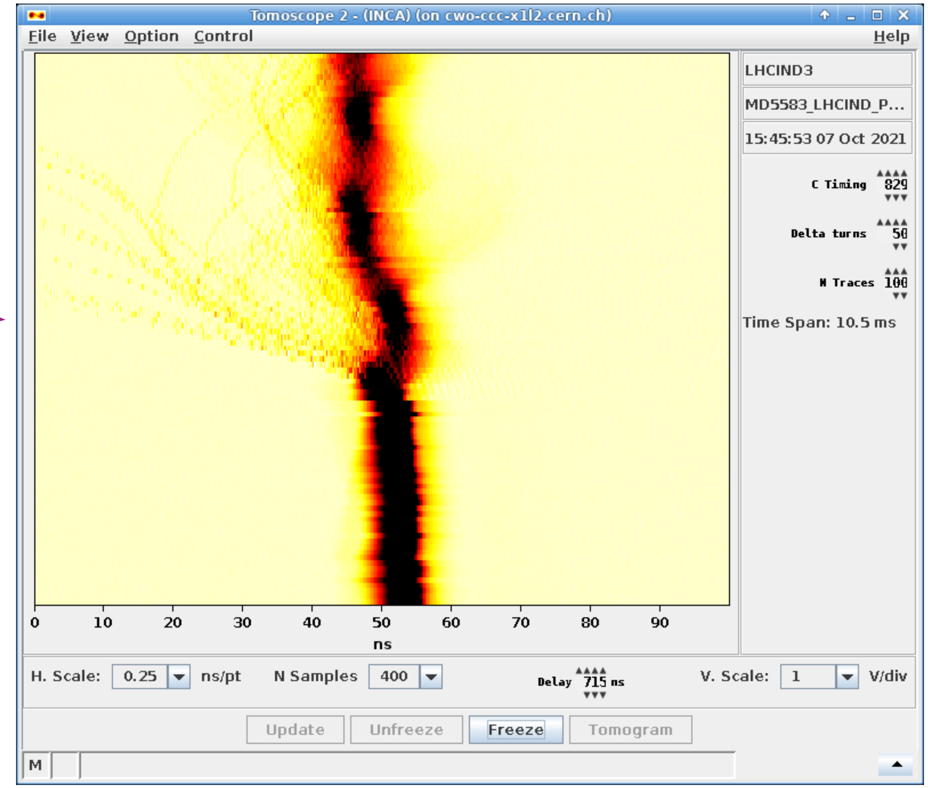

- Parameters comparable to the 2013 experiments could be obtained from the PSB, but the beam couldn't make it through the PS transition → Longitudinal instability
  - A. Lasheen found a frequency component that is compatible with the impedance of the sector valves (see backup). They have not changed between 2013 and 2021 → this new limitation is neither understood nor solved at the moment

Issue with low longitudinal emittances at the PS transition

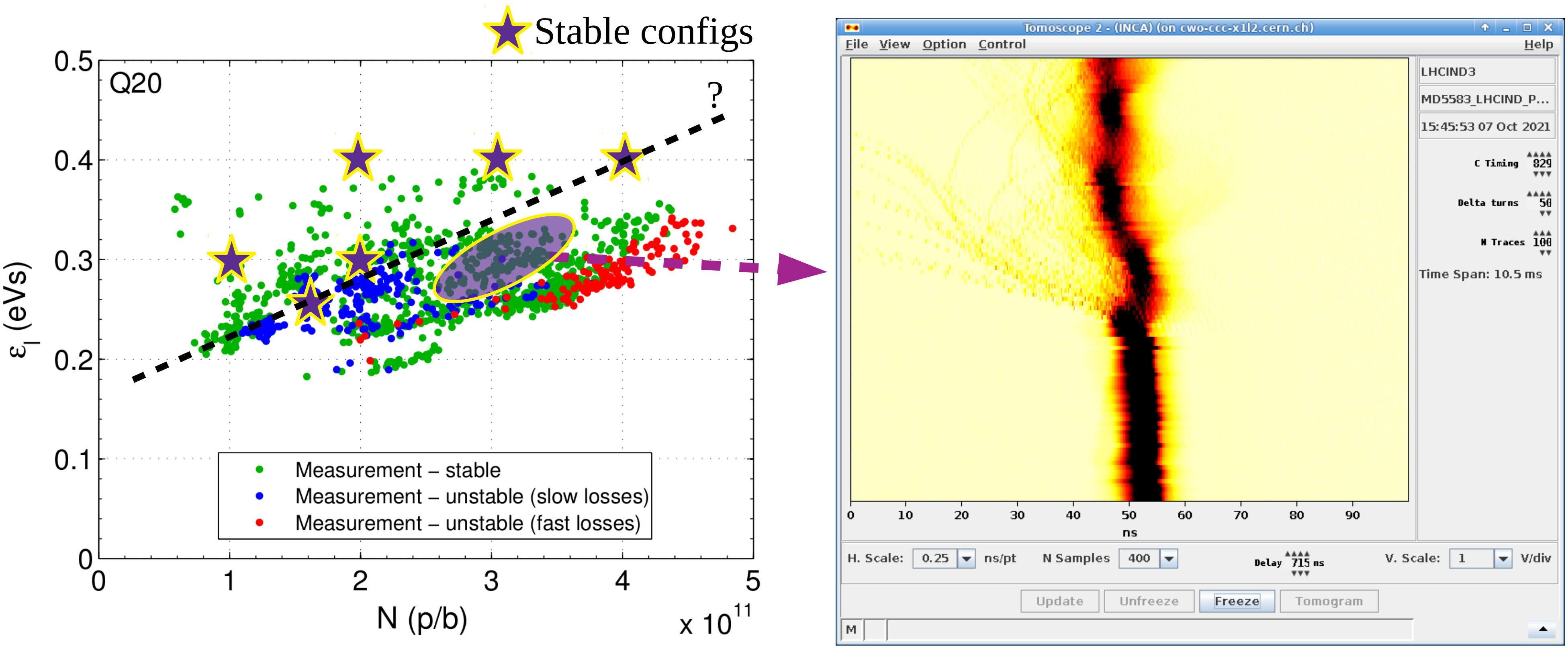

- Parameters comparable to the 2013 experiments could be obtained from the PSB, but the beam couldn't make it through the PS transition → Longitudinal instability
  - A. Lasheen found a frequency component that is compatible with the impedance of the sector valves (see backup). They have not changed between 2013 and 2021 → this new limitation is neither understood nor solved at the moment
- No instabilities were observed at the SPS with the Q20 optics using the available beams from the PS, compatibly with past results

→ Need the Q26 optics to study the TMCI until the issue at PS transition is solved

Stability threshold - intensity

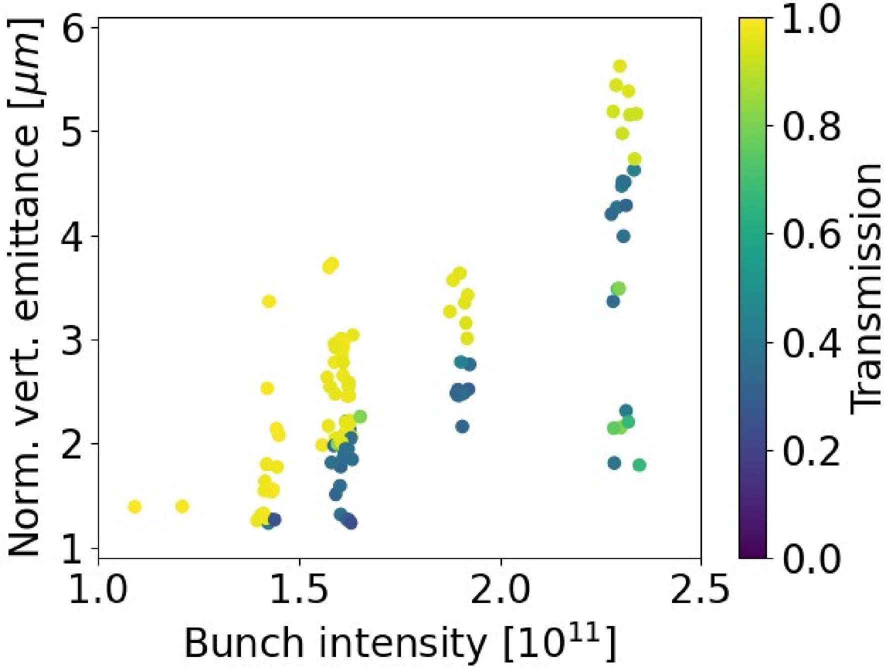

Stability threshold - intensity

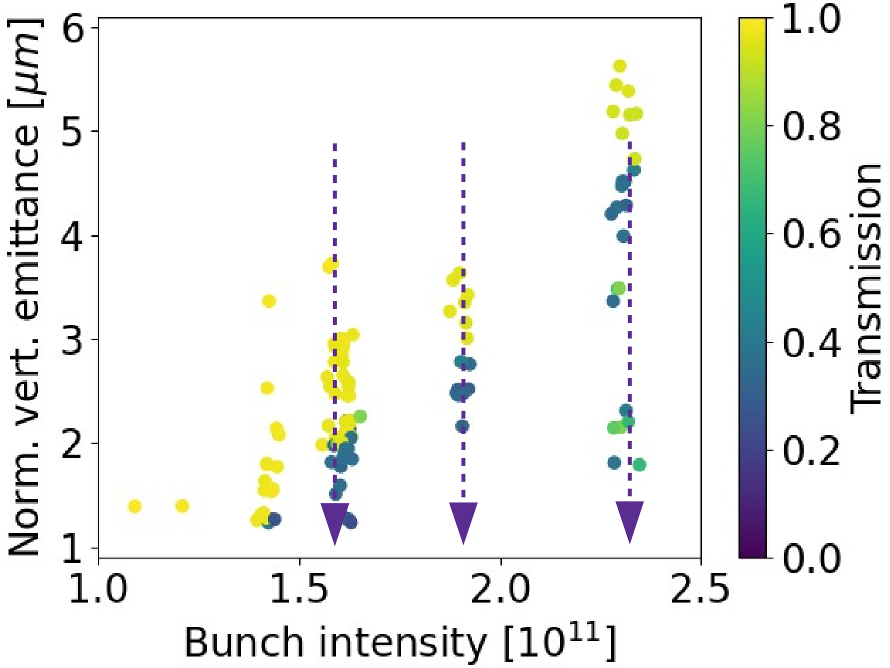

- For a given intensity and longitudinal emittance (i.e. **fixed wake field strength**), the beam is **stable with a large emittance** (low space-charge strength) and **unstable with a small emittance** (high space-charge strength)

Stability threshold - intensity

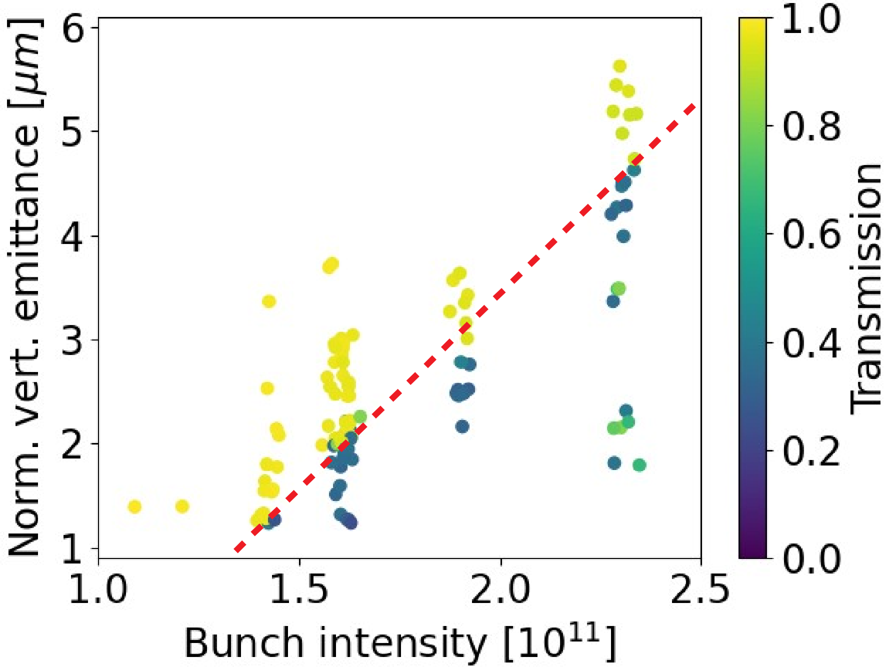

- For a given intensity and longitudinal emittance (i.e. **fixed wake field strength**), the beam is **stable with a large emittance** (low space-charge strength) and **unstable with a small emittance** (high space-charge strength)
- The transverse emittance threshold looks linear with the intensity

Stability threshold - intensity

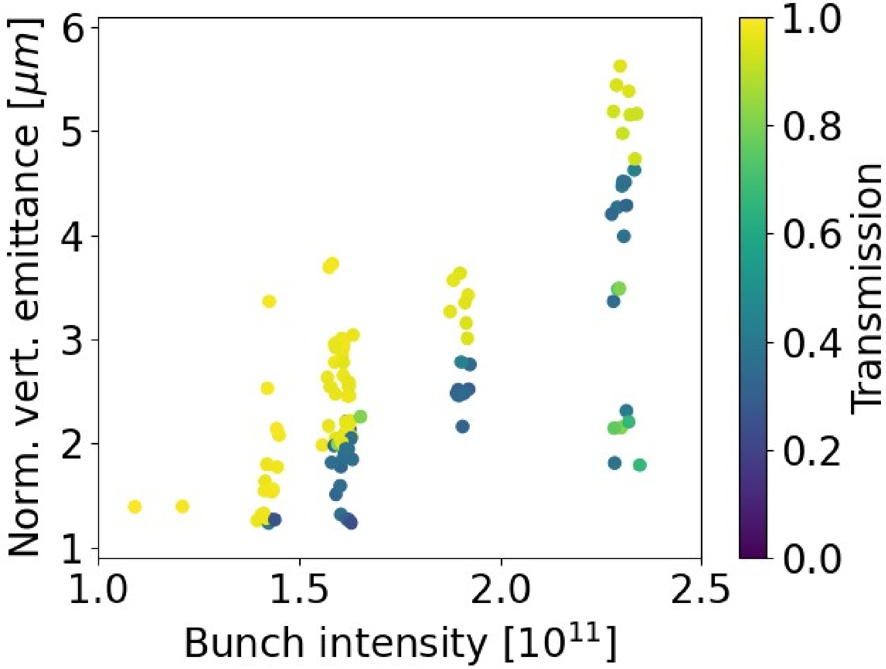

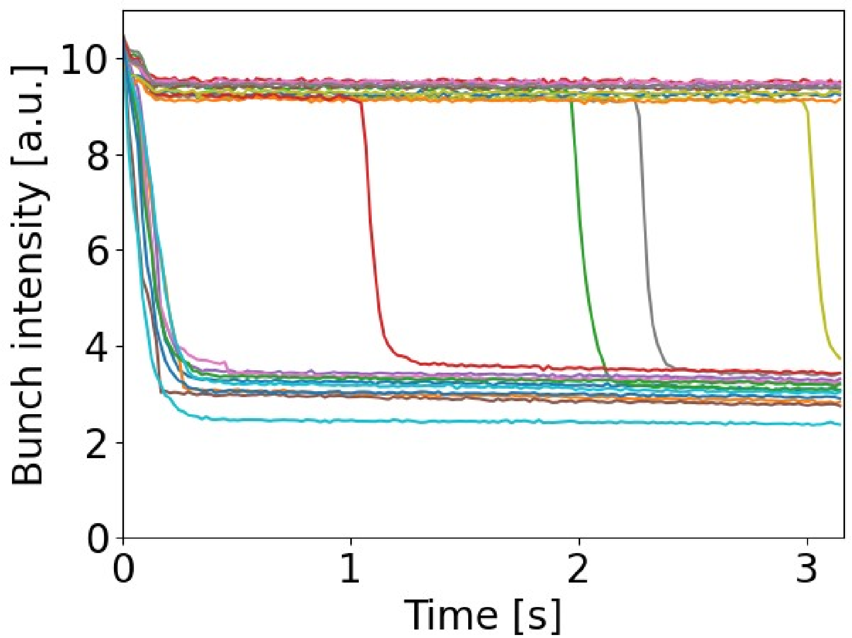

- For a given intensity and longitudinal emittance (i.e. **fixed wake field strength**), the beam is **stable with a large emittance** (low space-charge strength) and **unstable with a small emittance** (high space-charge strength)
- The transverse emittance threshold looks linear with the intensity

Stability threshold - intensity

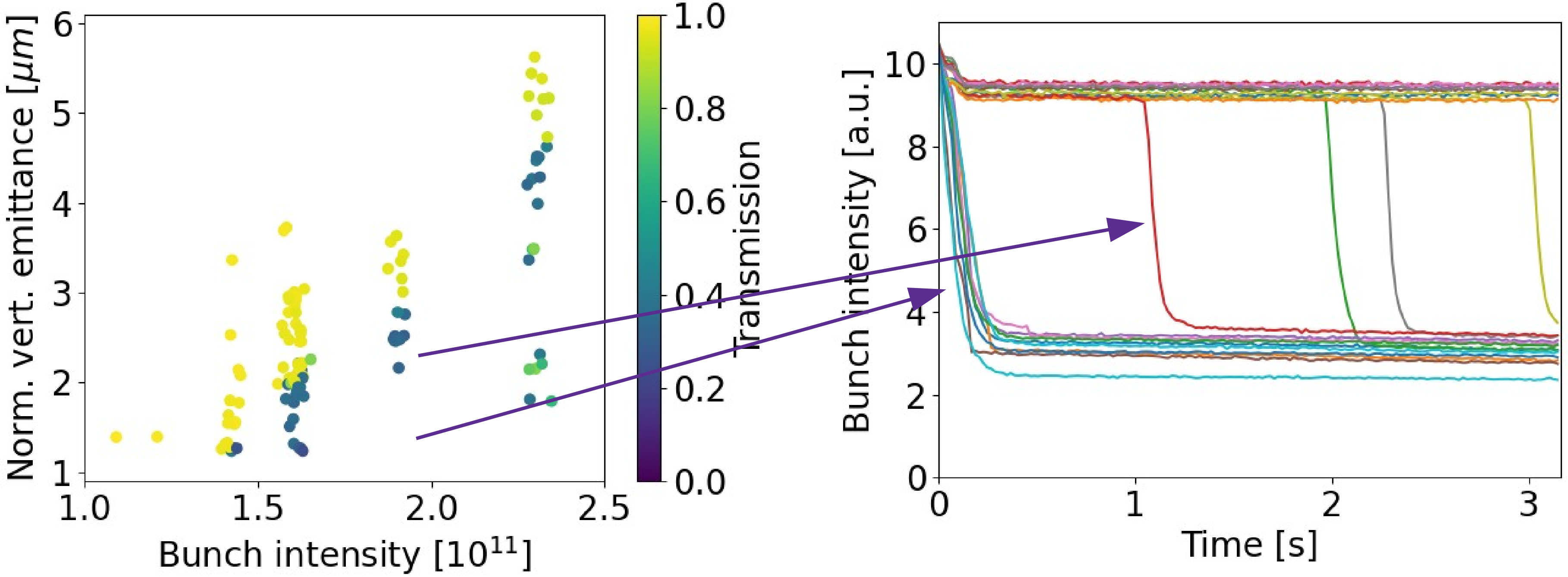

- For a given intensity and longitudinal emittance (i.e. **fixed wake field strength**), the beam is **stable with a large emittance** (low space-charge strength) and **unstable with a small emittance** (high space-charge strength)
- The transverse emittance threshold looks linear with the intensity
- Instabilites can be quite violent away from threshold and rather slow close to it

Stability threshold – longitudinal emittance

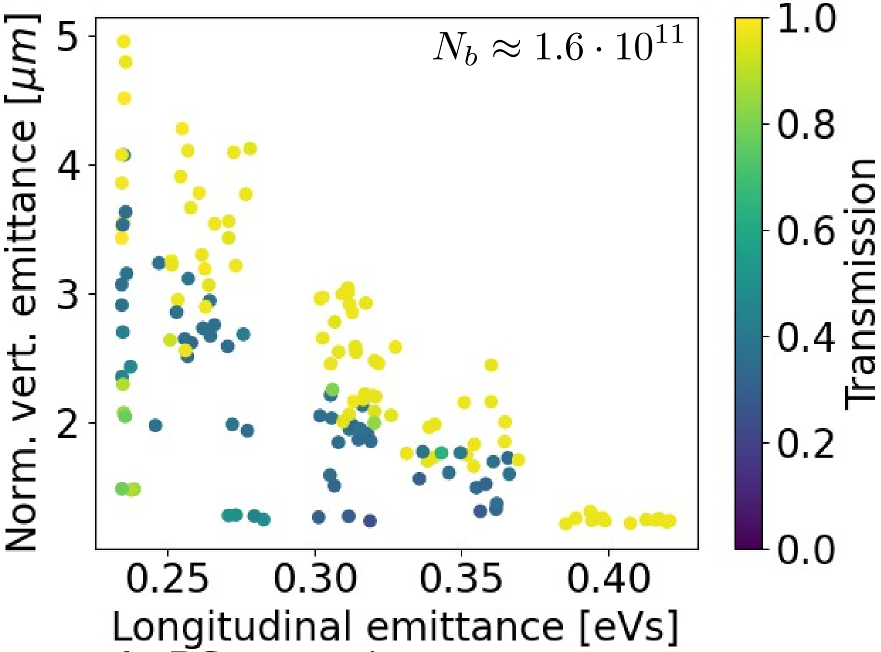

At PS extraction

- The instability threshold's dependence on the longitudinal emittance is also affected by the transverse emittance

  → This *hidden* dependence has likely impacted the 2013 study

Stability threshold – longitudinal emittance

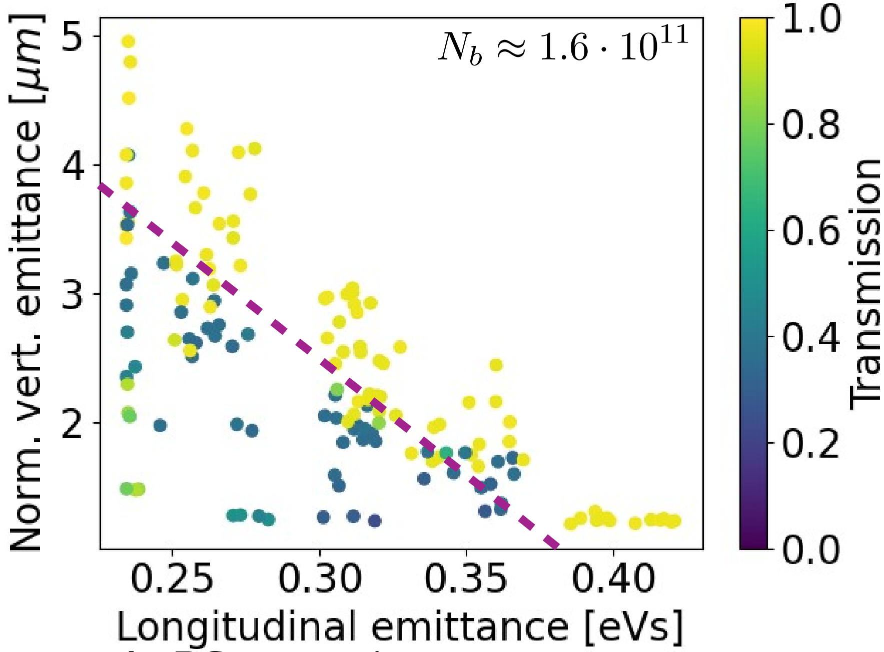

At PS extraction

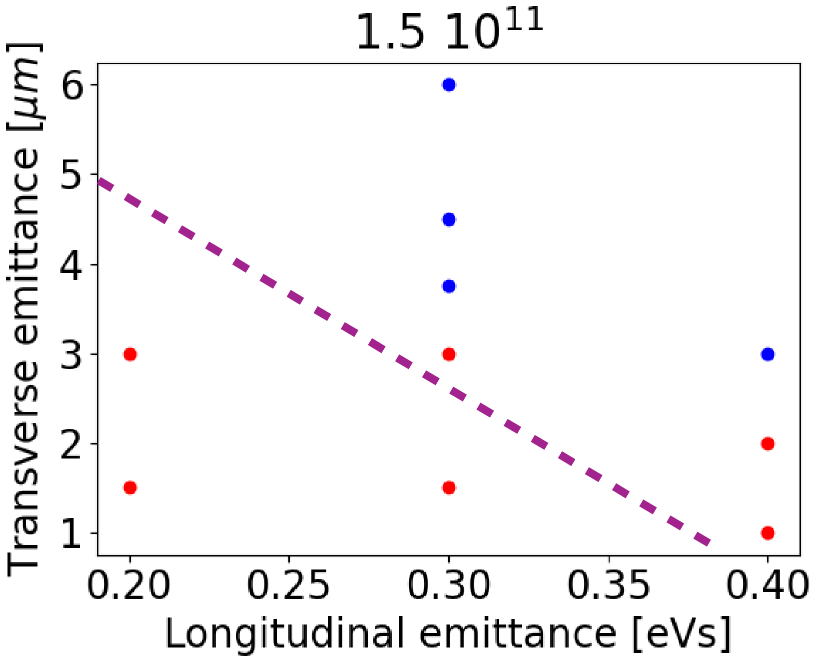

- The instability threshold's dependence on the longitudinal emittance is also affected by the transverse emittance

  → This *hidden* dependence has likely impacted the 2013 study

- More simulations and correction of the longitudinal emittance based on ABWLM are needed to conclude on the impact of the longitudinal emittance at fixed intensity

Beam oscillation (BBQ)

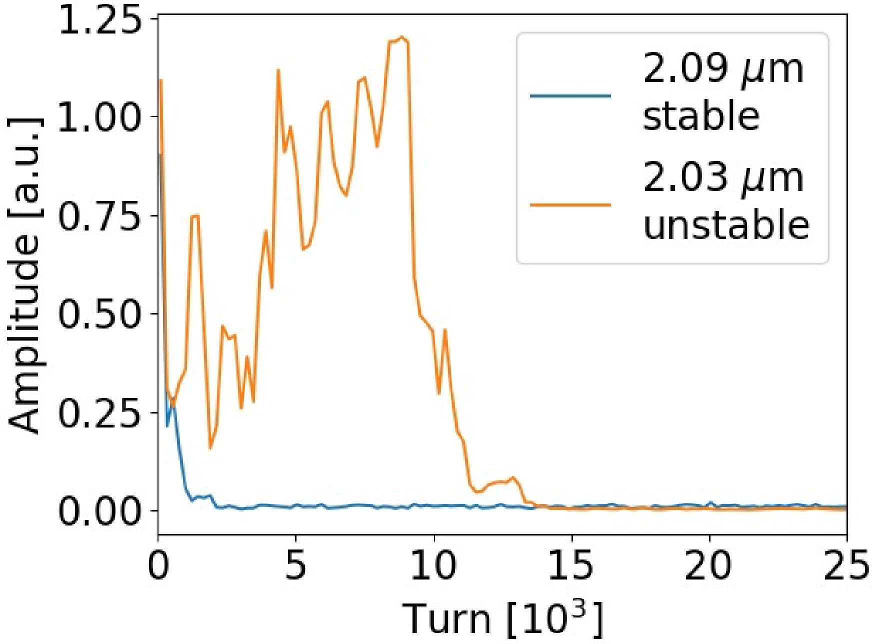

- The coherent signal is clearly visible in the BBQ

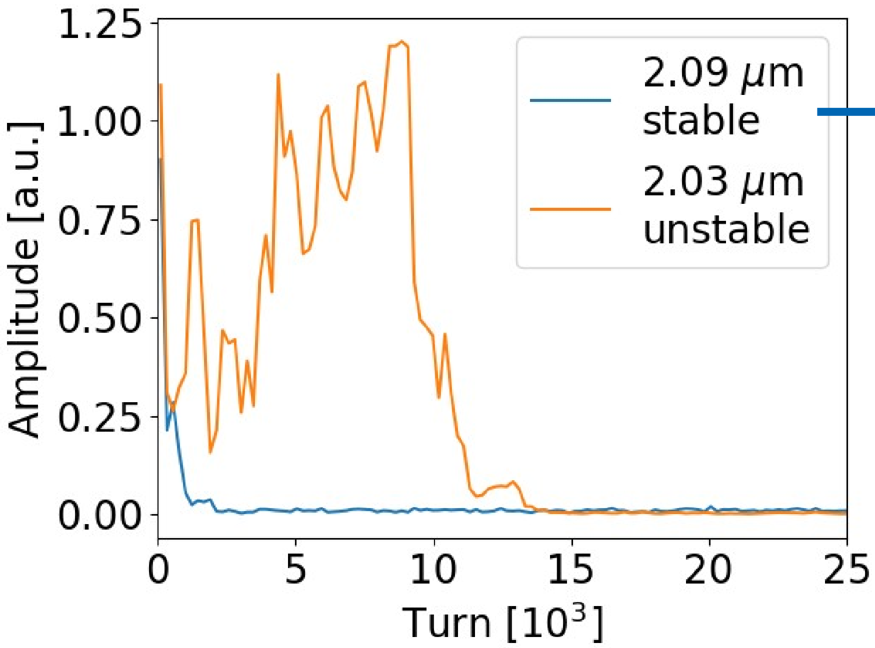

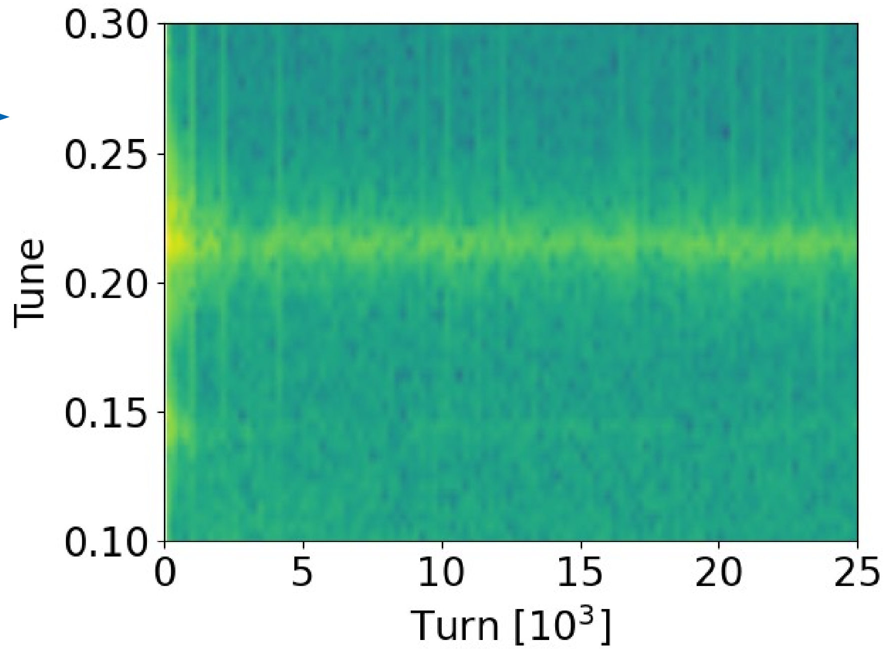

- The coherent signal is clearly visible in the BBQ

Beam oscillation (BBQ)

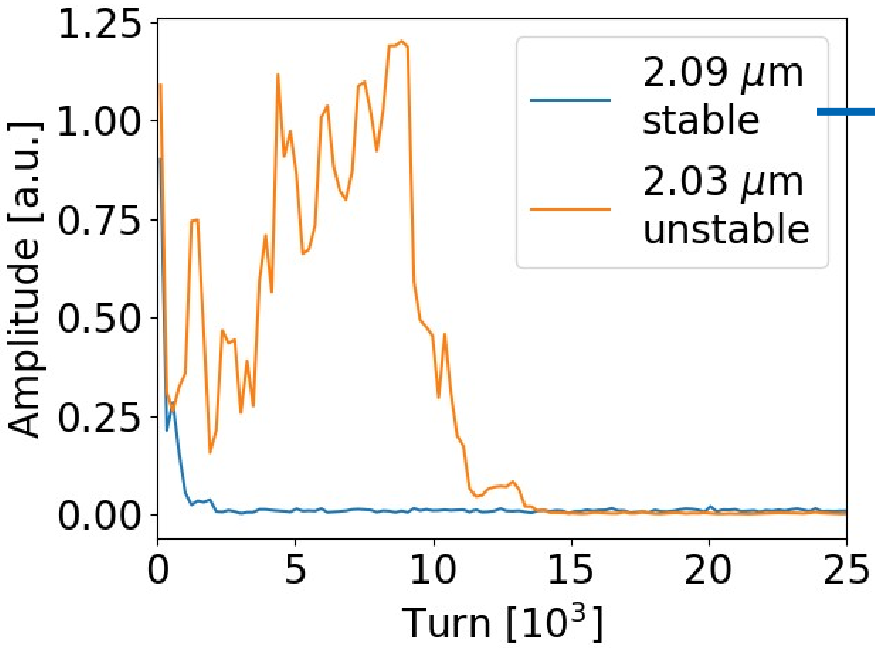

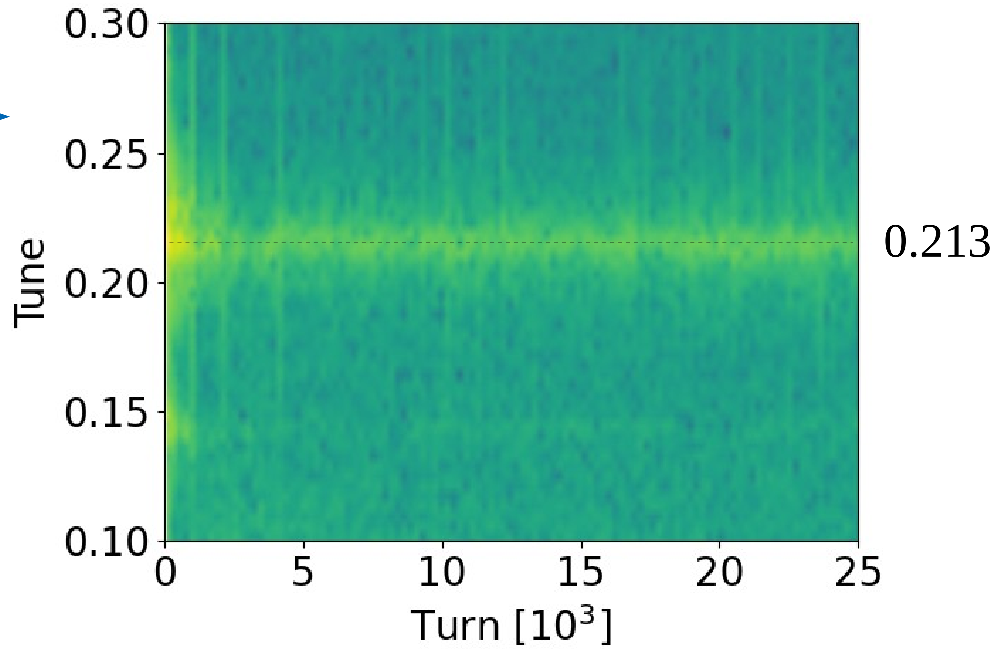

- The coherent signal is clearly visible in the BBQ

Beam oscillation (BBQ)

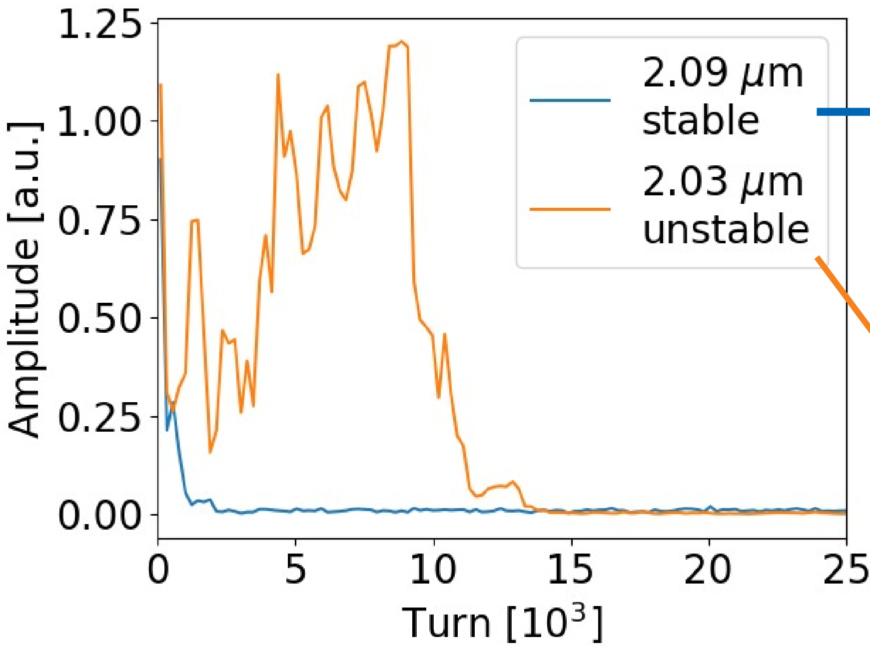

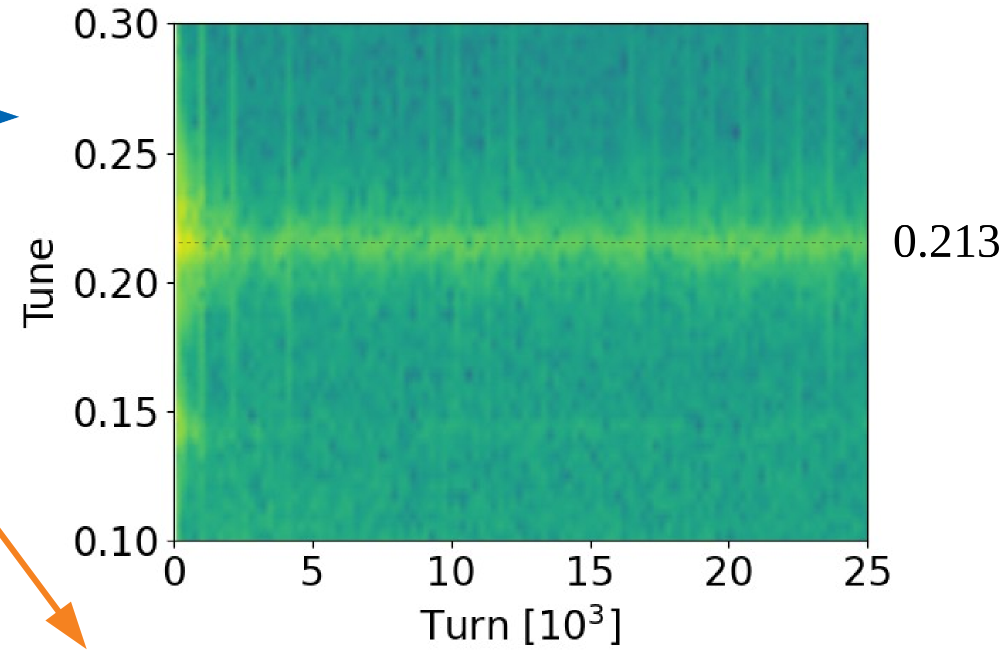

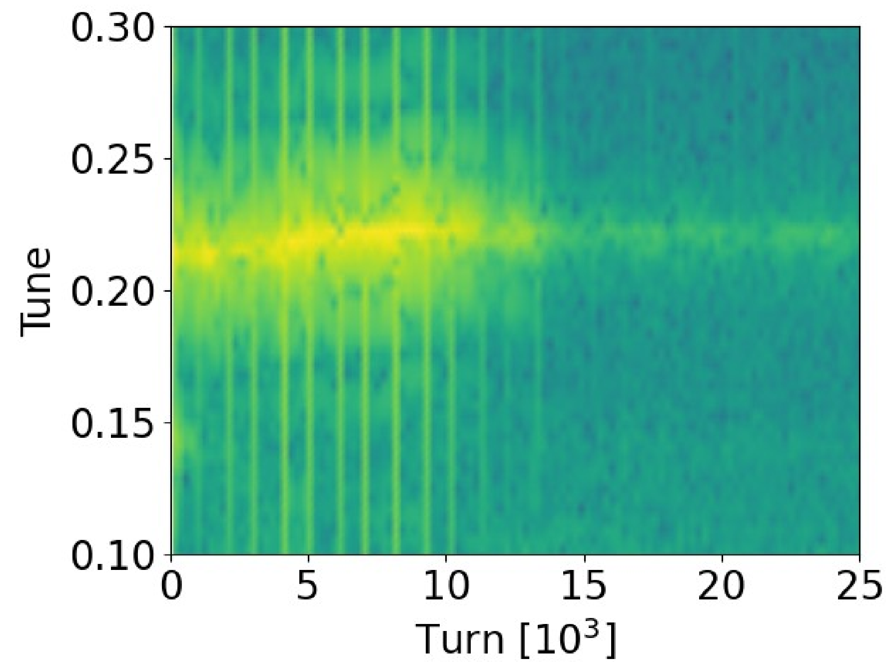

- The coherent signal is clearly visible in the BBQ

Beam oscillation (BBQ)

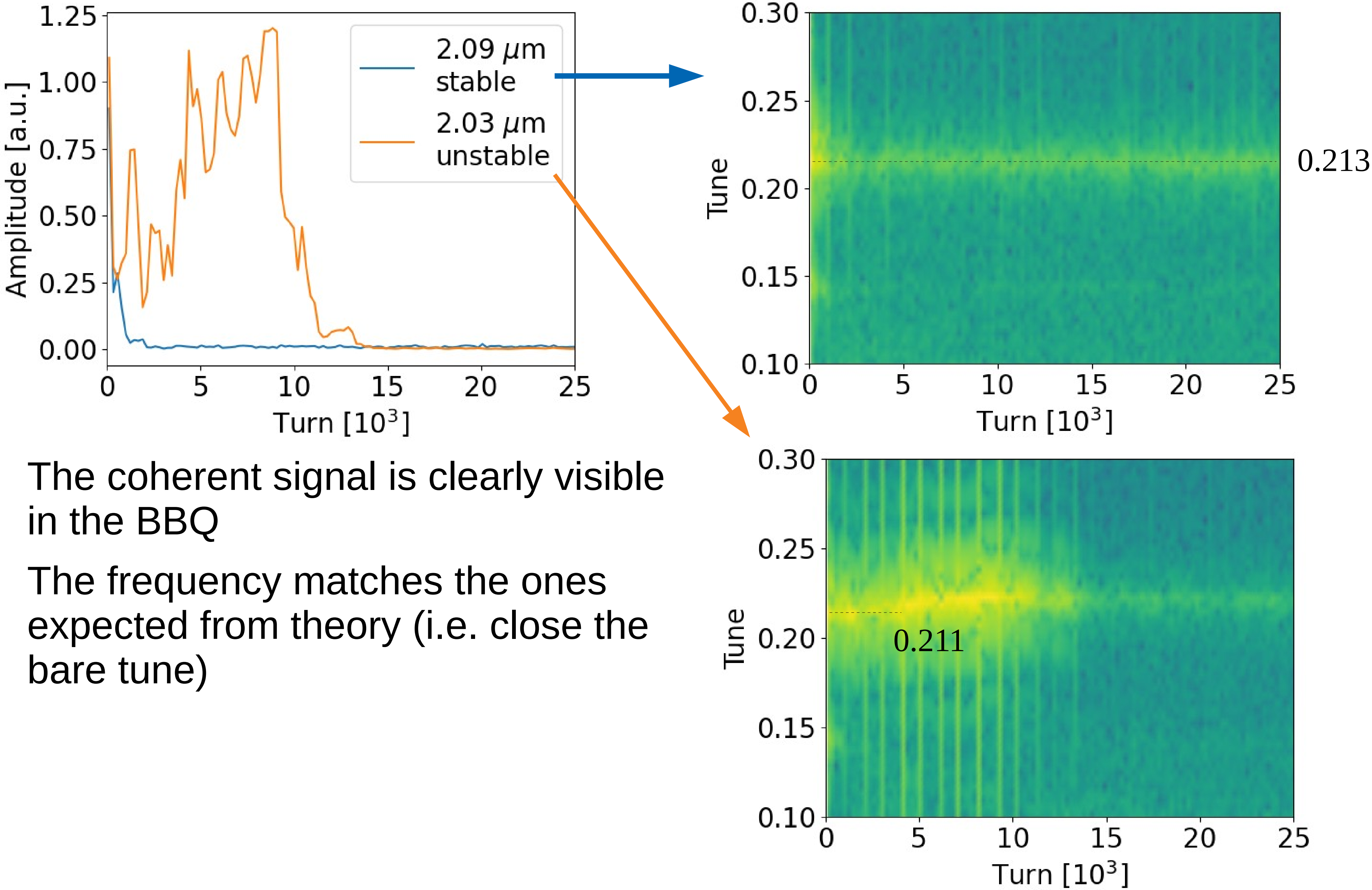

- The coherent signal is clearly visible in the BBQ
- The frequency matches the ones expected from theory (i.e. close the bare tune)

Beam oscillation (BBQ)

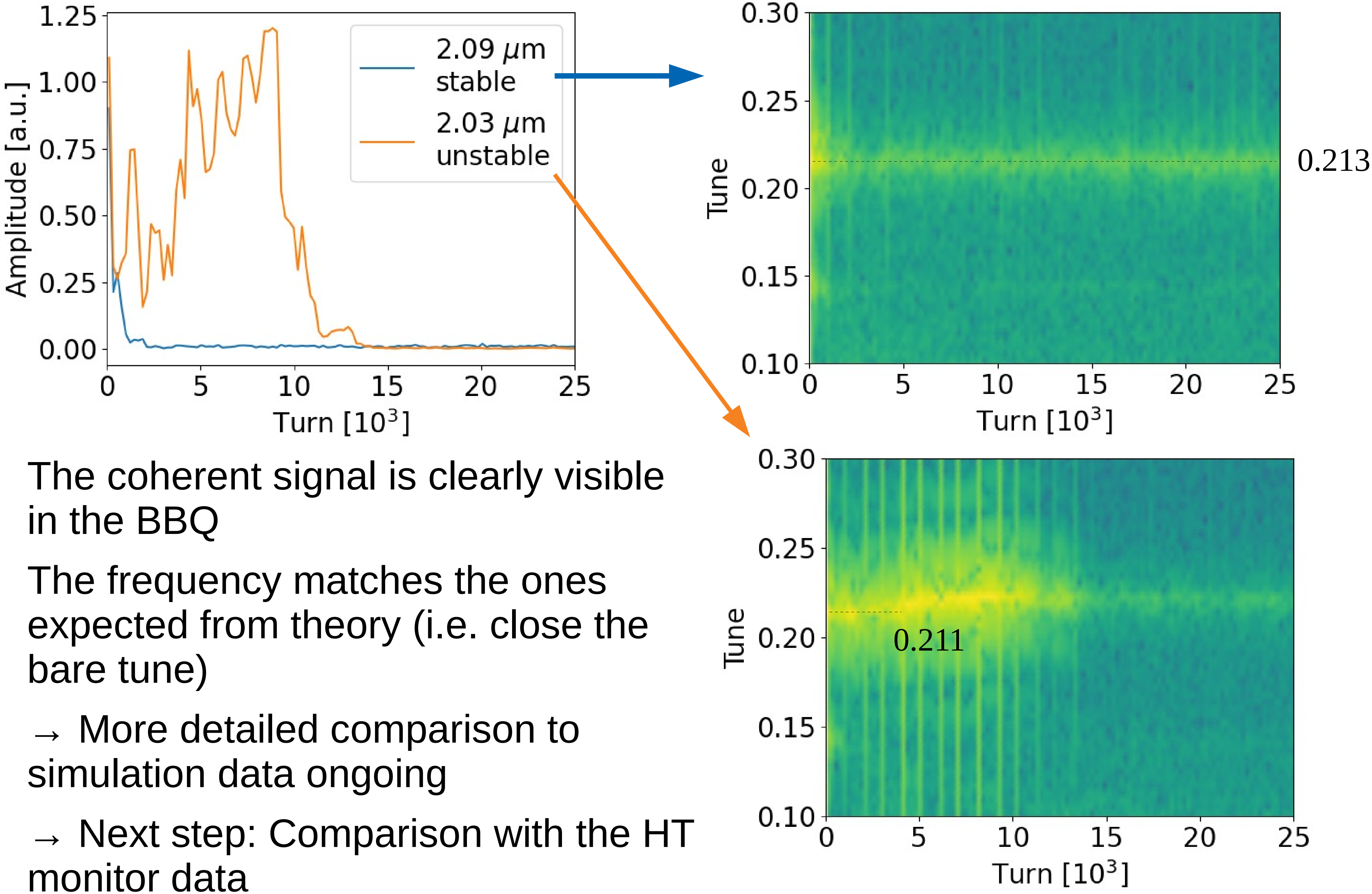

- The coherent signal is clearly visible in the BBQ
- The frequency matches the ones expected from theory (i.e. close the bare tune)

  → More detailed comparison to simulation data ongoing

  → Next step: Comparison with the HT monitor data

Sixtracklib – PyHEADTAIL simulations

- Sixtracklib does not support error tables as defined in MAD-X

  → Requires a copy of the error tables into the element strength

- The difference in third order chromaticity could be attributed to higher order terms leading to an artifact in the fit

	Horizontal PTC	Horizontal Fit	Vertical PTC	Vertical Fit
Q	0.15	0.15	0.22	0.22
Q’	2.96	2.3	2.2	2.5
Q’’	264	275	134	122
Q’’’ [10^3]	-479	-213	292	118

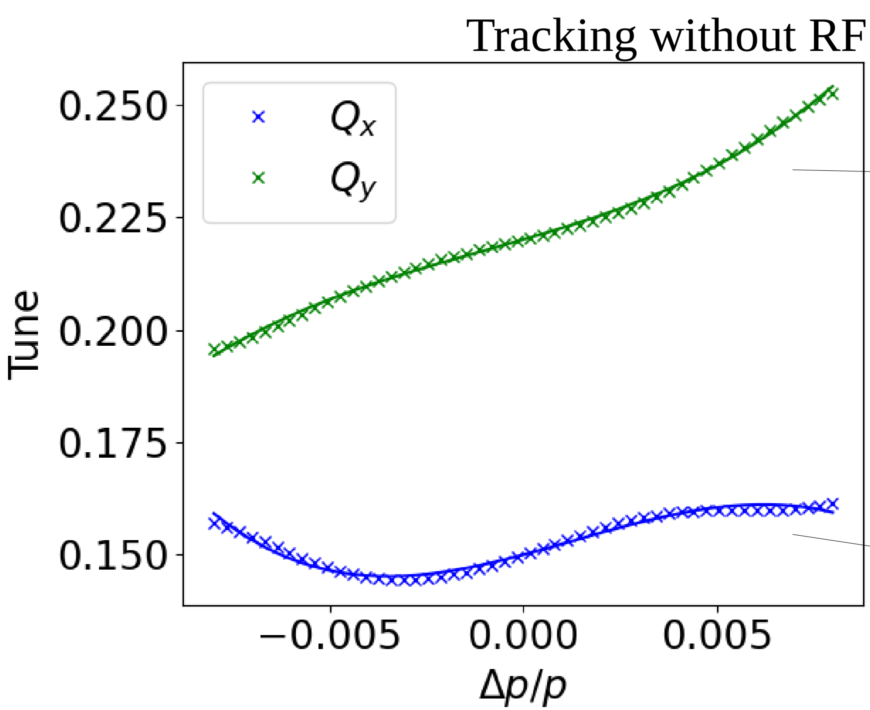

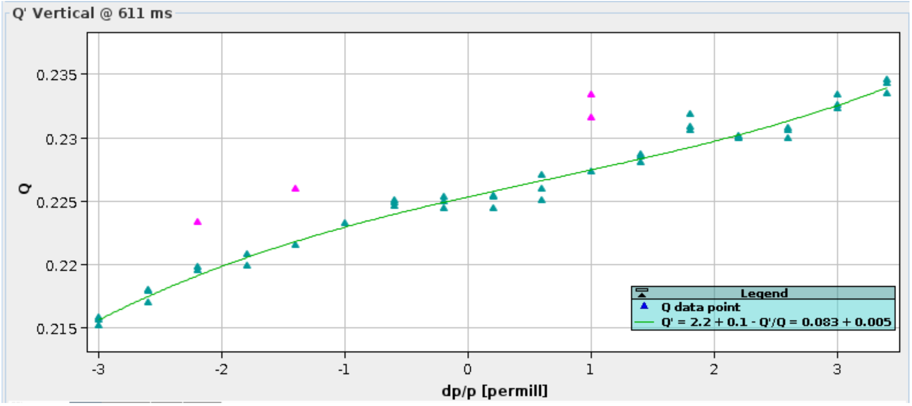

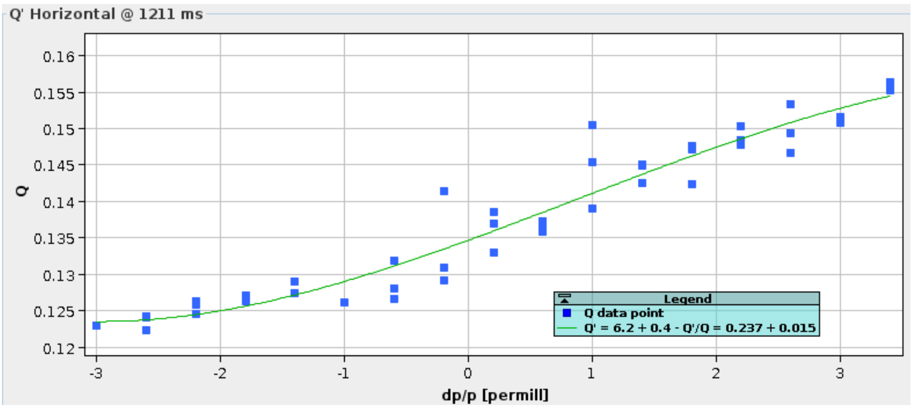

- Some theories *[Blaskiewicz, Burov09, Balbekov]* predict that the **TMCI should be suppressed by space-charge forces** while others not *[Chin, Alexahin]*
  - **The suppression of the instability is not observed** in some machines featuring strong space-charge forces

[Bartosik]

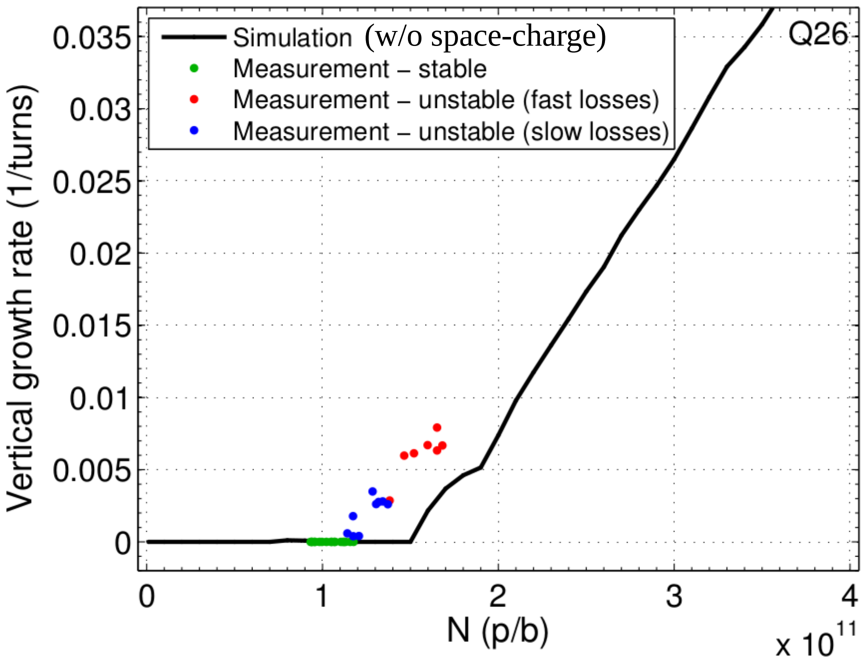

[Balbekov] V. Balbekov, Phys. Rev. Accel. Beams 20, 034401 (2017)
[Burov09] A. Burov, Phys. Rev. ST Accel. Beams 12, 044202 (2009)
[Burov19] A. Burov, Phys. Rev. Accel. Beams 22, 034202 (2019)
[Bartosik] H. Bartosik, PhD Thesis, Vienna, 2013 (CERN-THESIS-2013-257)

TMCI and space charge

- Some theories *[Blaskiewicz, Burov09, Balbekov]* predict that the **TMCI should be suppressed by space-charge forces** while others not *[Chin, Alexahin]*
  - **The suppression of the instability is not observed** in some machines featuring strong space-charge forces

[Bartosik]

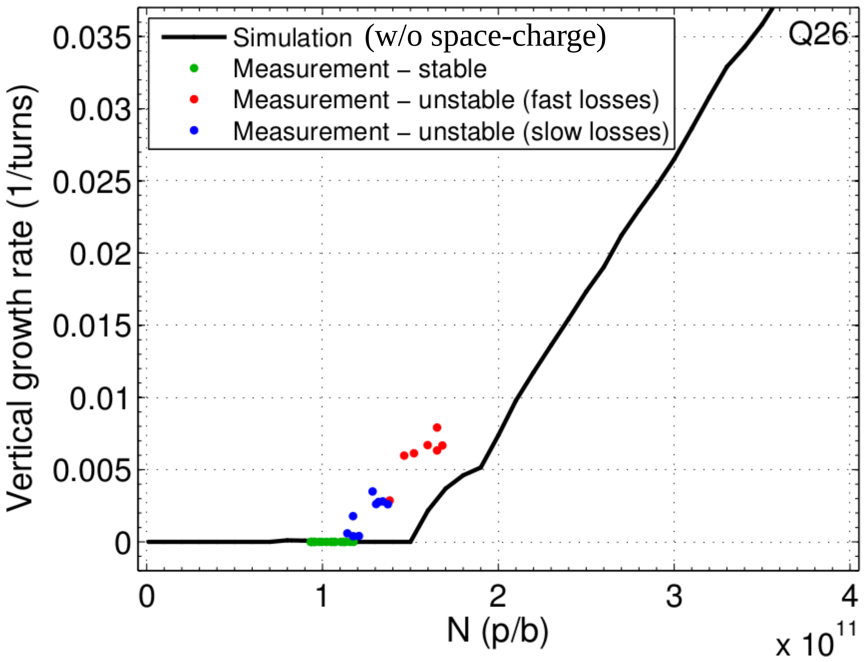

- It is claimed in [Burov19] that the missing ingredient in theories predicting the suppression of TMCI is the existence of 'convective instabilities'

→ We may formalise this ingredient by considering the **non-normal** aspect of these instabilities within the circulant matrix model

[Balbekov] V. Balbekov, Phys. Rev. Accel. Beams 20, 034401 (2017)
[Burov09] A. Burov, Phys. Rev. ST Accel. Beams 12, 044202 (2009)
[Burov19] A. Burov, Phys. Rev. Accel. Beams 22, 034202 (2019)
[Bartosik] H. Bartosik, PhD Thesis, Vienna, 2013 (CERN-THESIS-2013-257)

Beam stability without eigenvalues *[Trefethen]*

- Dynamical systems can exhibit transient growth even if all eigenvalues are stable

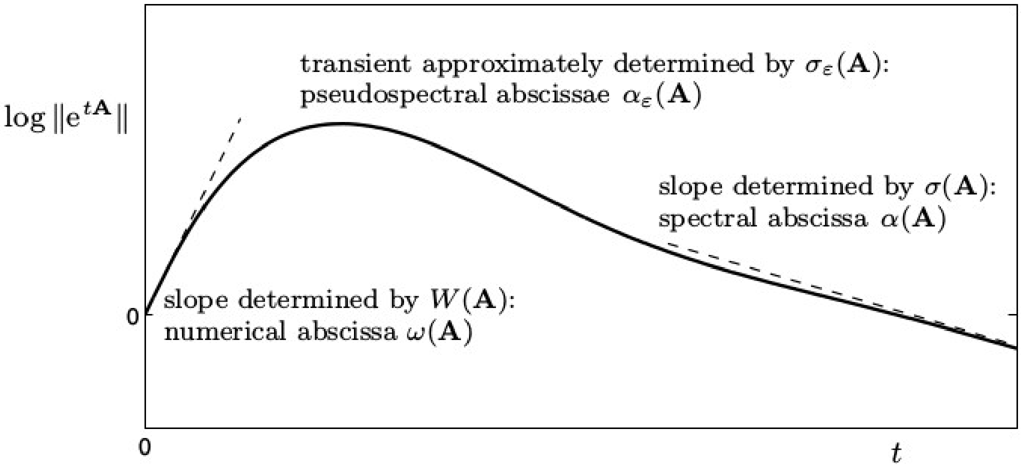

[Trefethen] L.N. Trefethen, M. Embree, Spectra and pseudospectra: The behaviour of non-normal matrices and operators, Princeton University Press (2005)

Beam stability without eigenvalues *[Trefethen]*

- Dynamical systems can exhibit transient growth even if all eigenvalues are stable

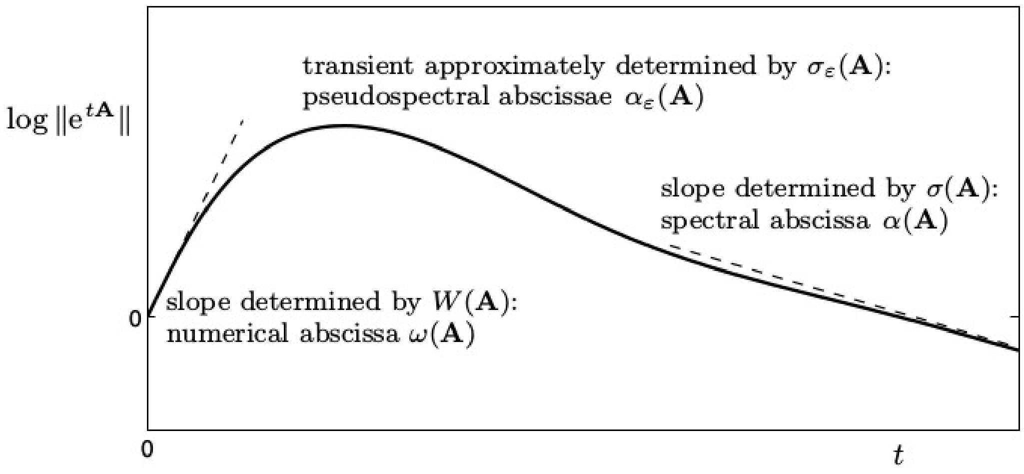

  - If the transient growth is sufficiently large, the observables may be similar to the one of a normal instability (here : head-tail oscillations and eventually beam losses and/or emittance growth)

[Trefethen] L.N. Trefethen, M. Embree, Spectra and pseudospectra: The behaviour of non-normal matrices and operators, Princeton University Press (2005)

Beam stability without eigenvalues *[Trefethen]*

- Dynamical systems can exhibit transient growth even if all eigenvalues are stable

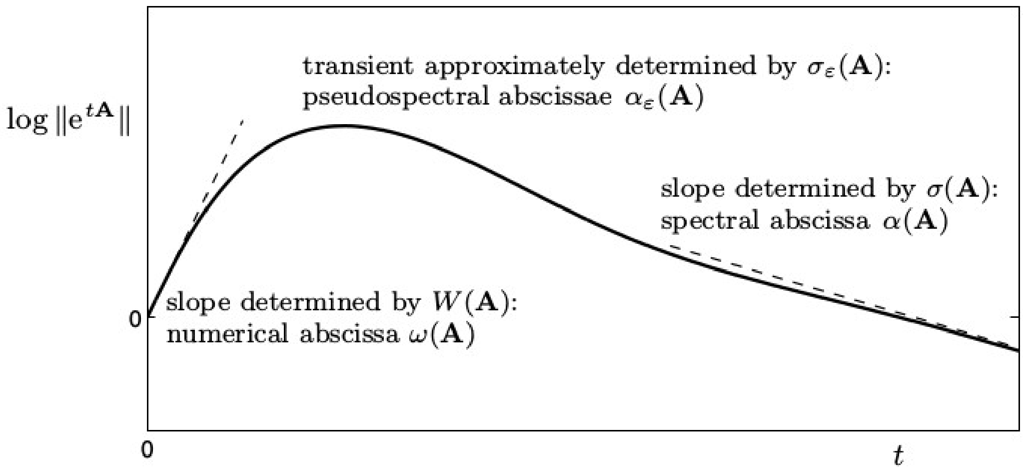

  - If the transient growth is sufficiently large, the observables may be similar to the one of a normal instability (here : head-tail oscillations and eventually beam losses and/or emittance growth)

- The notion of spectrum (i.e. eigenvalues) can be extended to characterise the sensitivity of a dynamical system to perturbations:

$$\mathrm{Spectrum}(M) = \{\lambda \in \mathbb{C} | \exists \overrightarrow{v} : (M - \lambda I) \cdot \overrightarrow{v} = 0\}$$

$$\mathrm{Pseudospectrum}(M, \epsilon) = \{\lambda \in \mathbb{C} | \exists \overrightarrow{v} : ||(M - \lambda I) \cdot \overrightarrow{v}|| < \epsilon\}$$

[Trefethen] L.N. Trefethen, M. Embree, Spectra and pseudospectra: The behaviour of non-normal matrices and operators, Princeton University Press (2005)

Beam stability without eigenvalues *[Trefethen]*

- Dynamical systems can exhibit transient growth even if all eigenvalues are stable

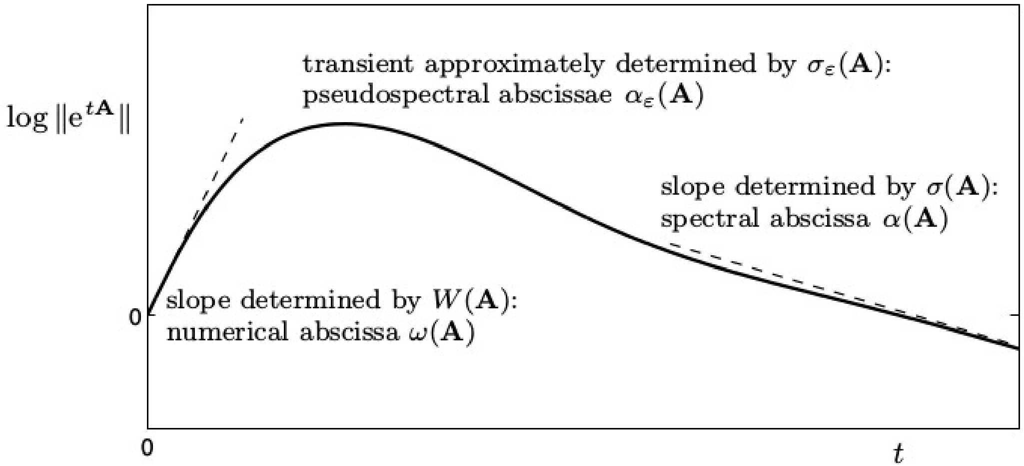

  - If the transient growth is sufficiently large, the observables may be similar to the one of a normal instability (here : head-tail oscillations and eventually beam losses and/or emittance growth)

- The notion of spectrum (i.e. eigenvalues) can be extended to characterise the sensitivity of a dynamical system to perturbations:

$$\mathrm{Spectrum}(M) = \{\lambda \in \mathbb{C} | \exists \overrightarrow{v} : (M - \lambda I) \cdot \overrightarrow{v} = 0\}$$

$$\mathrm{Pseudospectrum}(M, \epsilon) = \{\lambda \in \mathbb{C} | \exists \overrightarrow{v} : ||(M - \lambda I) \cdot \overrightarrow{v}|| < \epsilon\}$$

- The pseudospectrum answers the question “How much may the eigenvalues of a matrix change under a perturbation of order ε?”

- Numerically it can be obtained implicitly using the smallest singular value:

$$\epsilon(M, \lambda) = s_{min}(M - \lambda I)$$

[Trefethen] L.N. Trefethen, M. Embree, Spectra and pseudospectra: The behaviour of non-normal matrices and operators, Princeton University Press (2005)

The circulant matrix model

- The longitudinal distribution of the beam is discretised in polar coordinates
- In the transverse plane, each beamlet has the same distribution, described by their moments $\langle x \rangle_i$ and $\langle x' \rangle_i$

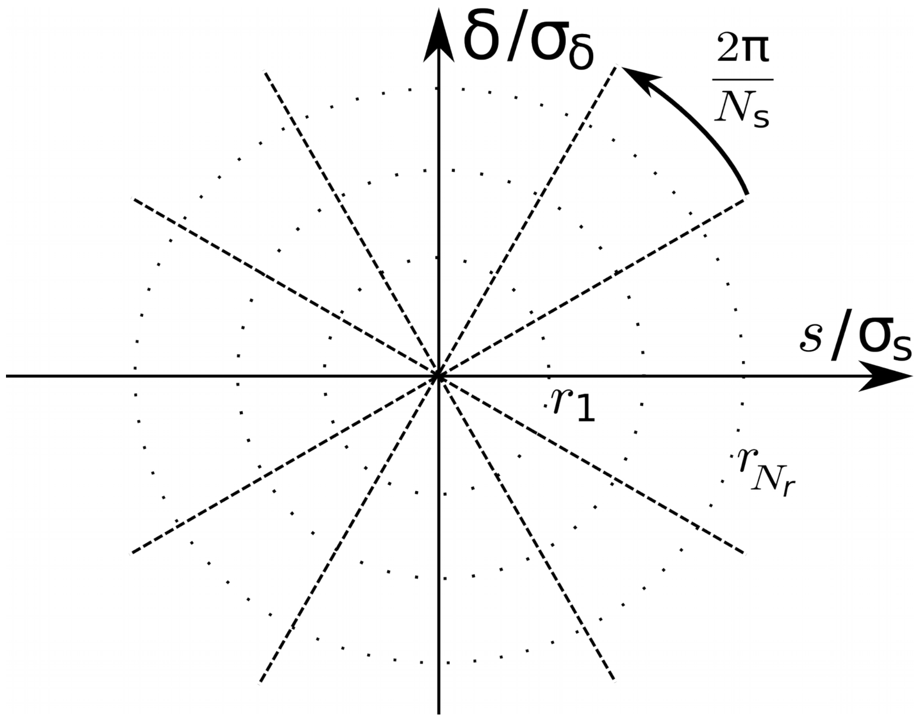

The circulant matrix model

- The longitudinal distribution of the beam is discretised in polar coordinates
- In the transverse plane, each beamlet has the same distribution, described by their moments $\langle x \rangle_i$ and $\langle x' \rangle_i$

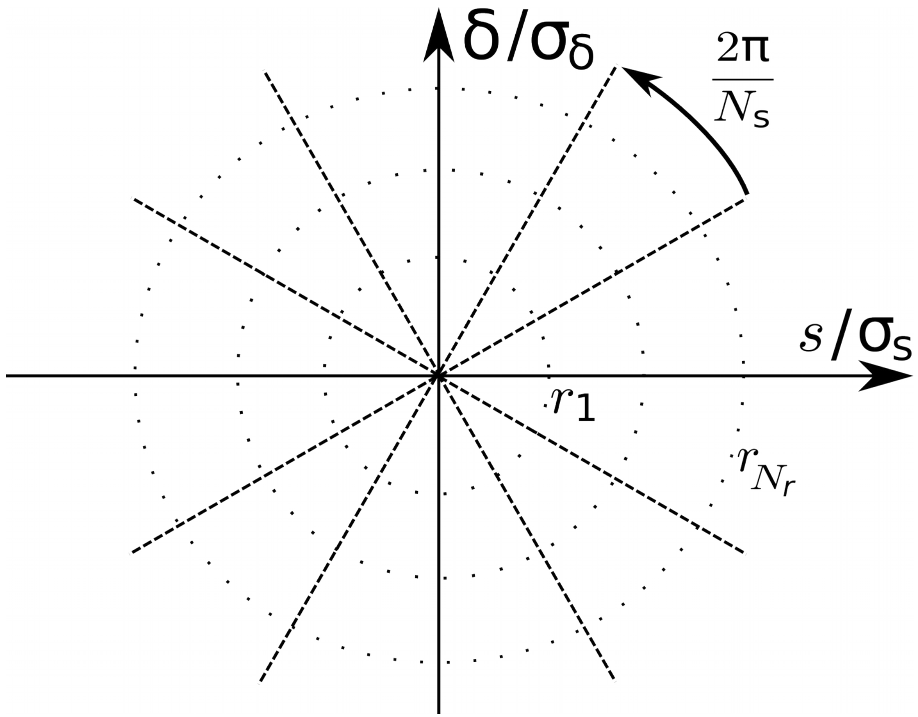

→ We write the one turn matrix for the average transverse positions and divergences, including the lattice linear rotation and the coherent forces (wakefields and linearised space charge), for details see the appendix

→ Diagonalising the matrix, we obtain the complex coherent tunes of the normal mode of oscillation (also called the *spectrum*)

Pseudospectrum example

- Let us consider a toy example:

$$M = \begin{pmatrix} \cos(2\pi 0.31) & \sin(2\pi 0.31) & 0 & 0 \\ -\sin(2\pi 0.31) & \cos(2\pi 0.31) & K/10 & 0 \\ 0 & 0 & \cos(2\pi 0.31) & \sin(2\pi 0.31) \\ K & 0 & -\sin(2\pi 0.31) & \cos(2\pi 0.31) \end{pmatrix}$$

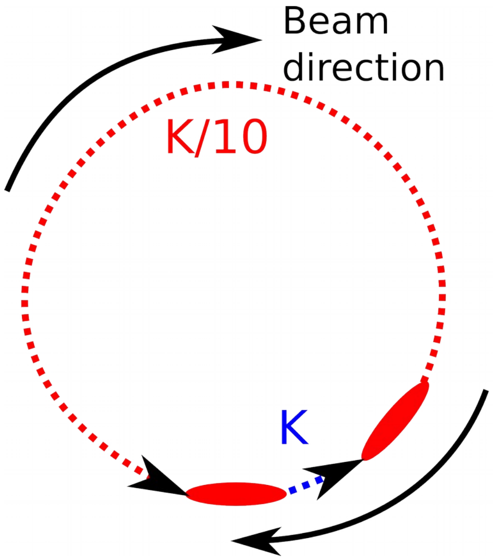

Pseudospectrum example

- Let us consider a toy example:

$$M = \begin{pmatrix} \cos(2\pi 0.31) & \sin(2\pi 0.31) & 0 & 0 \\ -\sin(2\pi 0.31) & \cos(2\pi 0.31) & K/10 & 0 \\ 0 & 0 & \cos(2\pi 0.31) & \sin(2\pi 0.31) \\ K & 0 & -\sin(2\pi 0.31) & \cos(2\pi 0.31) \end{pmatrix}$$

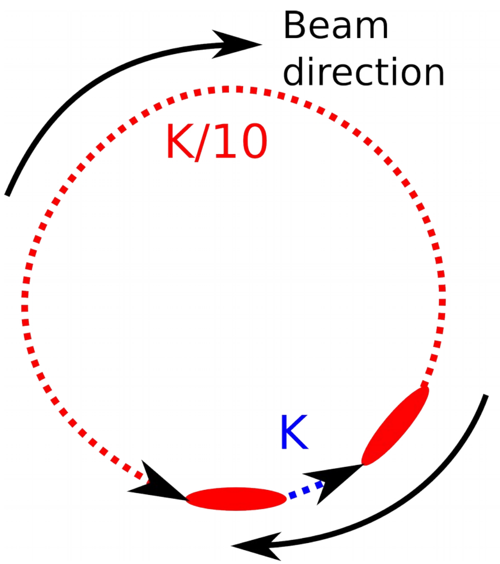

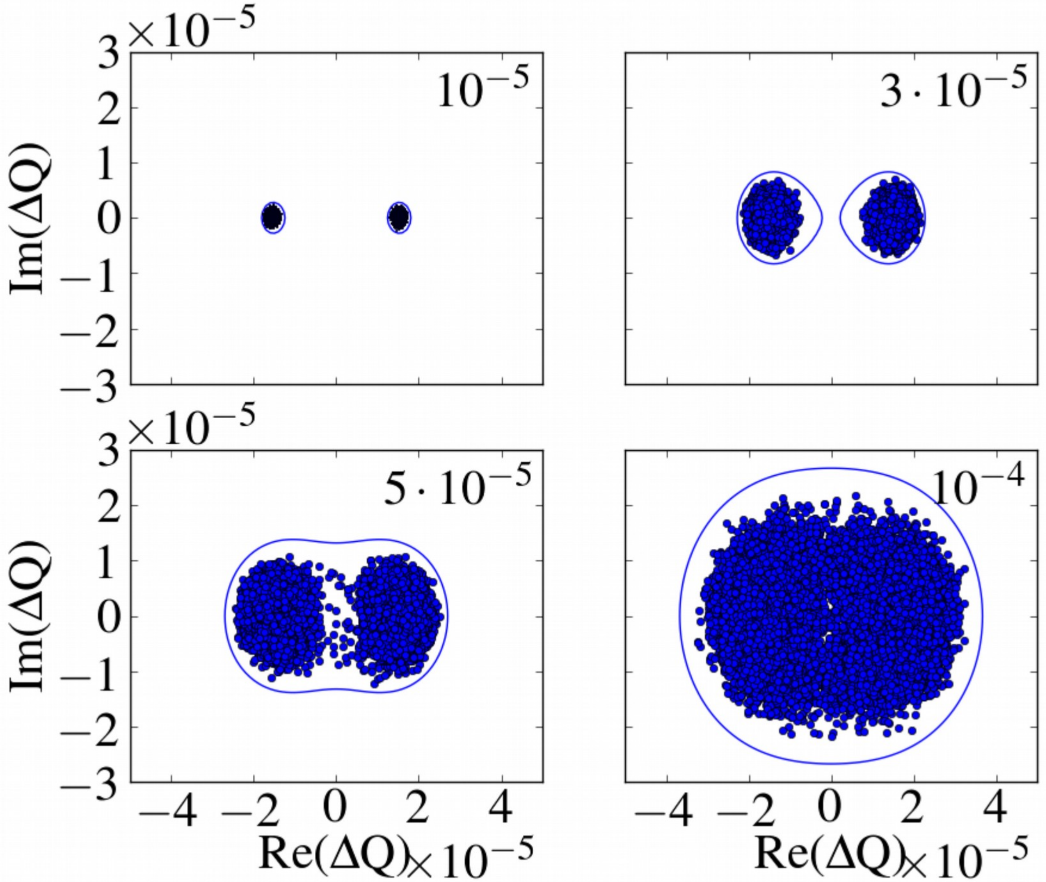

- The lines show the pseudospectrum for a fixed ε, i.e. all eigenvalues reachable with a perturbation of order ε
- The dots show the eigenvalues of M+E, where E is random matrix with ||E|| = ε

Pseudospectrum representation

- The pseudo spectrum is conveniently reported using contours of equal -$\log_{10}(\varepsilon)$
  - The eigenvalues appear as infinite dips (ε=0), then epsilon increases away from them

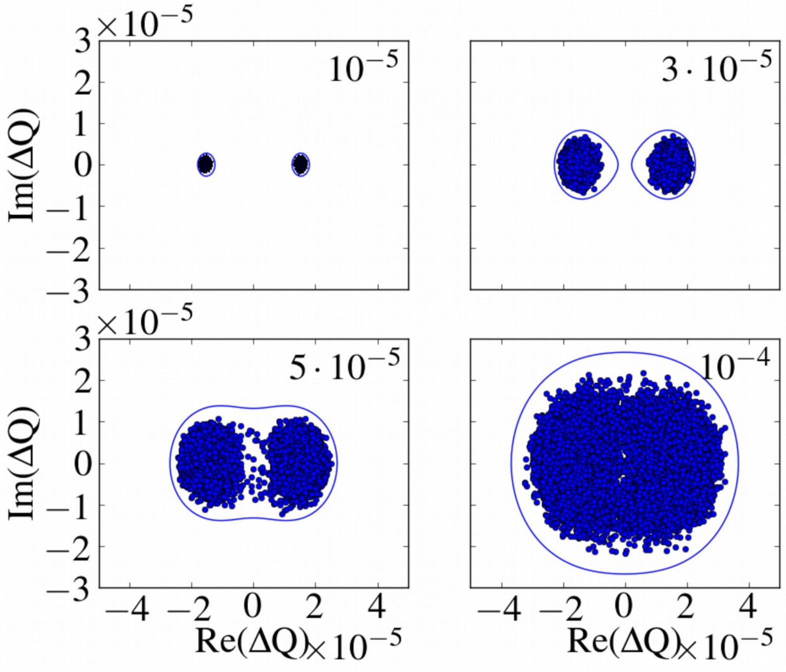

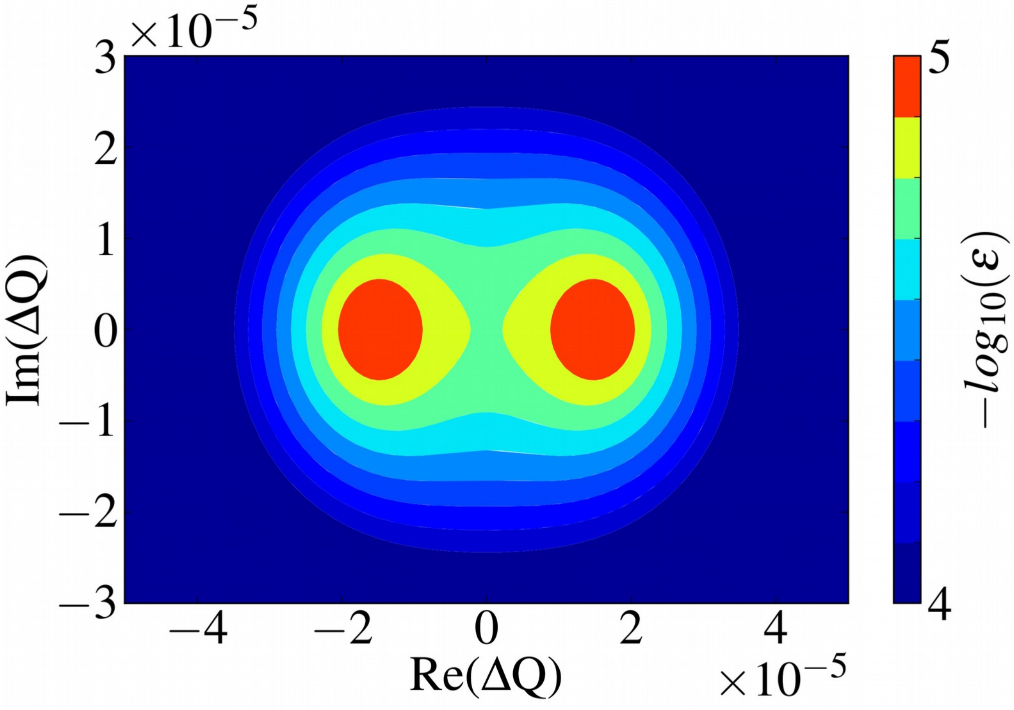

Pseudo spectrum in the presence of wake fields and space-charge

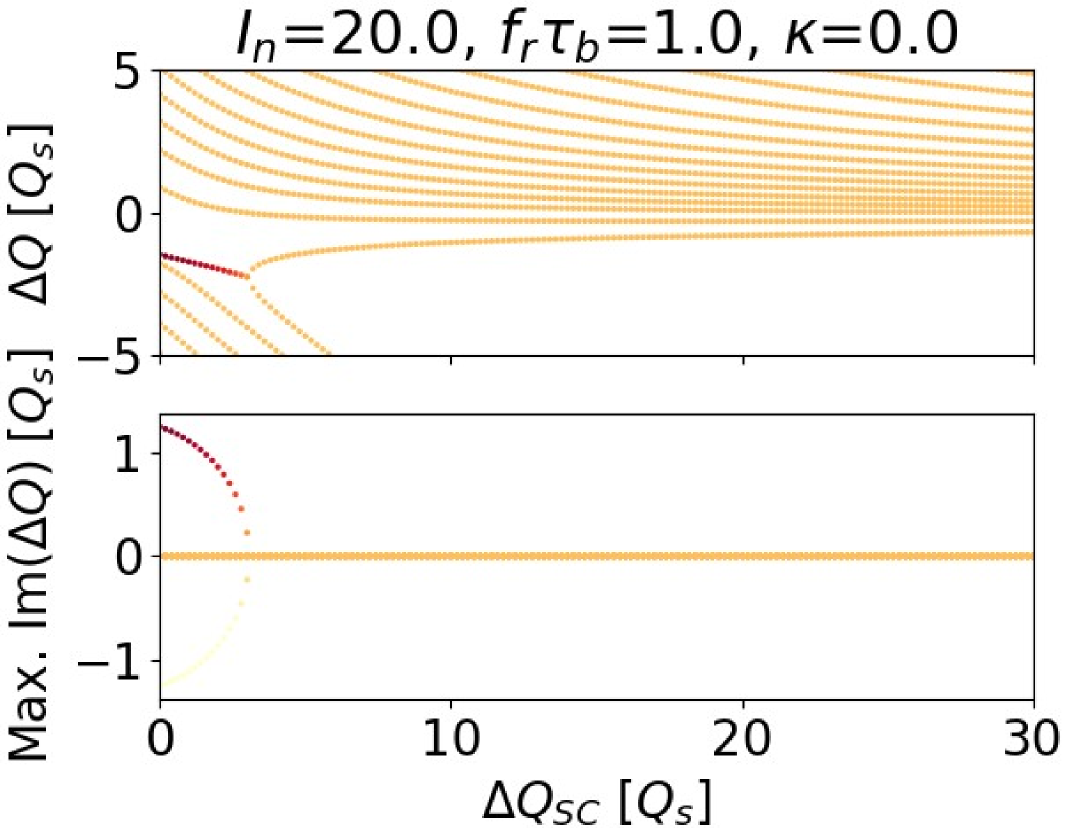

Pseudo spectrum in the presence of wake fields and space-charge

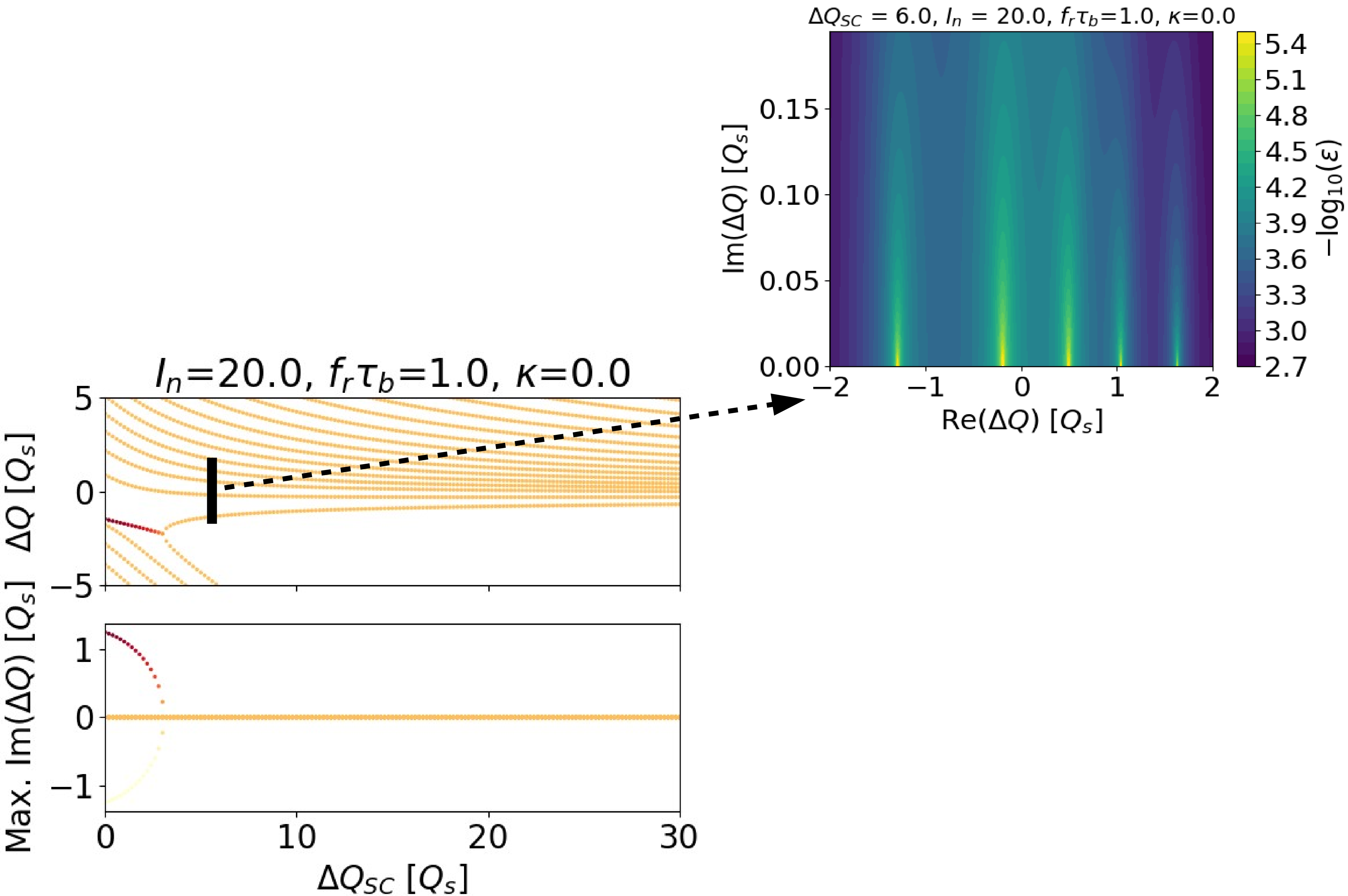

Pseudo spectrum in the presence of wake fields and space-charge

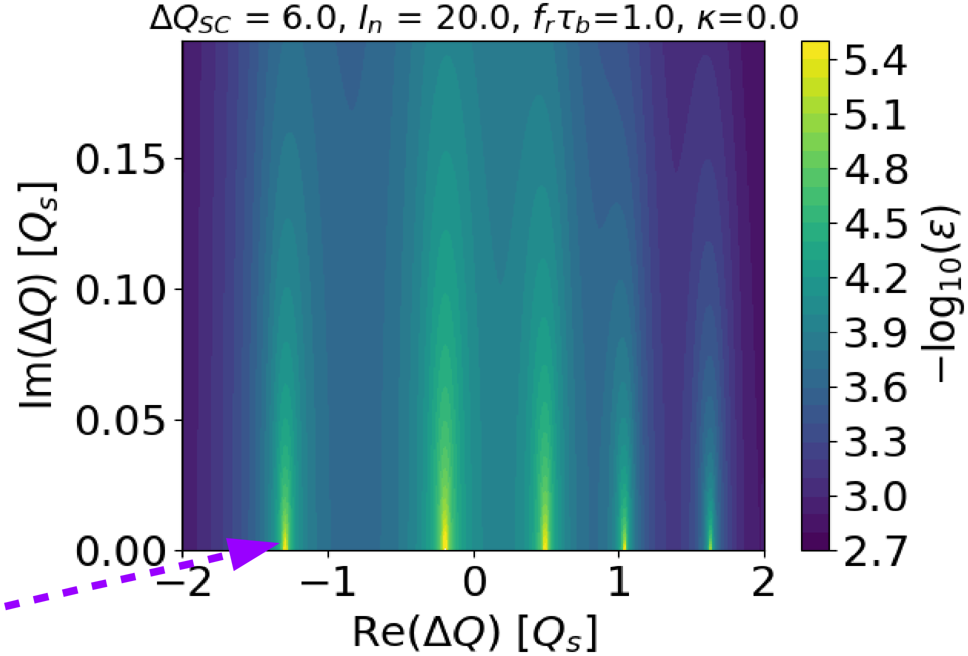

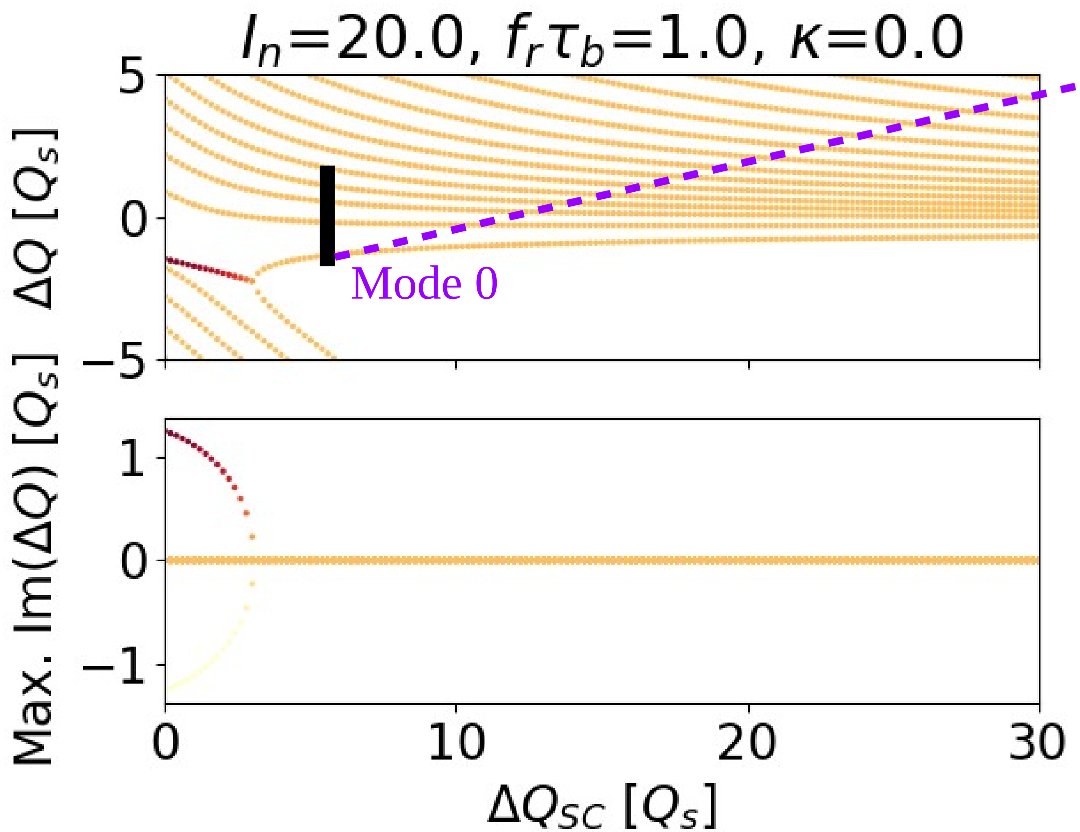

Pseudo spectrum in the presence of wake fields and space-charge

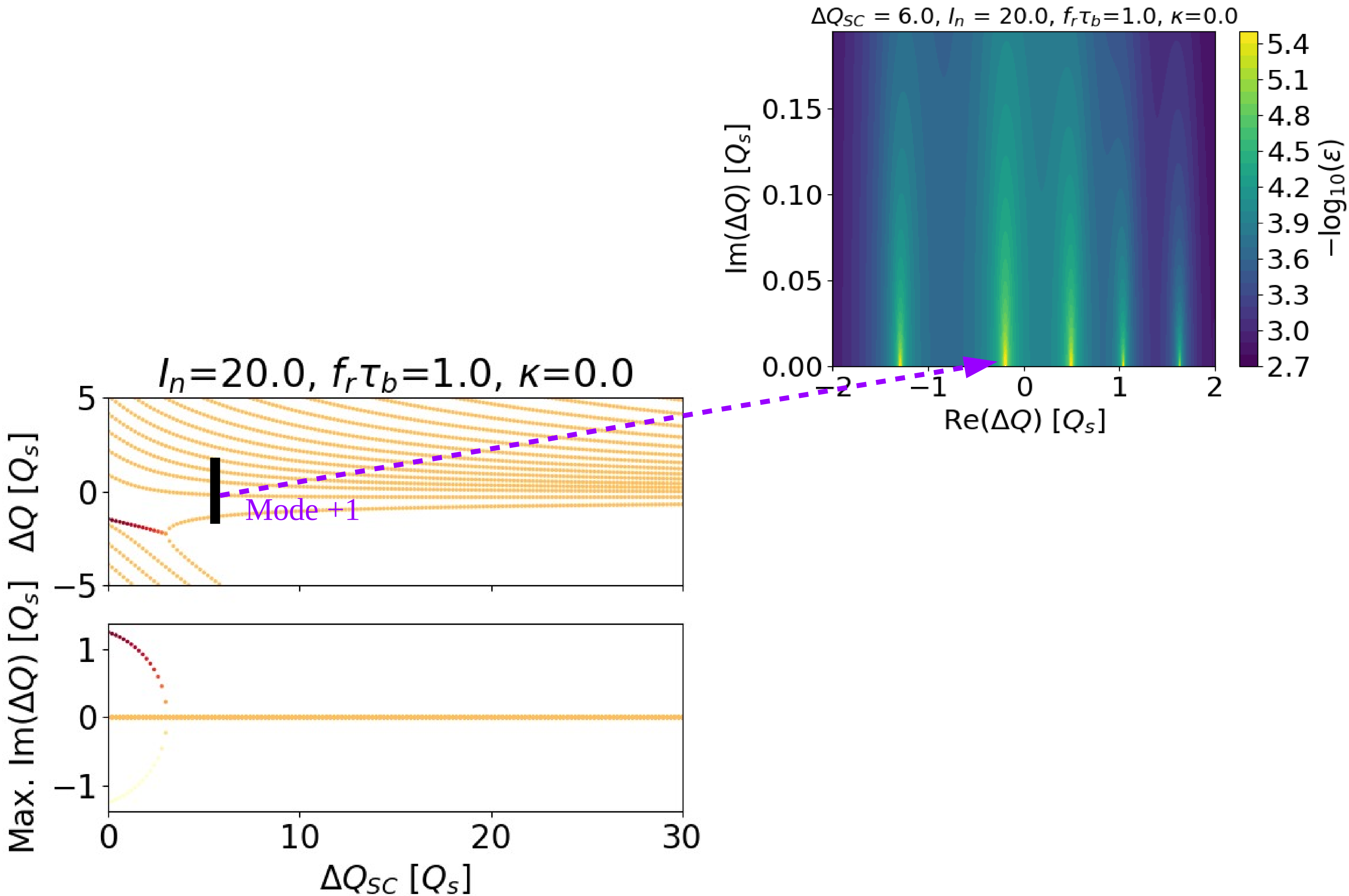

Pseudo spectrum in the presence of wake fields and space-charge

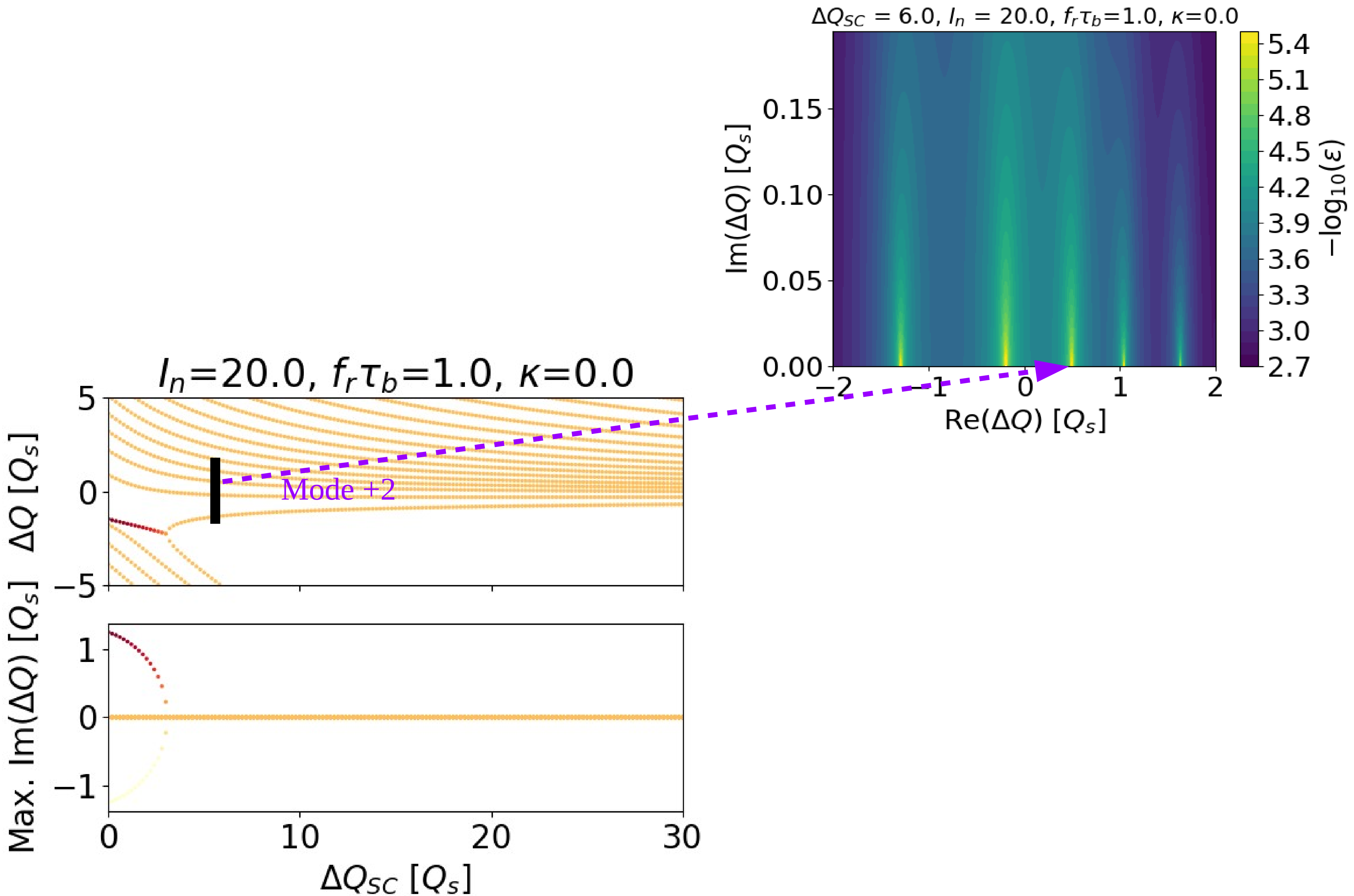

Pseudo spectrum in the presence of wake fields and space-charge

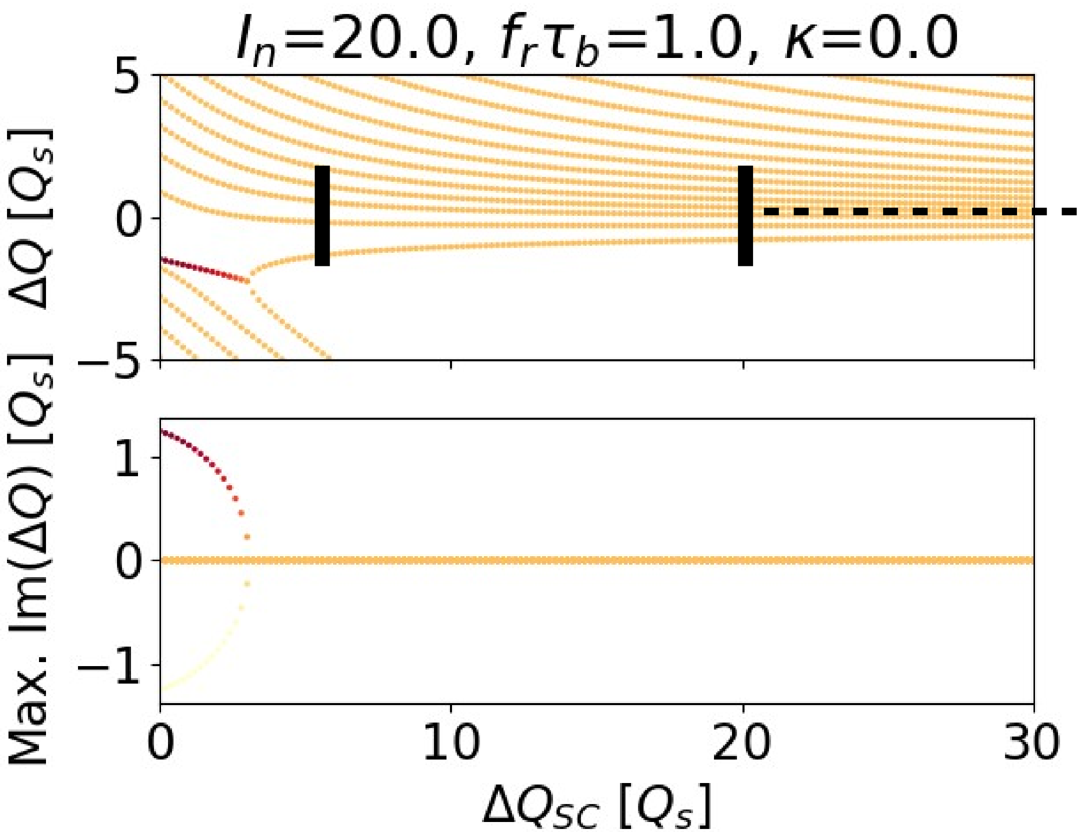

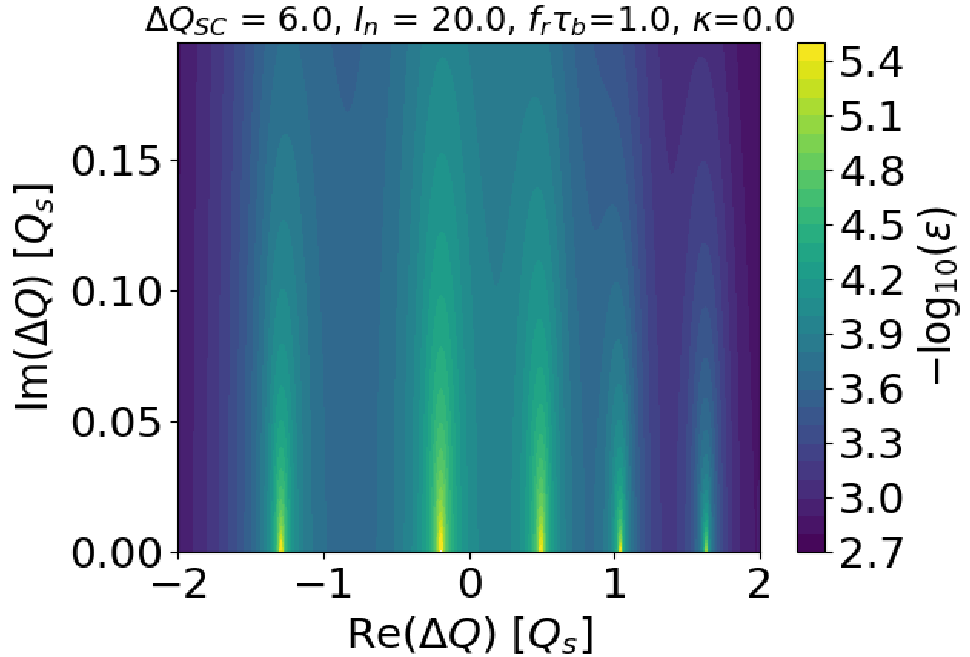

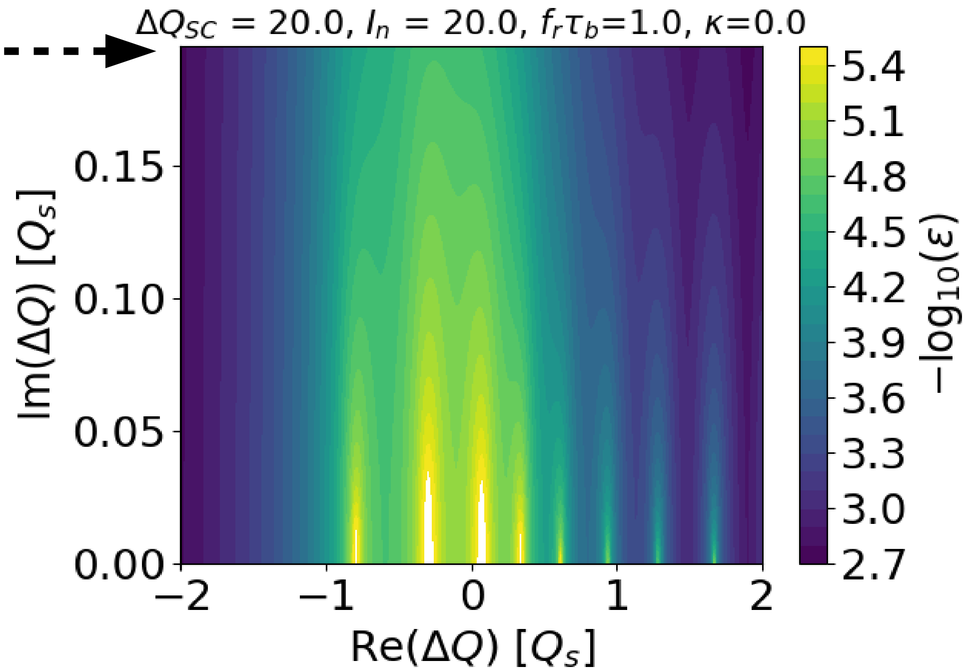

Pseudo spectrum in the presence of wake fields and space-charge

- Due to the **proximity of the eigenvalues** caused by space-charge, the pseudospectrum increases significantly close to ΔQ=0

  → The beam is more prone to instabilities under small perturbations

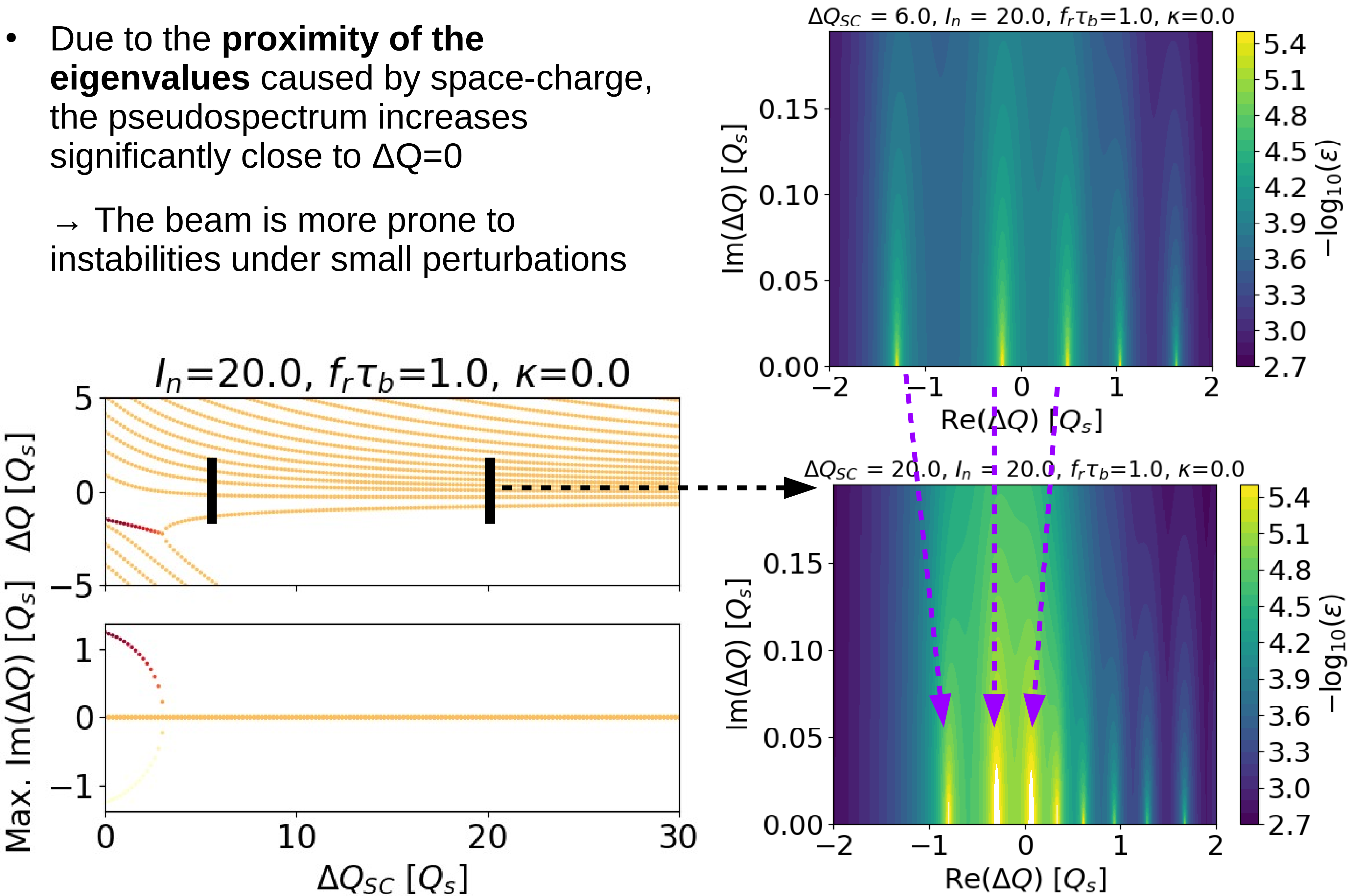

The Kreiss matrix theorem

[Trefethen]

- For a matrix M of size N, the maximum of the transient growth is bounded as follows:

$$\mathcal{K}(M) < \sup_{t>0} ||M^t|| < eN\mathcal{K}(M)$$

with K(M) the Kreiss constant

The Kreiss matrix theorem *[Trefethen]*

- For a matrix M of size N, the maximum of the transient growth is bounded as follows:

$$\mathcal{K}(M) < \sup_{t>0} ||M^t|| < eN\mathcal{K}(M)$$

with K(M) the Kreiss constant

Above TMCI, lifted by strong space charge

Above TMCI, lifted by weaker space charge

Below TMCI, without space charge

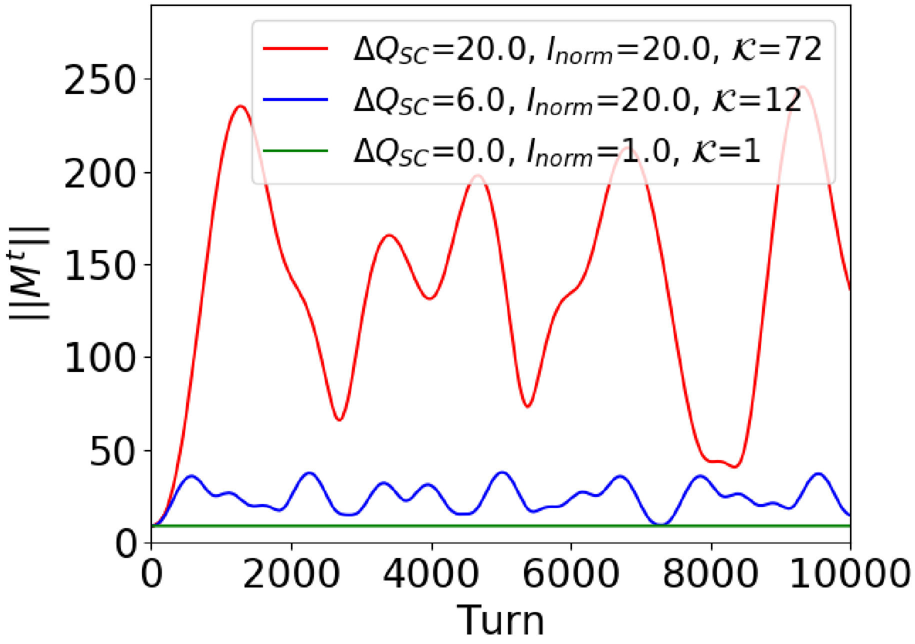

The Kreiss matrix theorem *[Trefethen]*

- For a matrix M of size N, the maximum of the transient growth is bounded as follows:

$$\mathcal{K}(M) < \sup_{t>0} ||M^t|| < eN\mathcal{K}(M)$$

with K(M) the Kreiss constant

Above TMCI, lifted by strong space charge

Above TMCI, lifted by weaker space charge

Below TMCI, without space charge

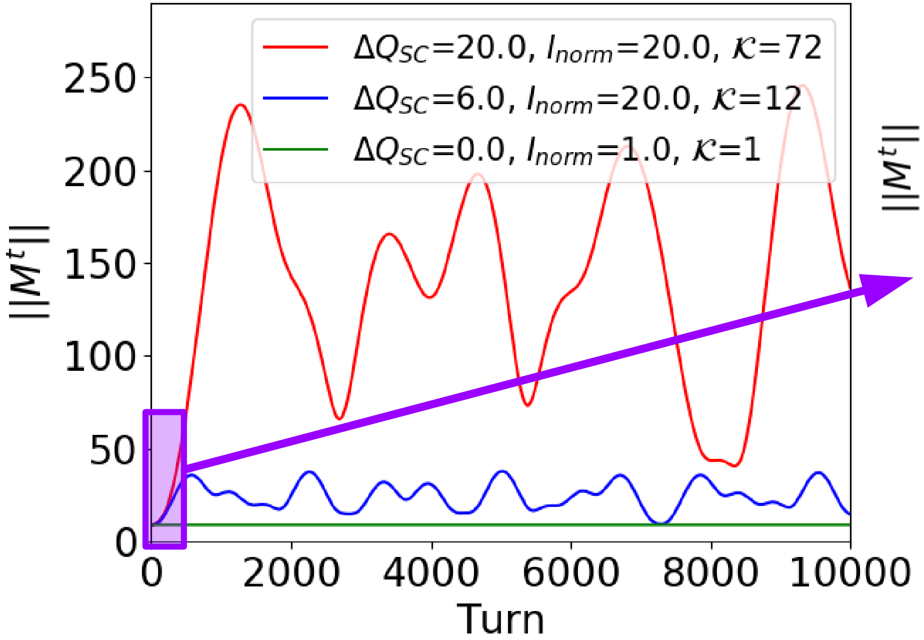

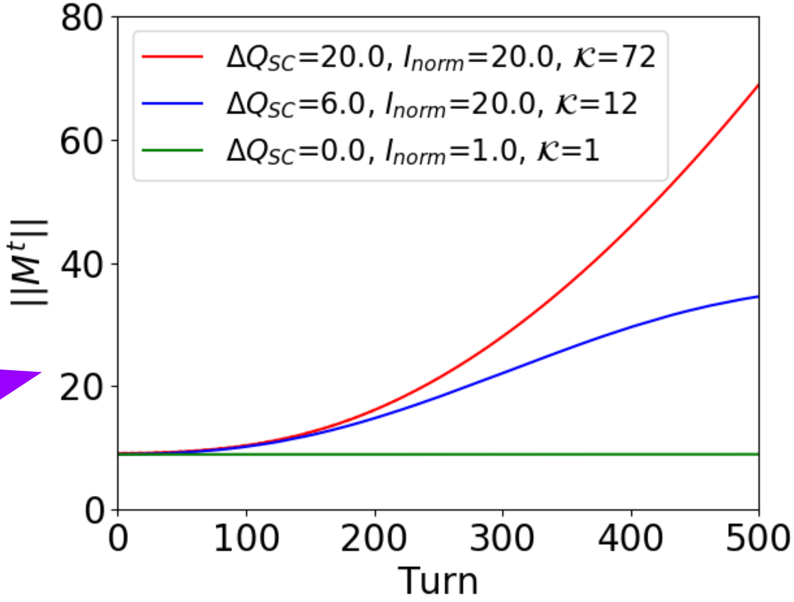

- For a matrix M of size N, the maximum of the transient growth is bounded as follows:

$$\mathcal{K}(M) < \sup_{t>0} ||M^t|| < eN\mathcal{K}(M)$$

with K(M) the Kreiss constant

Above TMCI, lifted by strong space charge

Above TMCI, lifted by weaker space charge

Below TMCI, without space charge

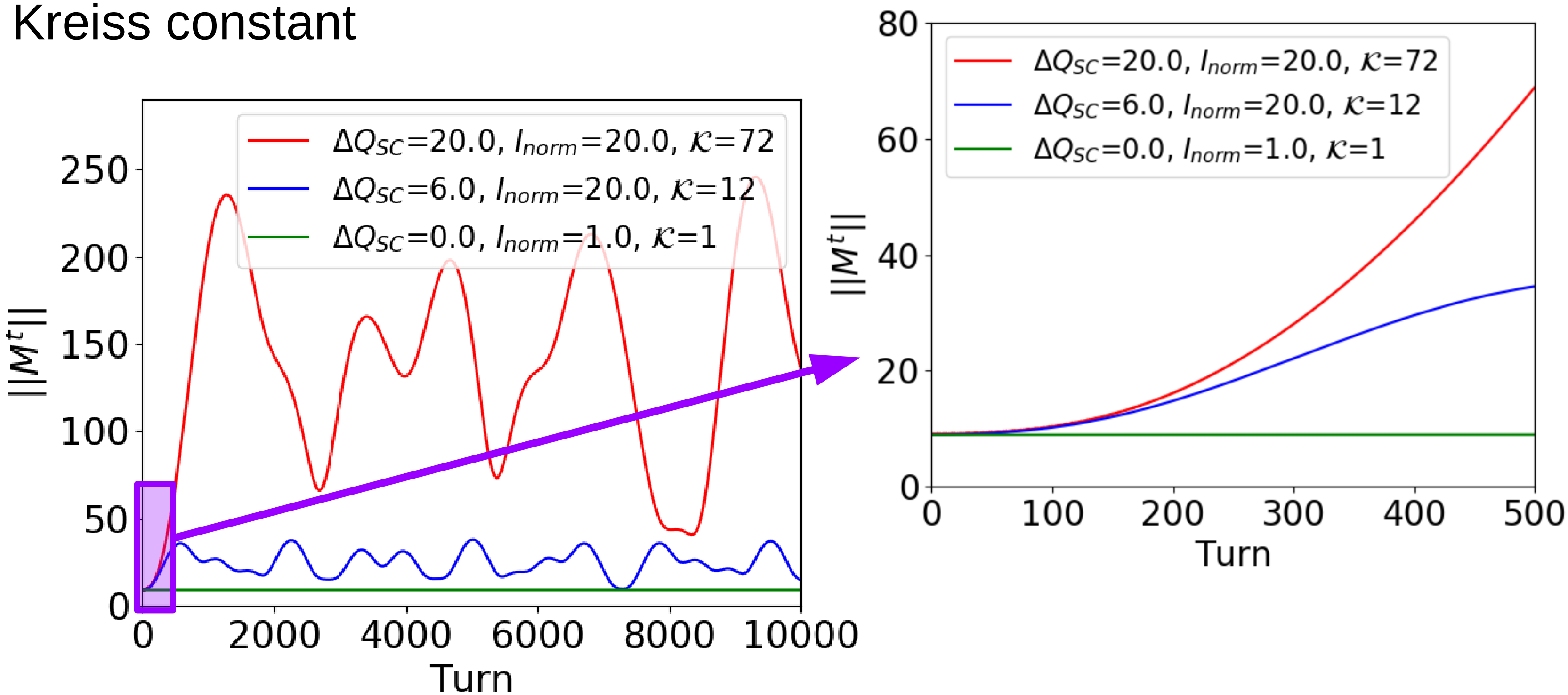

- The Kreiss constant can be obtained from the pseudospectrum:

$$\mathcal{K}(M) = \max_{\Im\lambda>0} \frac{||\lambda|| - 1}{\epsilon(M,\lambda)}$$

Transient growth in the presence of wake fields and space-charge

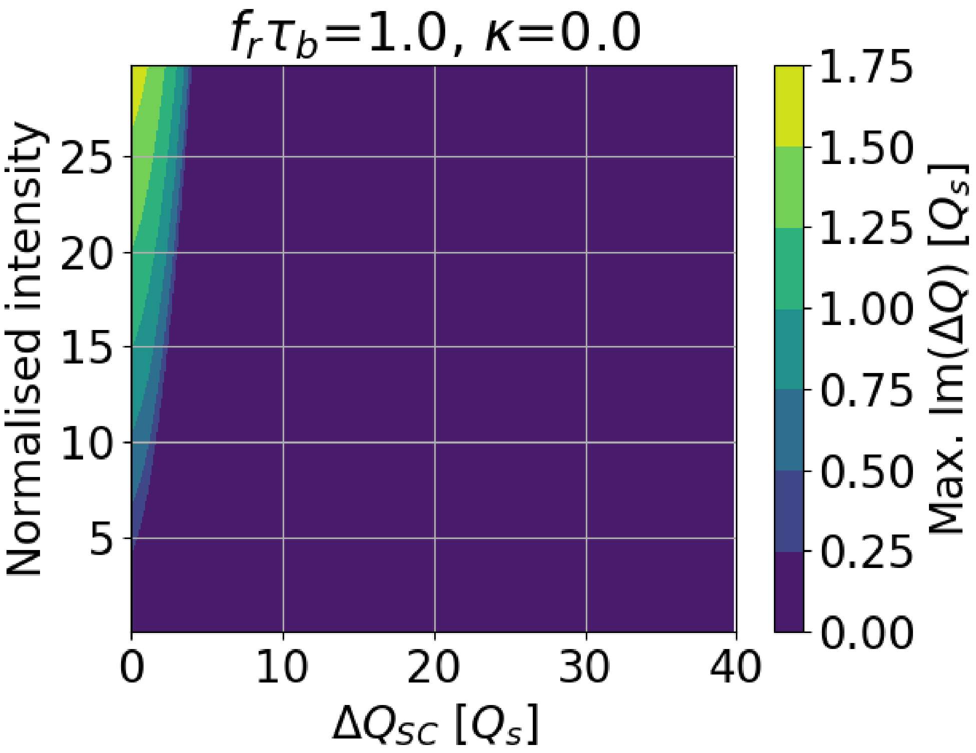

Transient growth in the presence of wake fields and space-charge

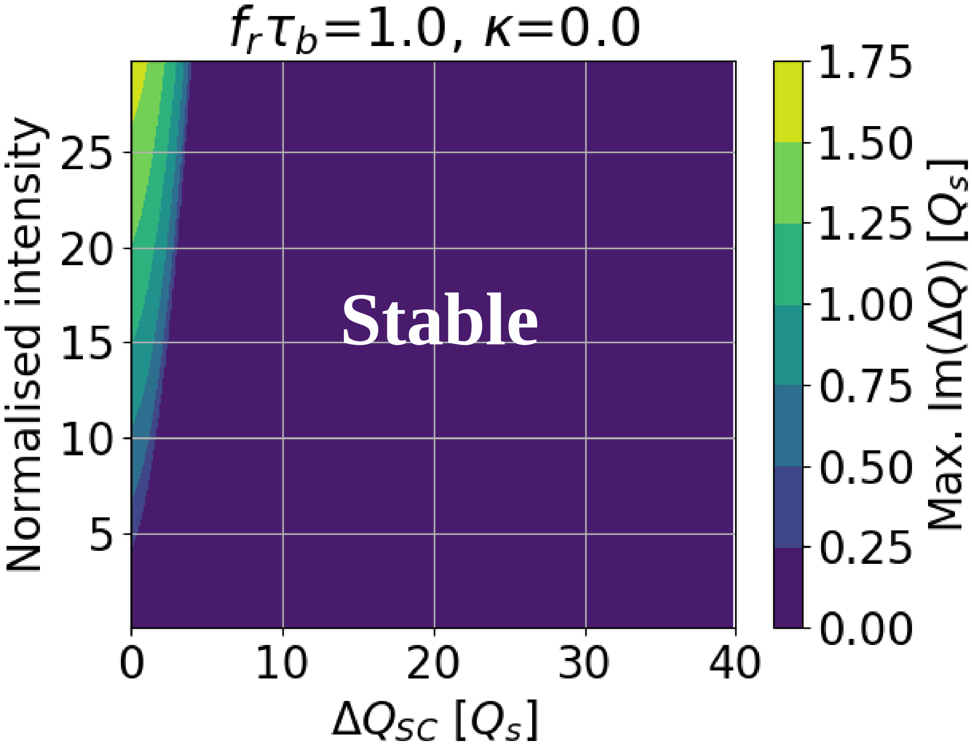

Transient growth in the presence of wake fields and space-charge

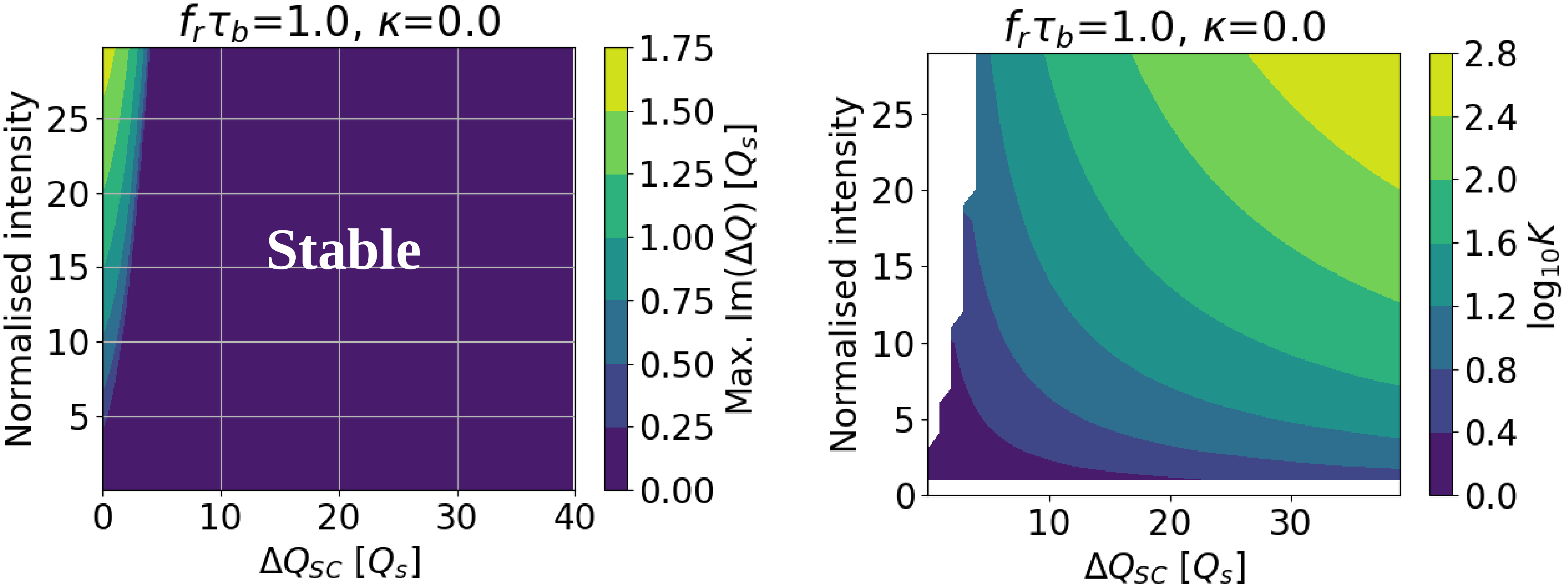

Transient growth in the presence of wake fields and space-charge

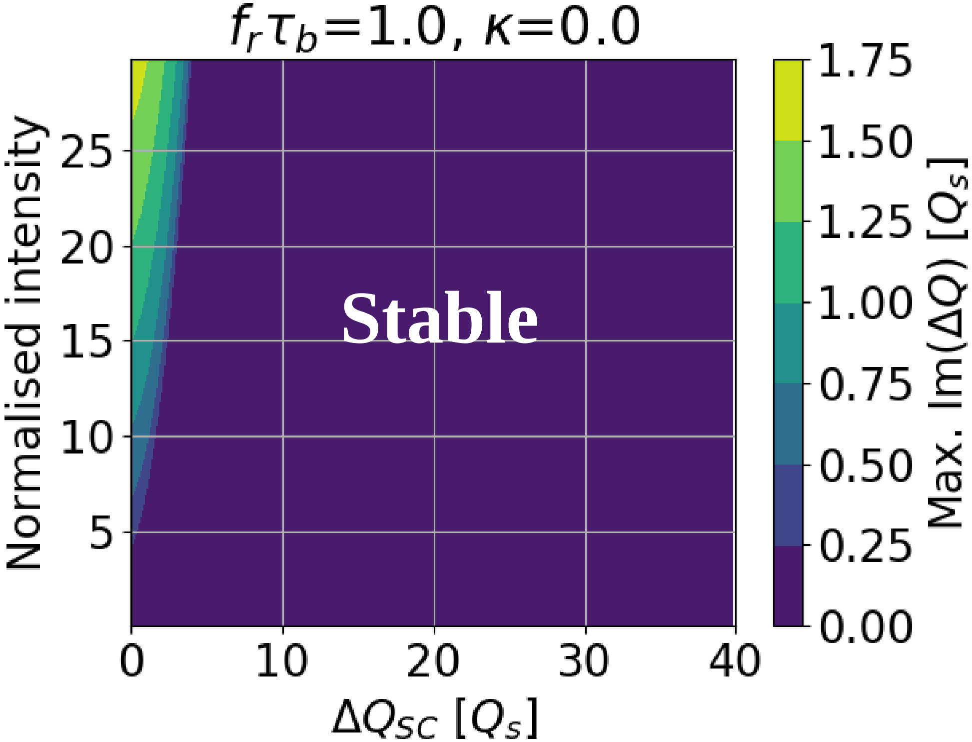

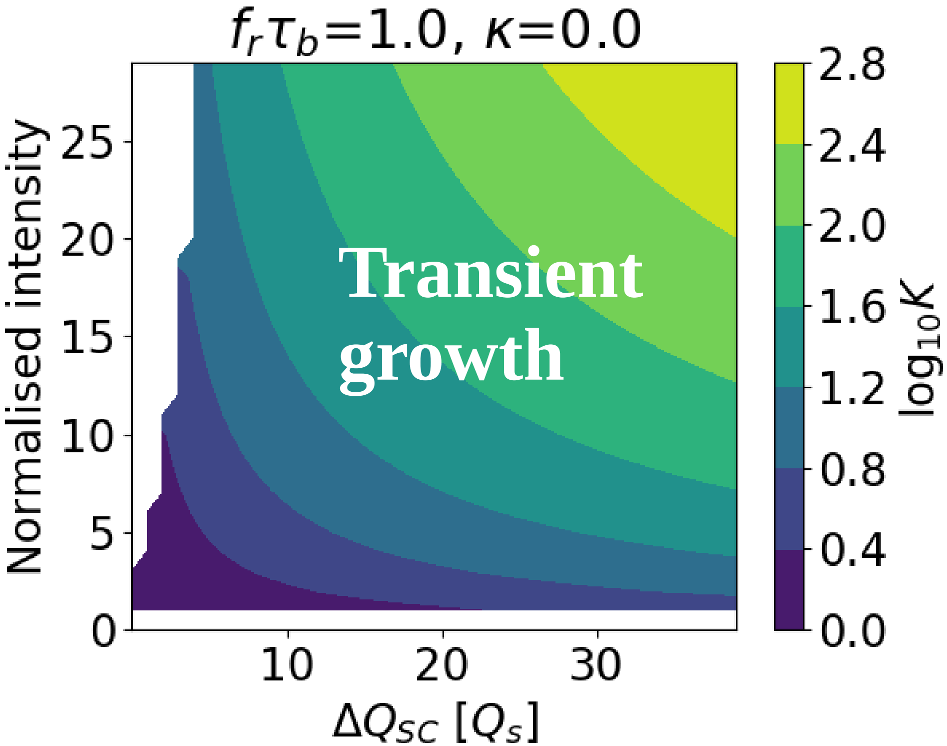

- In the area where the beam is stabilised by space-charge, the potential for transient growth increases

Transient growth in the presence of wake fields and space-charge

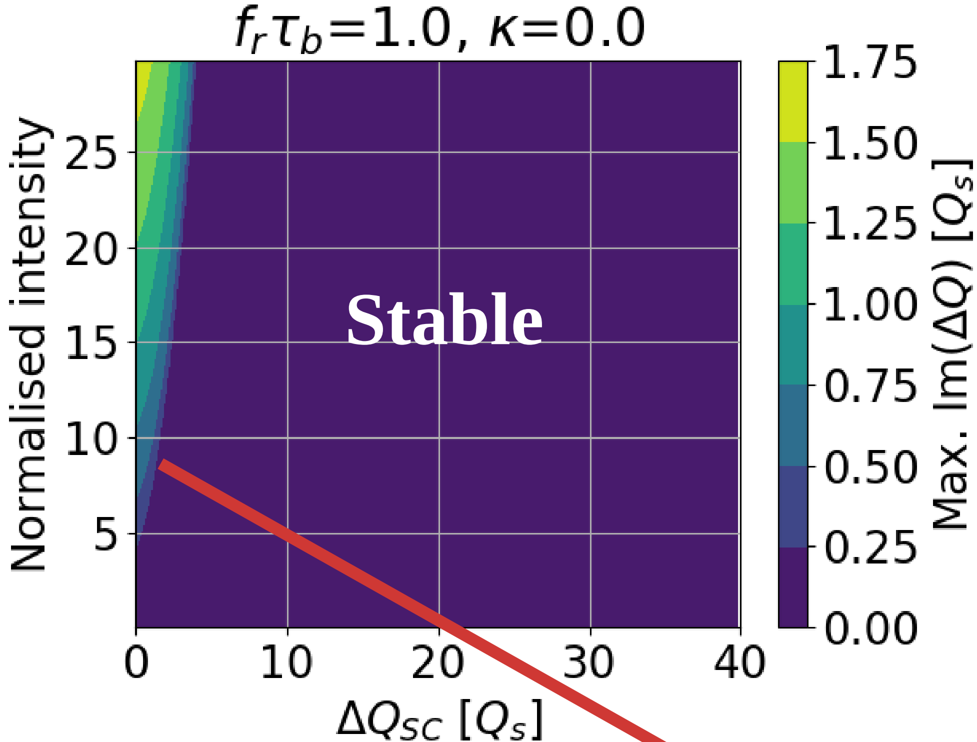

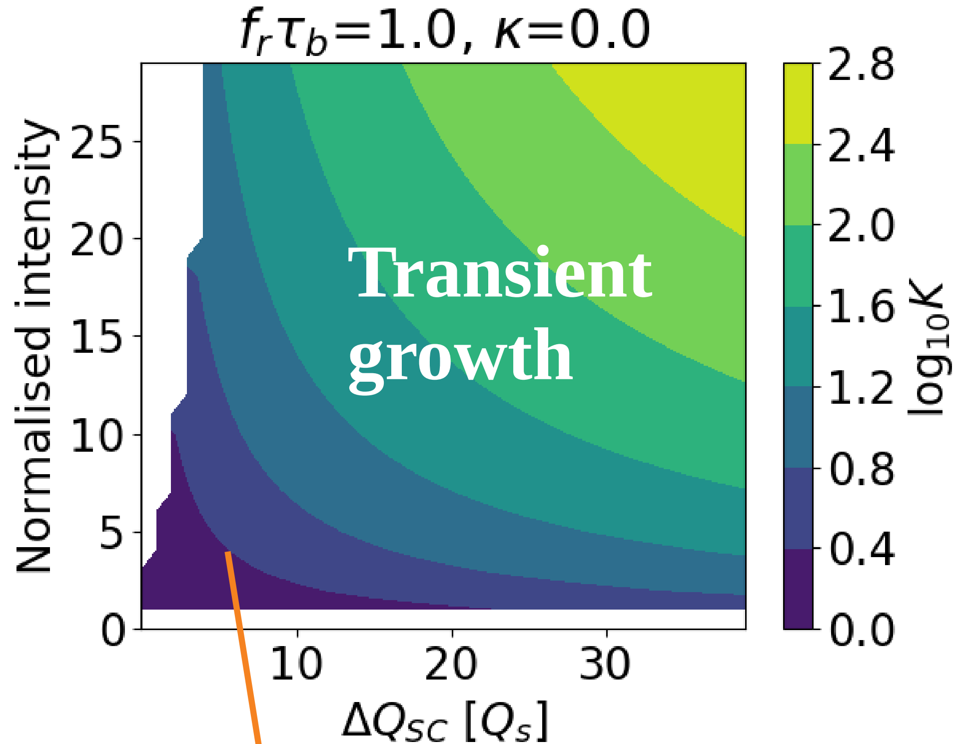

- In the area where the beam is stabilised by space-charge, the potential for transient growth increases
- The behaviour of the transient growth seems comparable to the one predicted by the 2 particle model *[Chin]*

[Chin]

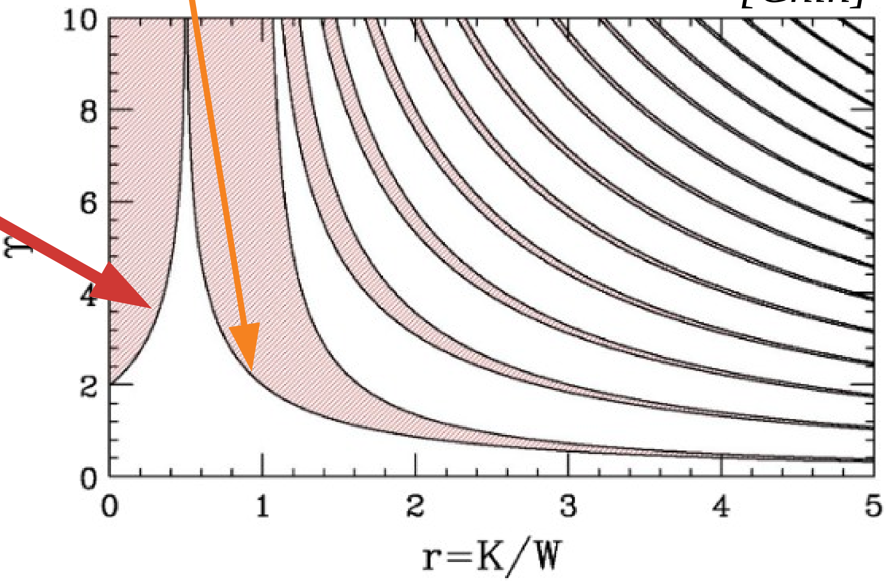

Transient growth in the presence of wake fields and space-charge

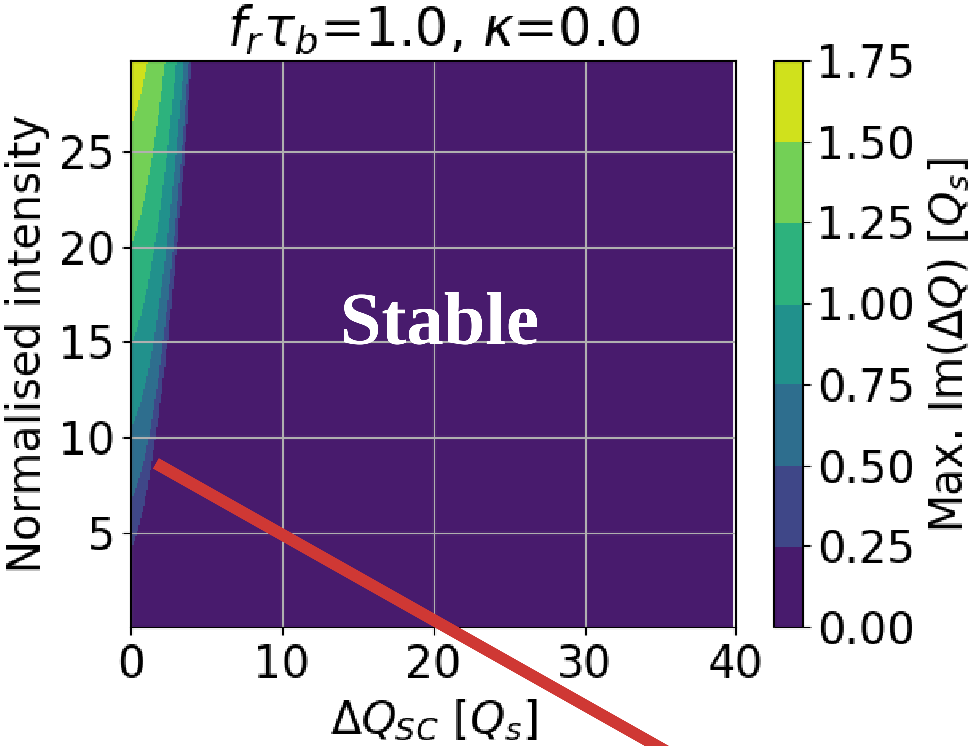

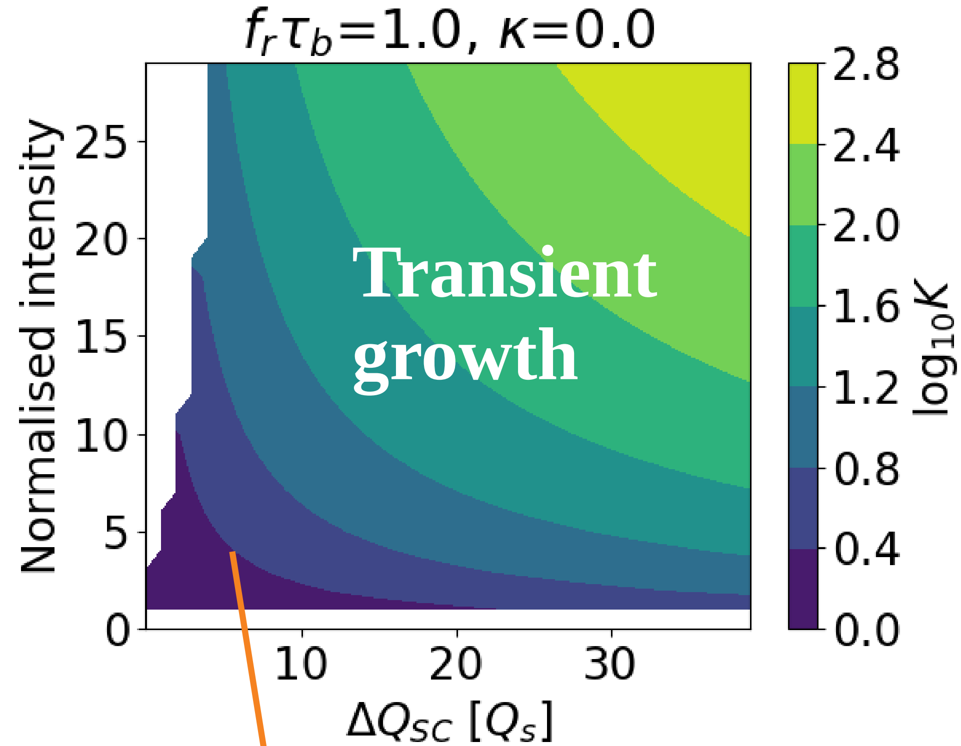

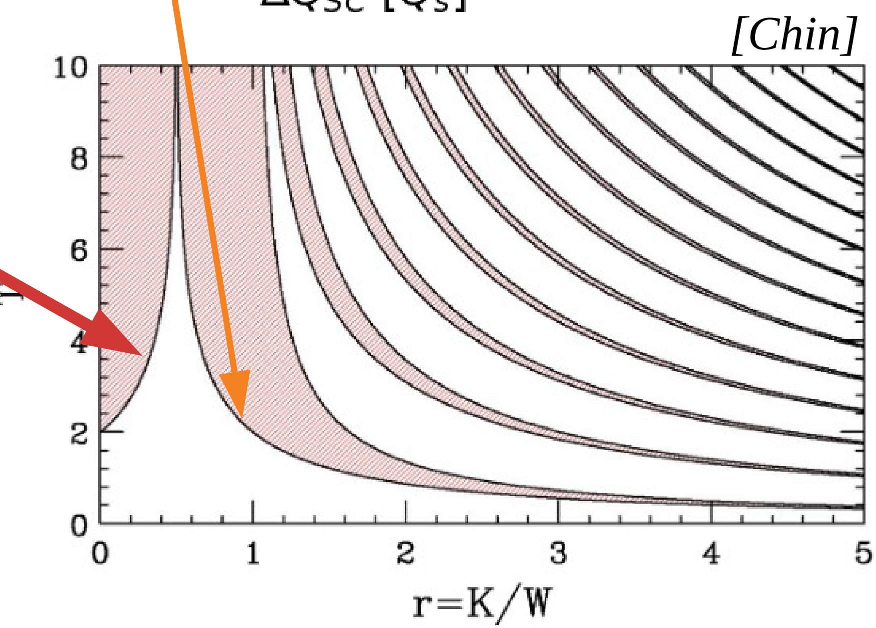

- In the area where the beam is stabilised by space-charge, the potential for transient growth increases
- The behaviour of the transient growth seems comparable to the one predicted by the 2 particle model *[Chin]*
- Such transient growth is often associated to convective instabilities, compatibly with *[Burov]*

Conclusion

- The results obtained with the ABS *[Blaskiewicz]* model were extended to a linear RF using the circulant matrix model (BimBim) with an air bag distribution

    → *Depression* of the coherent mode frequencies

    → Suppression of the TMCI by strong-space charge forces

Conclusion

- The results obtained with the ABS *[Blaskiewicz]* model were extended to a linear RF using the circulant matrix model (BimBim) with an air bag distribution

  → *Depression* of the coherent mode frequencies

  → Suppression of the TMCI by strong-space charge forces

- Using the pseudospectrum and the Kreiss constant of the one turn matrix, we find that the clustering of the coherent frequencies around ΔQ=0 results in large maximum transient growth (compatibly with the convective behaviour in *[Burov19]*)

  – This behaviour follows the same trend as the two particle model *[Chin]*.

Conclusion

- The results obtained with the ABS *[Blaskiewicz]* model were extended to a linear RF using the circulant matrix model (BimBim) with an air bag distribution

  → *Depression* of the coherent mode frequencies

  → Suppression of the TMCI by strong-space charge forces

- Using the pseudospectrum and the Kreiss constant of the one turn matrix, we find that the clustering of the coherent frequencies around ΔQ=0 results in large maximum transient growth (compatibly with the convective behaviour in *[Burov19]*)
  - This behaviour follows the same trend as the two particle model *[Chin]*.

- Today we considered an approximate model: The airbag distribution. By considering a more realistic distribution and including radial modes, the TMCI is recovered using normal analysis. We conclude that **the non-normal behavious is only an artifact of the simplified models**.

  → For example: The observations of instabilities in the SPS can be described with a normal TMCI mechanism (i.e. without considering non-normal analysis tools)

Space-charge in the circulant matrix model

- We write the equation of motion in the transverse plane of a test particle at transverse and longitudinal position x_t *and* z_t under the influence of a source beamlet with average position $\langle x \rangle_s$:

$$\frac{d^2 x_t}{ds^2} = -K(s)x_t + \frac{q}{m_p c^2 \beta_r^2 \gamma_r^3} E_s(s, x_t, \langle x \rangle_s, z_t)$$

Space-charge in the circulant matrix model

- We write the equation of motion in the transverse plane of a test particle at transverse and longitudinal position x_t *and* z_t under the influence of a source beamlet with average position $\langle x \rangle_s$:

$$\frac{d^2 x_t}{ds^2} = -K(s)x_t + \frac{q}{m_p c^2 \beta_r^2 \gamma_r^3} E_s(s, x_t, \langle x \rangle_s, z_t)$$

- We use the linearised electric field from a Gaussian beam (ultra-relativistic approx.):

$$E_s(s, x_t, \langle x \rangle_s) \approx \frac{q\lambda_s(z_t)}{2\pi\epsilon_0 m_p c^2 \beta_r^2 \gamma_r^3} \frac{x_t - \langle x \rangle_s}{\sigma_x(s)(\sigma_x(s) + \sigma_y(s))} \delta(z_t)$$

Space-charge in the circulant matrix model

- We write the equation of motion in the transverse plane of a test particle at transverse and longitudinal position x_t *and* z_t under the influence of a source beamlet with average position $\langle x \rangle_s$:

$$\frac{d^2 x_t}{ds^2} = -K(s)x_t + \frac{q}{m_p c^2 \beta_r^2 \gamma_r^3} E_s(s, x_t, \langle x \rangle_s, z_t)$$

- We use the linearised electric field from a Gaussian beam (ultra-relativistic approx.):

$$E_s(s, x_t, \langle x \rangle_s) \approx \frac{q\lambda_s(z_t)}{2\pi\epsilon_0 m_p c^2 \beta_r^2 \gamma_r^3} \frac{x_t - \langle x \rangle_s}{\sigma_x(s)(\sigma_x(s) + \sigma_y(s))} \delta(z_t)$$

- Integrating the equation of motion over one turn and using the smooth approximation, we get the integrated kicks from the lattice and space charge:

$$\Delta x'_r = -K x_t + \Delta x'_{SC}$$

$$\Delta x'_{SC} \approx \frac{q\lambda_s(z_t) C}{4\pi\epsilon_0 m c^2 \beta_r^2 \gamma_r^3 \beta \epsilon} (x_t - \langle x \rangle_s)\delta(z_t)$$

Space-charge in the circulant matrix model

- Rewriting the integrated space-charge kick using the source beamlet distribution in the longitudinal plane $\psi_s(z,\delta)$

$$\Delta x'_{SC} \approx A\sigma_z(x_t - \langle x\rangle_s) \int d\delta \Psi_s(z_t,\delta) \quad \text{with } A = \frac{qC}{4\pi\epsilon_0 mc^2\beta_r^2\gamma^3\beta\epsilon\sigma_z}$$

Space-charge in the circulant matrix model

- Rewriting the integrated space-charge kick using the source beamlet distribution in the longitudinal plane $\psi_s(z,\delta)$

$$\Delta x'_{SC} \approx A\sigma_z(x_t - \langle x\rangle_s) \int d\delta \Psi_s(z_t,\delta) \quad \text{with } A = \frac{qC}{4\pi\epsilon_0 mc^2\beta_r^2\gamma^3\beta\epsilon\sigma_z}$$

- We can now write the integrated kick of the source beamlet on a test beamlet with normalised distribution $\psi_t(z,\delta)$

$$\Delta x'_{SC} \approx A\sigma_z(\langle x\rangle_t - \langle x\rangle_s) \iiint d\delta_s dz_t d\delta_t \Psi_s(z_t,\delta_s)\Psi_t(z_t,\delta_t)$$

Space-charge in the circulant matrix model

- Rewriting the integrated space-charge kick using the source beamlet distribution in the longitudinal plane $\psi_s(z,\delta)$

$$\Delta x'_{SC} \approx A\sigma_z(x_t - \langle x\rangle_s) \int d\delta \Psi_s(z_t,\delta) \quad \text{with } A = \frac{qC}{4\pi\epsilon_0 mc^2\beta_r^2\gamma^3\beta\epsilon\sigma_z}$$

- We can now write the integrated kick of the source beamlet on a test beamlet with normalised distribution $\psi_t(z,\delta)$

$$\Delta x'_{SC} \approx A\sigma_z(\langle x\rangle_t - \langle x\rangle_s) \iiint d\delta_s dz_t d\delta_t \Psi_s(z_t,\delta_s)\Psi_t(z_t,\delta_t)$$

$$= A\sigma_z(\langle x\rangle_t - \langle x\rangle_s) \iiiint dz_s d\delta_s dz_t d\delta_t \Psi_s(z_s,\delta_s)\Psi_t(z_t,\delta_t)\delta(z_s - z_t)$$

Space-charge in the circulant matrix model

- Rewriting the integrated space-charge kick using the source beamlet distribution in the longitudinal plane $\psi_s(z,\delta)$

$$\Delta x'_{SC} \approx A\sigma_z(x_t - \langle x\rangle_s)\int d\delta \Psi_s(z_t,\delta) \quad \text{with} \quad A = \frac{qC}{4\pi\epsilon_0 mc^2\beta_r^2\gamma^3\beta\epsilon\sigma_z}$$

- We can now write the integrated kick of the source beamlet on a test beamlet with normalised distribution $\psi_t(z,\delta)$

$$\Delta x'_{SC} \approx A\sigma_z(\langle x\rangle_t - \langle x\rangle_s)\iiint d\delta_s dz_t d\delta_t \Psi_s(z_t,\delta_s)\Psi_t(z_t,\delta_t)$$

$$= A\sigma_z(\langle x\rangle_t - \langle x\rangle_s)\iiiint dz_s d\delta_s dz_t d\delta_t \Psi_s(z_s,\delta_s)\Psi_t(z_t,\delta_t)\delta(z_s - z_t)$$

- Change of variables to normalised polar coordinates: $\begin{cases} z_t & \longrightarrow r_t\sigma_z\cos(\theta_t) \\ \delta_t & \longrightarrow r_t\sigma_\delta\sin(\theta_t) \\ z_s & \longrightarrow r_s\sigma_z\cos(\theta_s) \\ \delta_s & \longrightarrow r_s\sigma_\delta\sin(\theta_s) \end{cases}$

$$\Delta x'_{SC} \approx A(\langle x\rangle_t - \langle x\rangle_s)\iiiint dr_s d\theta_s dr_t d\theta_t$$
$$\Psi_s^p(r_s,\theta_s)\Psi_t^p(r_t,\theta_t)\delta(r_s\sin(\theta_s) - r_r\sin(\theta_r))$$

Coherent tunes in the presence of space-charge

Air-bag, linear RF (BimBim)

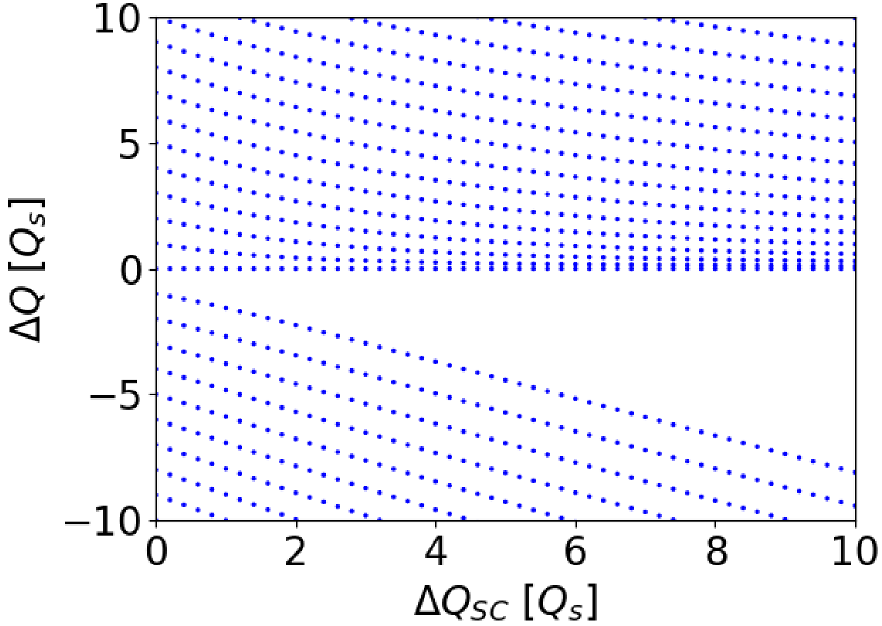

Air-bag, square potential well (M. Blaskiewicz)

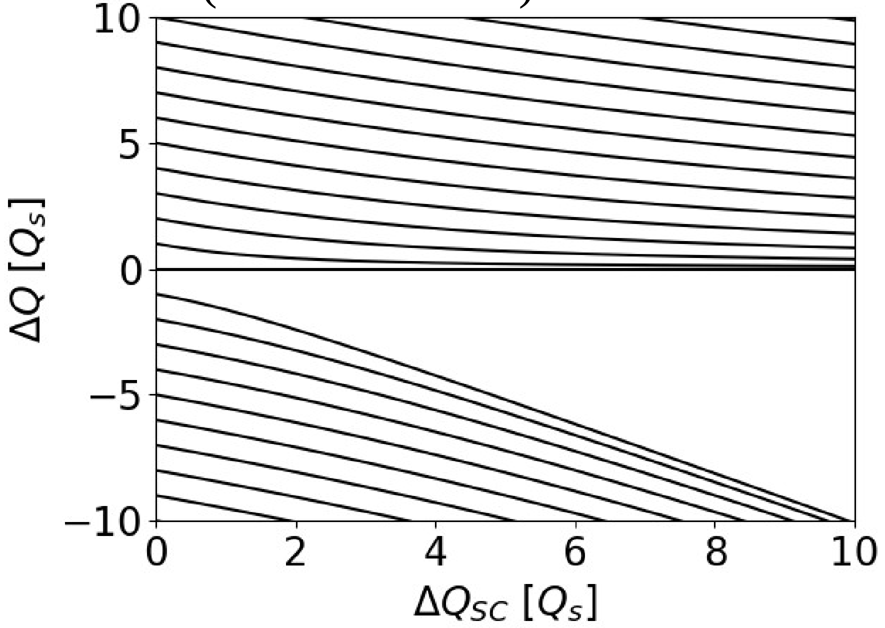

Coherent tunes in the presence of space-charge

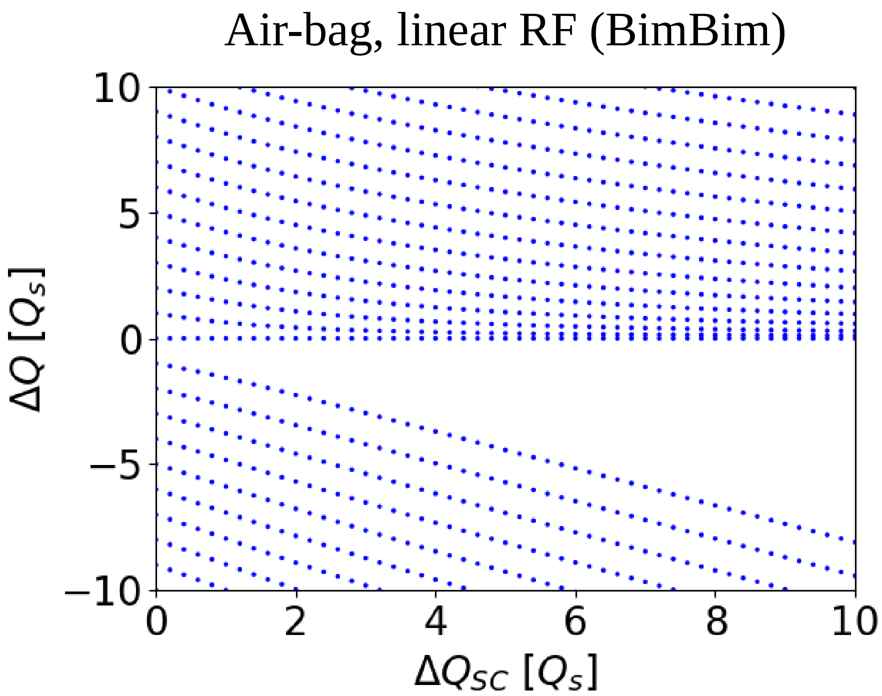

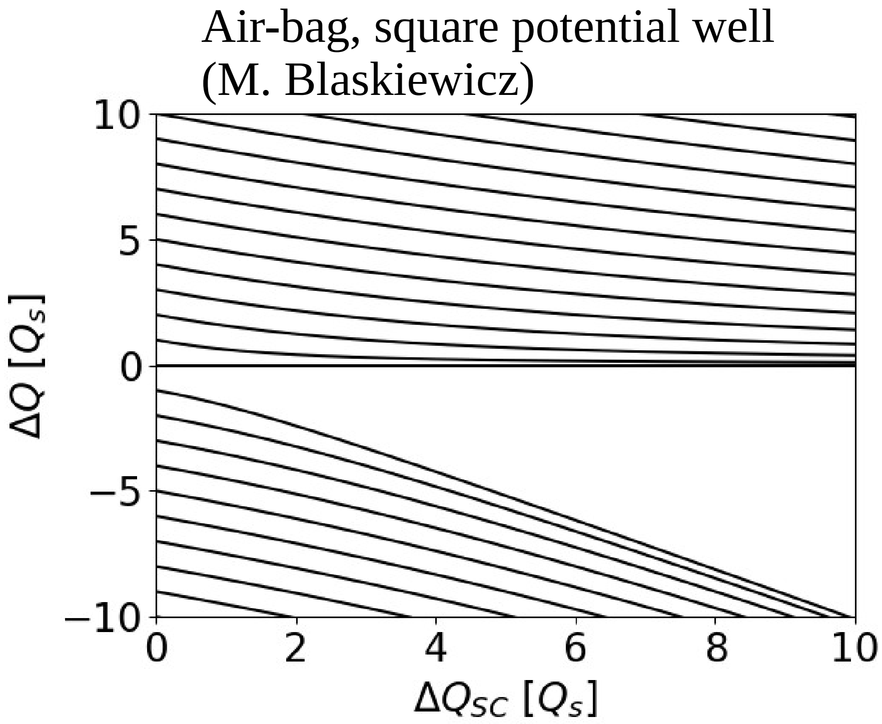

- The small differences between the two approaches result from the assumption on the RF, which affect the distribution and consequently the space-charge force

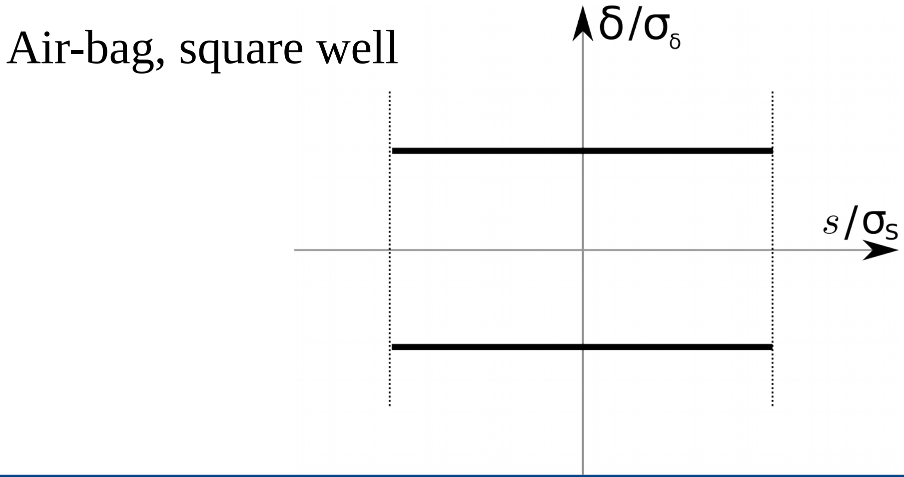

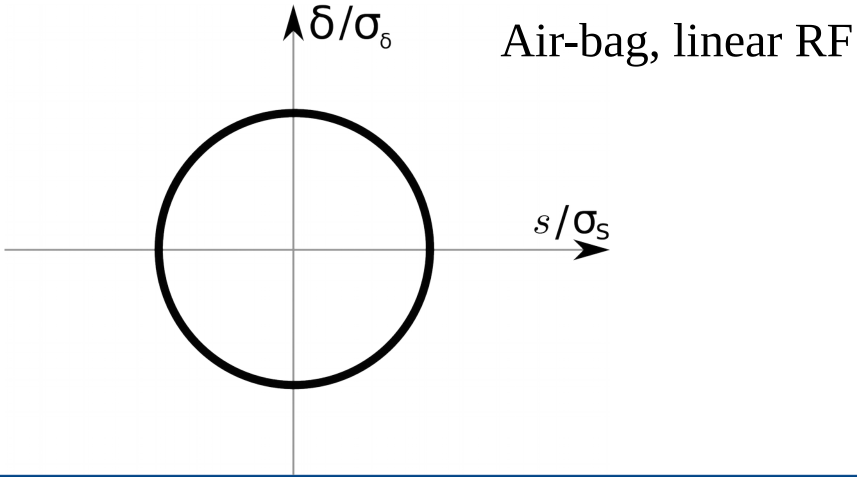

Space-charge in the circulant matrix model
Airbag distribution

- We consider an airbag of radius R_0 discretised into N_s chunks in polar angle:

$$\Psi_i^p(r,\theta) = \begin{cases} \frac{N_s}{2\pi}\delta(r-R_0) & \text{, if } \theta \in [\theta_i, \theta_{i+1}[\\ 0 & \text{, otherwise} \end{cases} \qquad \theta_i \equiv \frac{2\pi}{N_s}\left(i - \frac{1}{2}\right)$$

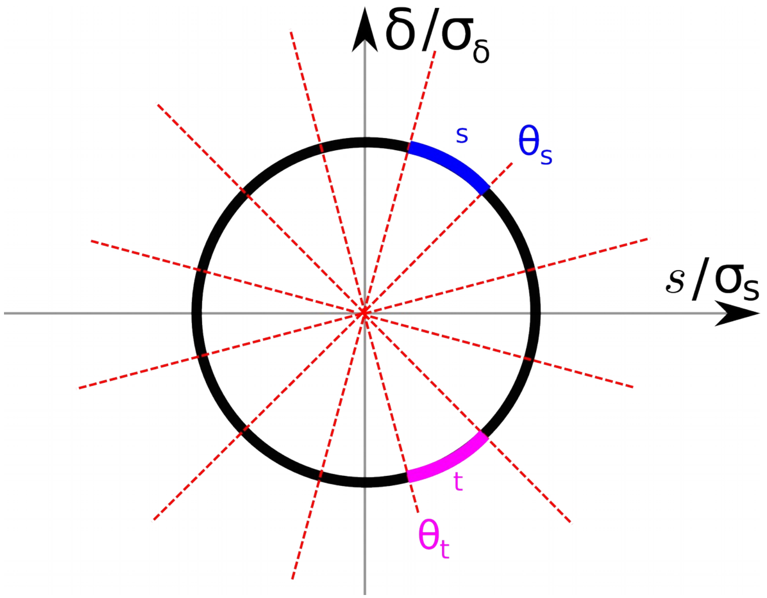

Space-charge in the circulant matrix model
Airbag distribution

- We consider an airbag of radius R_0 discretised into N_s chunks in polar angle:

$$\Psi_i^p(r,\theta) = \begin{cases} \frac{N_s}{2\pi}\delta(r-R_0) & \text{, if } \theta \in [\theta_i, \theta_{i+1}[\\ 0 & \text{, otherwise} \end{cases} \qquad \theta_i \equiv \frac{2\pi}{N_s}\left(i - \frac{1}{2}\right)$$

- The integrated kick of the source beamlet on the test beamlet is then:

$$\Delta x'_{s,t} \approx \frac{A}{4\pi R_0}(\langle x\rangle_t - \langle x\rangle_s)\int_{\theta_s}^{\theta_{s+1}}\int_{\theta_t}^{\theta_{t+1}} d\theta_s d\theta_t \delta(\cos(\theta_s) - \cos(\theta_t))$$

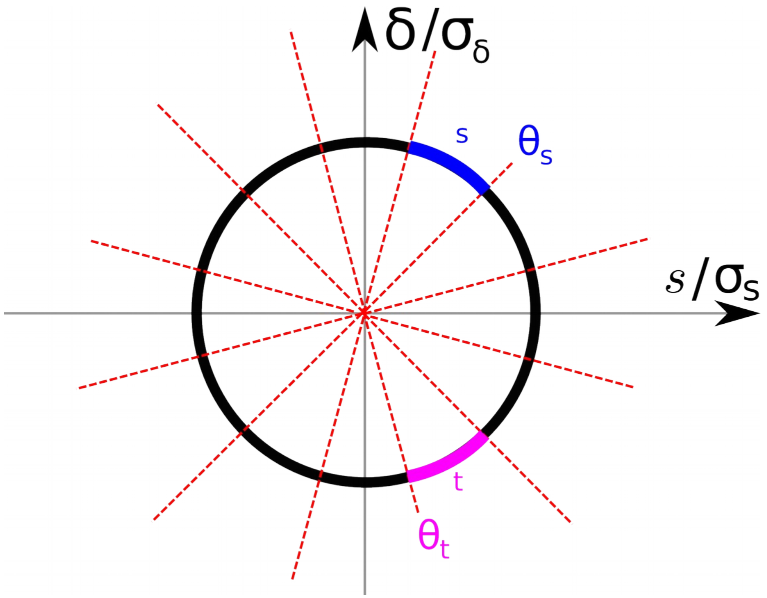

Space-charge in the circulant matrix model
Airbag distribution

- We consider an airbag of radius R_0 discretised into N_s chunks in polar angle:

$$\Psi_i^p(r,\theta) = \begin{cases} \frac{N_s}{2\pi}\delta(r-R_0) & \text{, if } \theta \in [\theta_i, \theta_{i+1}[\\ 0 & \text{, otherwise} \end{cases} \qquad \theta_i \equiv \frac{2\pi}{N_s}\left(i - \frac{1}{2}\right)$$

- The integrated kick of the source beamlet on the test beamlet is then:

$$\Delta x'_{s,t} \approx \frac{A}{4\pi R_0}(\langle x\rangle_t - \langle x\rangle_s) \int_{\theta_s}^{\theta_{s+1}} \int_{\theta_t}^{\theta_{t+1}} d\theta_s d\theta_t \delta(\cos(\theta_s) - \cos(\theta_t))$$

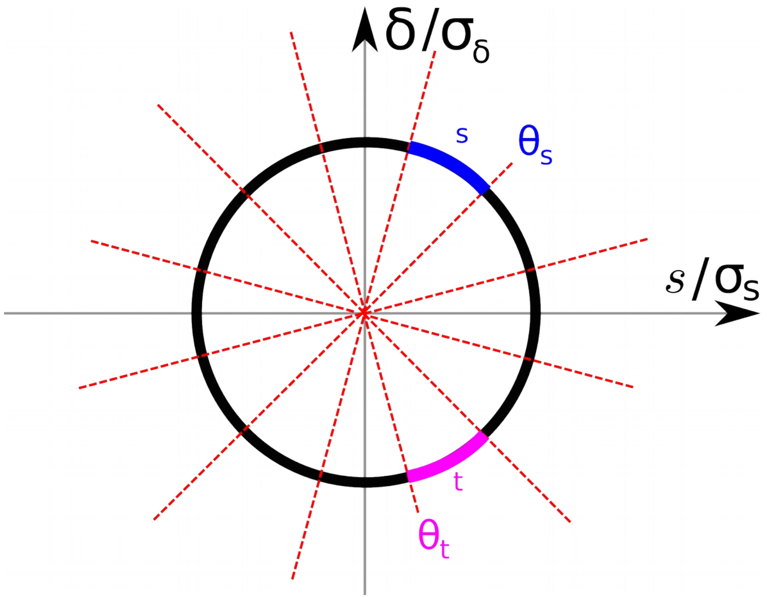

- Solving the integral with a change of variable

$$\begin{cases} \cos(\theta_s) & \longrightarrow u_s \\ \cos(\theta_t) & \longrightarrow u_t \end{cases} \qquad U_i = \cos(\theta_i)$$

Space-charge in the circulant matrix model
Airbag distribution

- We consider an airbag of radius R_0 discretised into N_s chunks in polar angle:

$$\Psi_i^p(r,\theta) = \begin{cases} \frac{N_s}{2\pi}\delta(r-R_0) & \text{, if } \theta \in [\theta_i, \theta_{i+1}[\\ 0 & \text{, otherwise} \end{cases} \qquad \theta_i \equiv \frac{2\pi}{N_s}\left(i - \frac{1}{2}\right)$$

- The integrated kick of the source beamlet on the test beamlet is then:

$$\Delta x'_{s,t} \approx \frac{A}{4\pi R_0}(\langle x\rangle_t - \langle x\rangle_s) \int_{\theta_s}^{\theta_{s+1}} \int_{\theta_t}^{\theta_{t+1}} d\theta_s d\theta_t \delta(\cos(\theta_s) - \cos(\theta_t))$$

- Solving the integral with a change of variable

$$\begin{cases} \cos(\theta_s) & \longrightarrow u_s \\ \cos(\theta_t) & \longrightarrow u_t \end{cases} \qquad U_i = \cos(\theta_i)$$

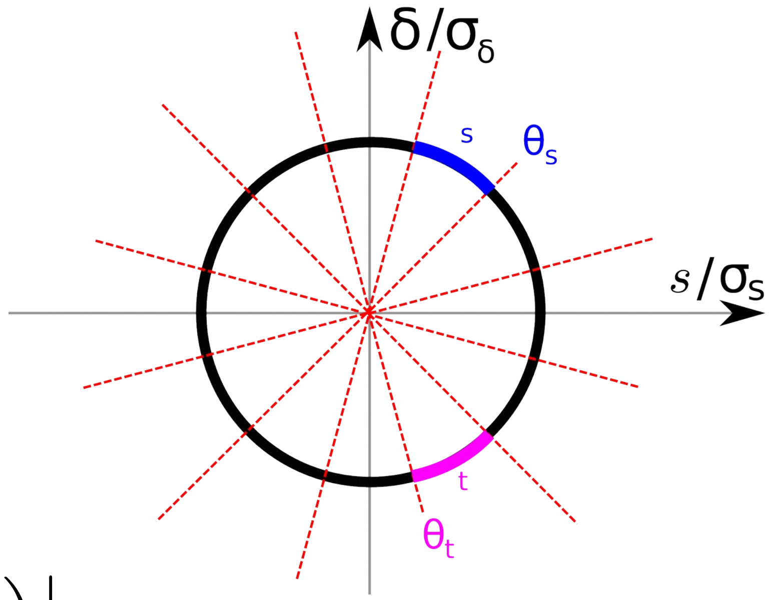

$$\Delta x'_{s,t} \approx \begin{cases} \frac{A}{8\pi^2 R_0}(\langle x\rangle_t - \langle x\rangle_s) \left|\log\left(\frac{1+U_{s+1}}{1-U_{s+1}}\frac{1-U_s}{1+U_s}\right)\right| & \text{, if } t+s = N_s \text{and } t \neq s \\ 0 & \text{, otherwise} \end{cases}$$